RUTGERS
School of Arts and Sciences

Samiah Moustafa
Department of Geography
Lucy Stone Hall, Room B254
Rutgers, The State University of New Jersey
54 Joyce Kilmer Avenue
Piscataway, NJ 08854-8045

samiah.moustafa@rutgers.edu

January 20th, 2015

Dear Editor,

We are grateful for the reviewers' comments and suggestions that we found very constructive. We have followed all major recommendations by the reviewers, which will improve the manuscript. Most importantly, we found that our interpretation of the bimodal MODIS albedo distributions from 2013 were not due to a shift from clean to dirty ice, but a shift from snow to an ice covered surface. We will update the manuscript accordingly. We will also add a new analysis of MODIS albedo distributions from 2012 that exhibit a more complex pattern than in 2013. In 2012, darker ice surfaces are exposed and are qualitatively different than other ice surfaces. Thus, we believe our revised manuscript of albedo of different ice surface types will provide a contribution to understanding Greenland ice sheet albedo in the ablation zone. We will revise the title of our manuscript to: Multi-modal albedo distributions in ablation zone in southwestern Greenland ice sheet. In addition, we would like to include three new coauthors to the manuscript who all made contributions to the revisions - Drs. L. Koenig, M. Hom, and C. Shuman.

A detailed response to each of the reviewers concerns and comments follows below.

In our response, we restate reviewers' comments and follow up with our responses in blue text. We use *italics* to highlight text that will be added or rewritten in the manuscript revisions. There might be minor changes to the manuscript from what is presented below to ensure the text flows well.

Sincerely,
Samiah Moustafa
PhD Candidate, Rutgers University

Response to comments by Dr. Pope

Response to comments on the Introduction section

1. **Surface albedo is defined as "is defined as the ratio of reflected to incident solar radiation upon a given surface (Schaepman-Strub et al., 2006)." However, that paper explicitly calls out the ambiguous use of the term "albedo." Even in common usage (as bihemispherical reflectance), "albedo" can refer to either the entire spectrum of solar radiation or the visible part of the spectrum (IASC Mass Balance Glossary). I do appreciate the desire to be pithy and concise, but I think it would help comprehension if you were more explicit in the introduction and through with the types of reflectance being compared and the wavelengths implied.

    - In the revised manuscript, we follow the advice of Dr. Pope and provide a more unambiguous term for surface albedo – identifying it as the bihemispherical reflectance across the visible and near-infrared wavelengths (case 9 in Schaepman-Strub et al., 2006). Throughout the manuscript, we provided explicit terminology for different types of reflectance and associated wavelengths as requested.

2. **The first paragraph continues on to describe positive albedo feedbacks as observed in previous studies. The was confusing to me as the reader because those studies (as summarized by Stroeve) show "The downward albedo trends indicate both a reduction in the duration of snowcover over low albedo bare ice, and an expansion of the bare ice area (Box et al., 2012; Tedesco et al., 2011)." This paper, on the other hand, avoids snow altogether and instead describes change in albedo on clean/dirty ice surfaces and cryoconite. This juxtaposition was misleading to at least this reader. To me, it would have been clearer to me to immediately move on to the more relevant content of the 2nd paragraph. (Another way to say this is that many studies focus on the whole of the GrIS – to be self-consistent, this paper should be highlighting studies / processes which focus on what happens after bare ice is exposed.)

    - We will rewrite the first paragraph to include reduction in snow cover as another mechanism for albedo decline. It reads:

      Over the last decade, an observed decline in albedo has been linked to less summer snow cover, expansion of bare ice area, and enhanced snow grain metamorphic rates from atmospheric warming, amplified by the melt-albedo feedback (Box et al., 2012; Stroeve et al., 2013; Tedesco et al., 2011). This positive feedback entails snow grain growth owing to melt, reducing surface albedo,…

    - We have decided to keep the first paragraph in the manuscript because it serves to draw the reader's attention to the importance of surface albedo on the GrIS, as well as its role in modulating the mass balance of the ice sheet (via the ice-albedo feedback and snow grain metamorphic rates).

**Page 4740, Lines 13-15 affirm that negative albedo trends are "linked to a darkening of the ice surface from increased surface coverage of meltwater, cryoconite holes, and impurity-rich surface types (Bøggild et al., 2010; Chandler et al., 2014; Wientjes and Oerlemans, 2010)." It would be clearer to say that ablation facies have expanded relative to accumulation facies (i.e. Box: "the strength of albedo feedback is determined more by the surface albedo decrease

associated with a loss of seasonal snow cover than the reduction in snow albedo due to snow metamorphosis because of the large difference between snow and bare ice albedo values.") rather than this sentence, which implies darkening ice surfaces, which is not previously substantiated in the literature as far as I am aware.

- We have corrected the text as requested. The revised text will read:

  Furthermore, negative albedo trends since 2000 (Box et al., 2012) are linked to an expansion of ablation facies relative to accumulation facies.

Response to comments on the ASD Data Collection section

3. **You mention the use of a foreoptic for solar illumination collection. Was no foreoptic used at all for data collection? And if not, were data collected with the sensor oriented in different directions horizontally so as not to bias measurements on particular sensor fibers? Also, was each spectrum really only 5 samples, or was each sample actually also a repeat of 'x' scanes (e.g. 25-50 scans), as is standard with ASD software?

   - We have rewritten the methods section to clarify that the ASD was fitted with a Remote Cosine Receptor (RCR), but no additional fiber optics was attached. We also clarified that each of the five consecutive samples consists of 10 dark currents per scan and 10 white reference measurements. The new text will read:

     The ASD was mounted on a tripod at 0.4 m distance, and with no foreoptic attached (i.e., bare fiber), had a 25º field-of-view, corresponding to a spot size of ~0.18 m diameter on the surface.

     At each sample location, five consecutive spectra consisting of 10 dark currents per scan and 10 white reference measurements were recorded and averaged.

4. **You say that αASD is averaged over the whole spectral range (of 325-1075 nm). Instead, for better comparison with MODIS as is done later, would it make more sense to use MODIS relative spectral response functions to weight the spectra? Or does the increased MODIS range (300-3000 nm) really change the comparison enough already to make this not worthwhile?

   - We have revised our methodology to compute α_{ASD} as a weighted average based on incoming solar radiation in each wavelength described in response reviewer 2 General Comment #4. This should provide a more accurate value for α_{ASD}. We will revise the manuscript text to make it very clear that the comparison between α_{ASD} and α_{MOD} are not directly comparable. We decided not to calculate α_{ASD} based on the spectral response of MODIS for two reasons. First, as Dr. Pope points out, the limited spectral range of the α_{ASD} compared to MODIS will not allow a calculation of a directly comparable variable. Second, we don't aim to make a comprehensive validation between α_{MOD} and α_{ASD}, but rather use MODIS qualitatively to provide spatial and temporal context. While the absolute values will differ, the difference between the two products should not change spatial and temporal patterns.

5. **Your regression αASD vs αMET as presented on Page 4746 / Figure 4 seems very skewed to the datapoint on the left. Afterall, αASD ranges from 0.45 to 0.6 beside that one 0.15 value, while the αAMET are well spread between 0.3 and 0.65. To me, this puts

into question the regression (and use of a 40% variance statistic). While I think there is likely some truth to your statement that "The discrepancy is likely due to differences in exact sample locations and instrumentation", I think your regression puts the ASD and MET data into question more than reinforcing their intercomparison.

- We have replotted Figure 4 and updated it with revised α_{ASD} values calculated with the broadband albedo calculation described in response to reviewer 2 General Comment #4. Furthermore, we discovered that the outlier point was identified as 'low quality' and included in the figure by mistake. The revised figure shows a stronger fit between the two variables. The figure is shown below:

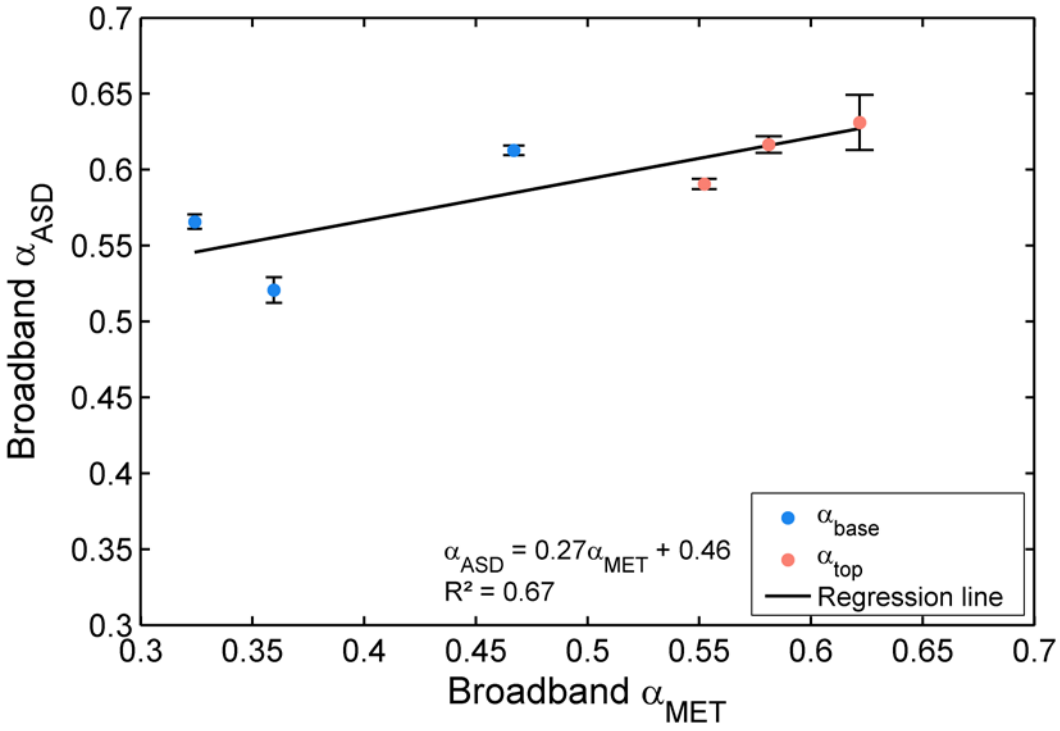

Figure 4. Broadband α_{base} (blue dots) and α_{top} (pink dots) vs. α_{ASD} and α_{MET} (i.e., both α_{base} and α_{top}) measurements fitted to a linear regression equation (R^2 = 0.67). The value of α_{ASD} error is based on the standard deviation of individual α_{ASD} measurements.

Response to comments on the Melt section

6. **Small note: Page 4748, Line 16 makes an assumption about net longwave radiation being negligible for surface melt. Since you go on to later talk about relative rates anyway, you might not need to state this assumption, and just acknowledge you are addressing shortwave flux only? Either that, or back up your assumption with a reference.

- We will revise the text to acknowledge that we are only addressing shortwave flux here in our computation of relative surface melt rates as suggested.

Response to comments on the Distribution Discussion section

7. **Page 4750, Lines 15-22: I might be misunderstanding, but these numbers don't all seem

to match up. E.g. the difference between 5.8 and 7.0 is 1.2, not 2.3. Or am I misunderstanding? Same comment for the subsequent set of numbers, too.

- Indeed, the numbers are incorrect. We corrected this error and the numbers now match up. These revised numbers will also be updated in Figure 8 and Table 4.
- These values were originally provided in units of m d^{-1} and converted to SI units of m s^{-1}.

8. **Fig 12: The term "spatial scale" is ambiguous to me. As I understand it, you are varying the spatial extent, not the spatial resolution. Apologies if I misread that. SO – this figure is possibly two populations that are snow & ice, as opposed to "ice" and "dirty". Could you address how you are sure that there is no influence of snow in the scenes? Also, why else would he the spatial extent matter (as opposed to being able to see things at different spatial resolutions, i.e. small patches of dark things wouldn't be resolved, etc.)
    - Yes, we are varying the spatial extent and not the spatial resolution. In the revised manuscript, the term 'spatial scale' will be replaced throughout the text to instead reflect the less ambiguous term 'spatial extent'.
    - After carefully analyzing the conditions in our study area in 2013, we have come to the conclusion that snow did in fact influence the MODIS scenes. As will become clear in the response to reviewers 1 and 2 below, we have made major revisions to the manuscript to address this issue.
    - Snow did influence the probability density distributions (PDDs) at the MODIS 100x100 and 150x150 spatial extents in 2013, as seen in Figure 12. The bimodality identified for the 100x100 MODIS pentad averages is likely associated with the population of snow and ice surfaces.
    - To verify the presence of snow in our study area and MODIS spatial extents, we examined hourly precipitation and air temperature measurements collected by a meteorological station installed near the ice sheet edge (at the proglacial and ice sheet margin interface). Near surface air temperature measurements from the shorter Base Met Stations time series were also examined to demonstrate roughly how much colder it was on the ice. To confirm that solid precipitation fell, we used NASA's WorldViewer to browse daily MODIS reflectance imagery (bands 7-2-1 and 3-6-7) to identify textural or brightness changes related to precipitation events. The identification of snowfall events will be added to the Methods section.
    - Several precipitation events occurred throughout the 2013 melt season as shown in the figure below. Two snowfall events were identified on 28-29 June and after 14-15 August. The 28-29 June 2013 precipitation event has been identified as a snowfall event. NASA WorldViewer imagery reveal cloud cover on 28-29 June followed by a brightening of the surface on 30 June. The 28-29 June snowfall event corresponds to the bimodal distribution observed in the MODIS 30 Jun - 4 July pentad average (see Figure 13), corresponding to a brief 'jump' in the PDD (associated with higher albedo values of ~0.6 and 0.7). The bimodal distribution seen in the 2013 MODIS data is associated with a transition from ice to snow, rather than clean to dirty ice. The results of this snowfall event, and its role in creating a bimodal distribution in the MODIS 2013 data will be added to the Results section, and further fleshed out in the Discussion section.

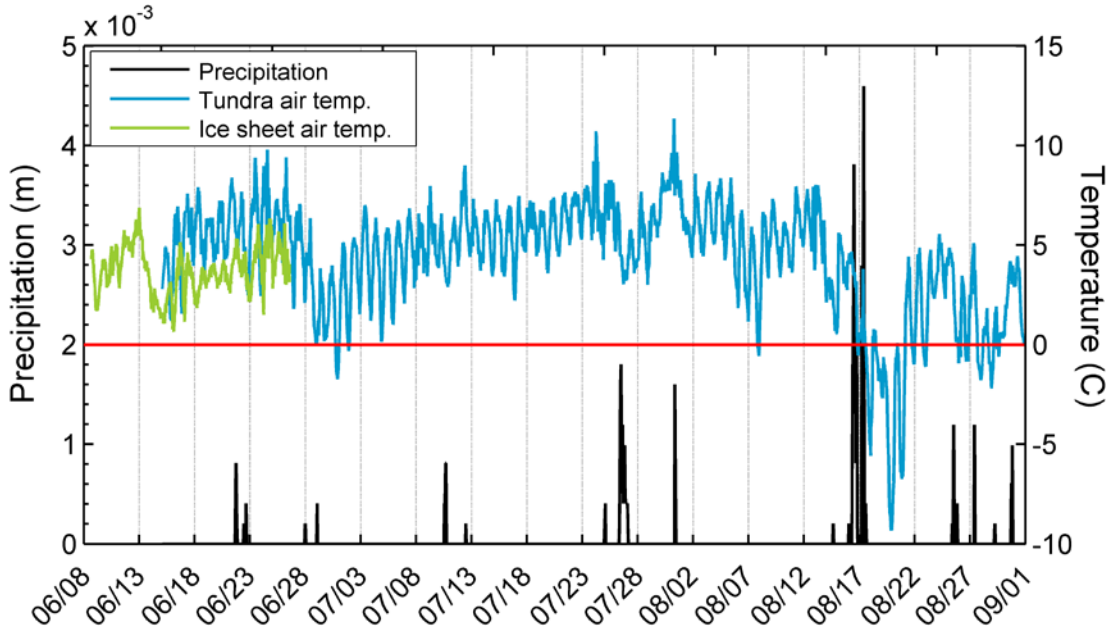

New Figure. Summer 2013 precipitation (left y-axis; black line) and near surface air temperature (right y-axis; blue line) time series collected from a meteorological station installed at the edge of the pro-glacial tundra environment. Base Met Station near surface air temperature time series is available from 8 – 26 June 2013 (green line). The difference in tundra and ice sheet near surface air temperatures is ~3 °C. The zero degree line is in red.

- To verify our findings in 2013, we also included an analysis of possible snowfall events in 2012 based on precipitation and air temperature meteorological station time series data, as shown in the figure below. Snowfall events likely occurred on 6 and 13 June 2012, prior to the start of the meteorological station log (8 June 2012), and on 14-15 August 2012, based on NASA WordViewer imagery. Calculation of 100x100 MODIS 2012 pentad averages reveal that the only exception to low albedo averages is on 6 June 2012, when snow likely fell (as verified with NASA's WorldViewer and tundra meteorological station data; see figure below and our response to reviewer 1 Major Comment #3 below). The results of the 2012 snowfall event identification, as well as its impact on MODIS albedo and pentad averages will be added to the Results section.

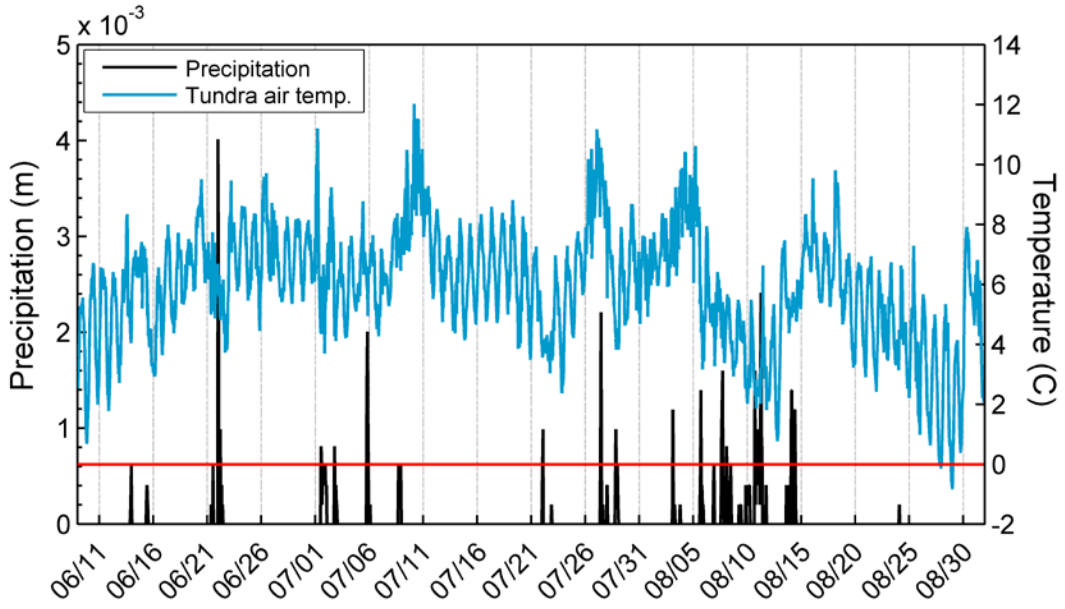

New Figure. Summer 2012 precipitation (left y-axis; black line) and near surface air temperature (right y-axis; blue line) time series collected from a meteorological station installed at the edge of the pro-glacial tundra environment. The zero degree line is in red.

9. **Overall in figs & discussion: I think the term "bimodal distribution" really needs to be used with caution (as opposed to single peak with a shoulder, wide peak, etc.) as this has important implications for later interpretation.

   - After revising our work and discovering more complex albedo distributions, we agree with the reviewer, and have adopted a more cautious and nuanced approach to writing about our results and their interpretation.

Response to Anonymous Referee #1

Response to General comments

Although Moustafa et. al. touch a very interesting and important research topic (i.e. the seasonal evolution of ice surface types in the GrIS ablation zone) that is very rele- vant for (future) surface mass balance estimations, there are several main issues and a variety of smaller comments that need to be clarified and corrected (see major and detailed comments below).
Generally, I do think that Moustafa et. al. are overcriticizing the existent SMB models while simultaneously overinterpreting their own results. For example, the latest genera- tion of SMB models does take the major variability in ablation zone albedo into account (i.e., snowfall events, spatial variability (e.g. Van Angelen et. al., 2012). Therefore they should already account for the major albedo variability in this study, which I also tend to attribute to (degraded) snow and spatial

variability. In that context, I do believe they are obtaining results that are very close to the results obtained by Alexander et. al. (2014). Moreover, by comparing the differences in melt relative to melt with unrealistic high ice albedo values of 0.7 they are overestimating the impact of their study.

In the response to the reviewer's major and minor comments below, it will become clear how we have addressed the reviewer's general comments. Briefly, we have revised the manuscript to better represent the state-of-the-art surface mass balance models, recalculated in-situ ASD albedo values (now more realistic), and clarified how our study differ from Alexander et. al.'s study, thereby strengthening the weaknesses pointed out by the reviewer.

2 Response to Major comments

1. Moustafa et. al. state motivate their work based on the clear separation be- tween the albedo schemes of ablation zones in current surface mass balance models (e.g. in RCMs) and the albedo values they observe. In their motivation they implicitly take two assumptions. Firstly, they assume that a constant and spatially uniform ice albedo is being used throughout the ablation season in the existent SMB models and, consequently, they assume there is no seasonal variation in the ablation zone albedo. Secondly, they assume that last winter's or wind redistributed snow does not play a role in their data and, consequently, they assume that they are observing only evolution of ablation zone ice surfaces.

    - We will revise the manuscript and better described SMB models and acknowledge that SMB models represent seasonal variation in ablation zone albedo. For example, we have rewritten the introduction to say:
      State-of-the-art SMB models consider the presence of water ponding, bare ice, and snow surfaces to characterize seasonal variations in ablation zone albedo (Alexander et al., 2014; Van Angelen et al., 2012).
    - We have also added an analysis to consider the possibility of snow cover in explaining high albedo values. Indeed, several high albedo events are likely due to snowfall and expansion of snow-covered ice. Further details are provided in the response to Dr. Pope's Comment #8.

2. Although I agree 100% with the importance of understanding/assessing the seasonal evolution of ablation zone albedo, I don't agree with this separation. Firstly, because recent SMB models (e.g. in RACMO; Van Angelen et. al., 2012) take the spatial variability in ice albedo into account (e.g., spatially variable ice albedo background map that accounts for spatial differences in dark material, etc.). Secondly, because snow in these models also results in a bimodal albedo distribution (e.g. Fig. 5 of Van Angelen et. al. (2012)) as short term snowfall periods or re-distribution of blowing snow on top of the underlying ice can result in variations in ablation zone albedo (i.e., here the bimodal distribution is the result of the deposition/change/removal of the snow layer on top of the ice layer). Thirdly, they assume that the observed changes in albedo are completely independent of snow (redistribution) events, whereas I think the observed fractions of white ice are very closely related to these (earlier) snow events. Therefore, I do not see this clear separation between ablation zone albedo in SMB models and evolution of ablation zone albedo in this study.

    - After conducting further analysis, we agree with the reviewer, to a large extent. Indeed,

the bimodal distribution seen in MODIS albedo data in 2013 was due to differences in snow and ice covered area (see response to Dr. Pope's Comment #8). We will update the manuscript throughout to correct our error. However, we expanded our analysis to also include MODIS albedo data observed in 2012. This analysis is explained in reviewer 1 Major Comment #3 below and shows that 'dark' ice regions exist, but were not visible in 2013 due to snow cover. Thus, our claim that dust and sediment on Greenland's ice sheet surface can influence surface albedo stands.

3. Although I agree that SMB models don't have the evolution of ice surfaces (e.g. dust deposition/accumulation, cryoconite development, roughness evolution, etc.), they do have variations in ablation zone albedo (e.g. on top of a spatially variable ice background (Van Angelen et. al., 2012) or as a function of ponding water (MAR)) as a result of the deposition/redistribution of snow which also results in a bimodal distribution. I am convinced that large part of the albedo evolution in Fig.6 is closely related to this bimodal distribution (presence/absence of snow or at least the remnants in the form of white ice) which is also in the SMB models if they model it correctly. For example, if I look at Fig. 13, I have the impression that this 'bimodal distribution' is the effect of the presence of snow or degraded snow (which you call white ice), which perhaps is also in Alexander et al. (2014). Therefore, I think you should prove that this bimodal distribution is effectively not the result of the disappearing (already degraded) snow instead of the evolving ice itself (i.e., completely independent of previous snowfall events) and/or what the contribution of (degraded) snow to this bimodal distribution is?

- As explained in our response to reviewer one's Comment #1 and Dr. Pope's comment #8, we concur with the reviewer that the bimodal distribution in Figure 13 is due to snow. However, the albedo evolution in Figure 6 cannot have been caused by presence/absence of snow alone. We will revise the manuscript to clarify that Figure 6 shows albedo for the two MODIS pixels that overlap with our transect and that snow had melted from this region before mid-June 2013. We will also clarify that there were no snowfall events in this area between 9-25 June 2013. Finally, we will revise our text to acknowledge that while albedo has a slight negative trend from June to mid-August, there is variability that could be caused by occasional snowfall events.

- While the 2013 MODIS albedo bimodal distribution shown in Figure 12 and 13 actually are a result of snow and ice albedo, subsequent analysis of MODIS (MOD10) 2012 data, for the 100x100 spatial extent pentad averages, reveal a more complex distribution (see figure below). This distribution cannot be explained due to the presence/absence of snow and ice. Very low albedo values are likely due to sediment and dust-enriched ice in the so-called 'dark-band' region (see figure of spatial distribution of 100x100 MODIS albedo data in 2012 and 2013 below). In the revised manuscript, this new analysis will be included to provide evidence for the importance of low albedo surfaces caused by surface dust and sediments. In our revised discussion, we hypothesize that higher resolution satellite imagery (finer than MODIS) might capture such regions closer to the ice sheet margin. Furthermore, we postulate that the area of these regions may grow in size over the melting season as demonstrated on local scales by Chandler's in-situ observations.

- Here, 2012 MODIS pentad averages exhibit more variability and center at lower albedo values (between ~0.3 – 0.5 albedo values) as compared to 2013 pentad averages (see figure below). The higher probability of substantially low albedo values is expected since 2012 was identified as an extreme melt year (e.g., see Nghiem et al., 2012). These points will be

brought up in the Results section along with its implications in the Discussion section (e.g., this greater variability may be related to changes in meltwater ponding).

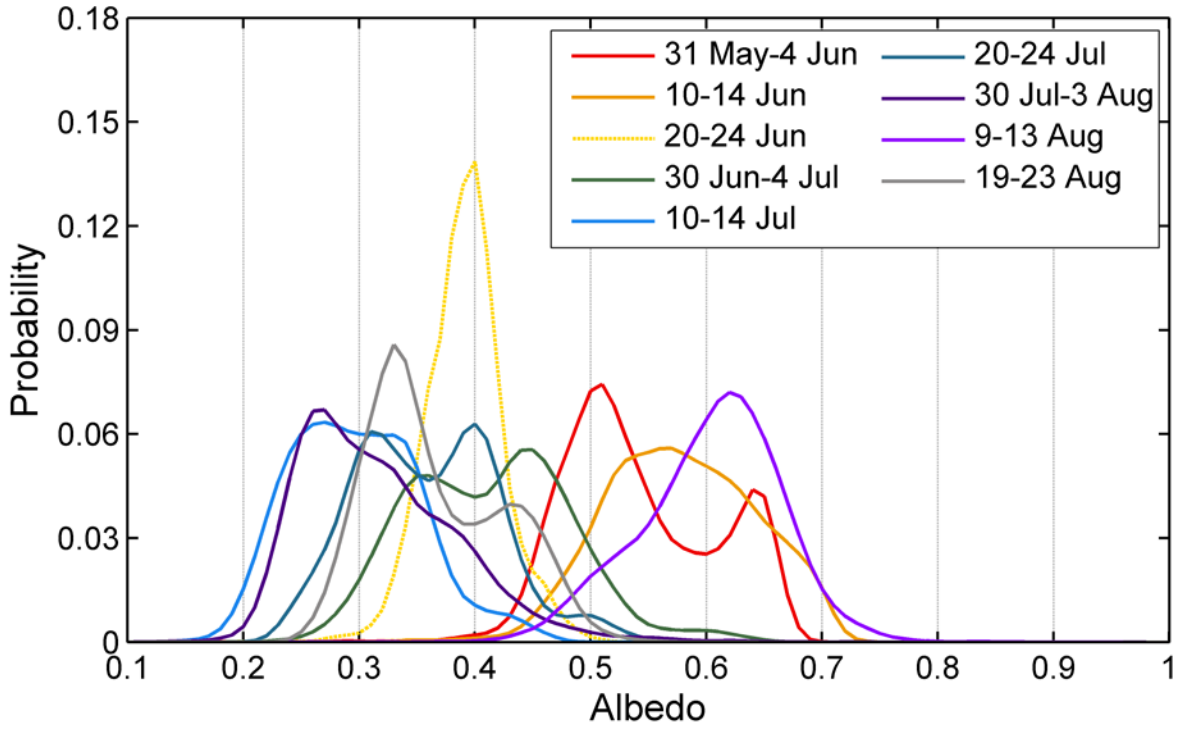

New Figure. MODIS 100x100 spatial extent pentad average albedo distributions for the 2012 melt season. Note, the 20-24 June pentad (yellow stippled line) is erroneous due to an outlier in the MODIS data for on 21-22 June 2012. This figure will be updated accordingly.

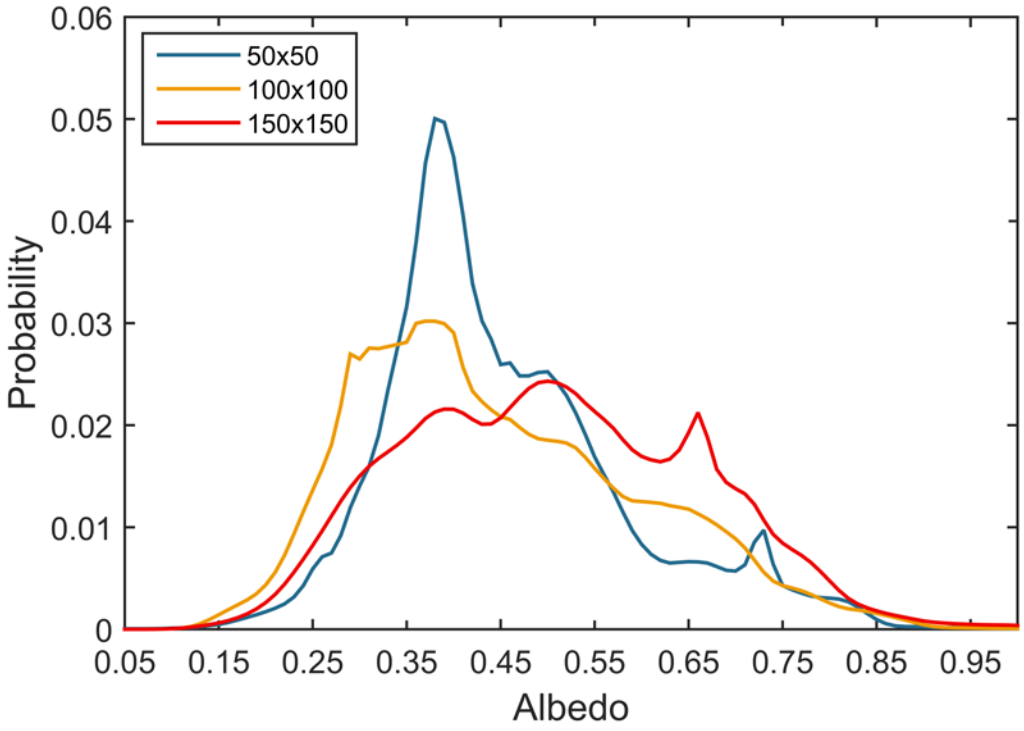

New Figure. MODIS 2012 seasonal average albedo probability density distributions at three spatial extents. The MODIS 2012 seasonal average albedo probabilities for the 100x100 and 150x150 spatial extents reveal a high probability of low albedo values (0.2 – 0.3). This is likely influenced by the expansion of the 'dark band' region in these spatial extents.

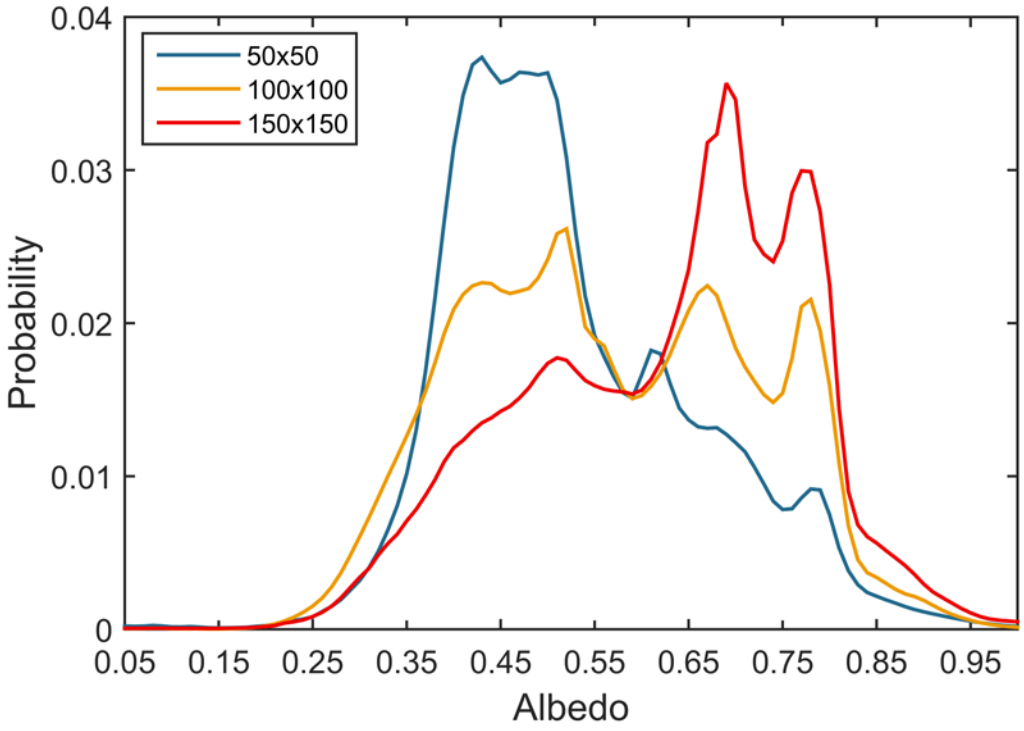

Updated Figure 12. MODIS 2013 seasonal average albedo probability density distributions at three spatial extents. The bimodal distribution seen at the 100x100 spatial extent is likely the result of snow and ice facies characterizing the two peaks.

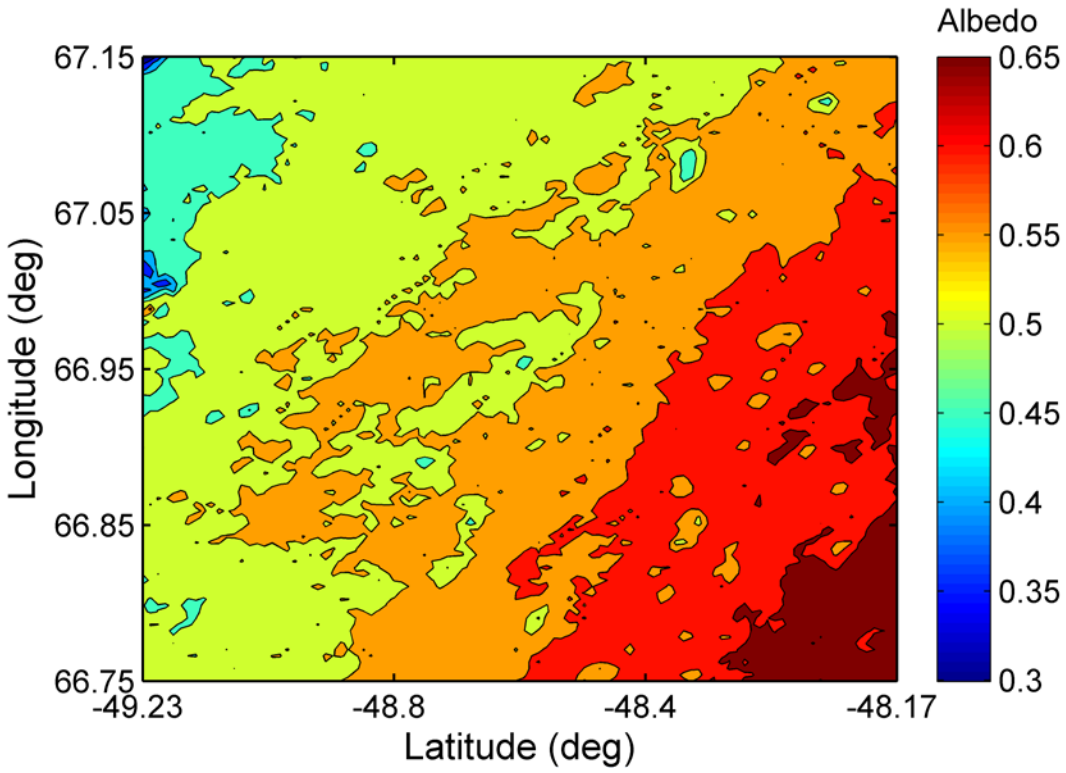

New Figure. MODIS 2013 spatial average for the 100x100 spatial extent. Overall higher MODIS albedo values are observed in 2013, without a 'dark band' region surface expression.

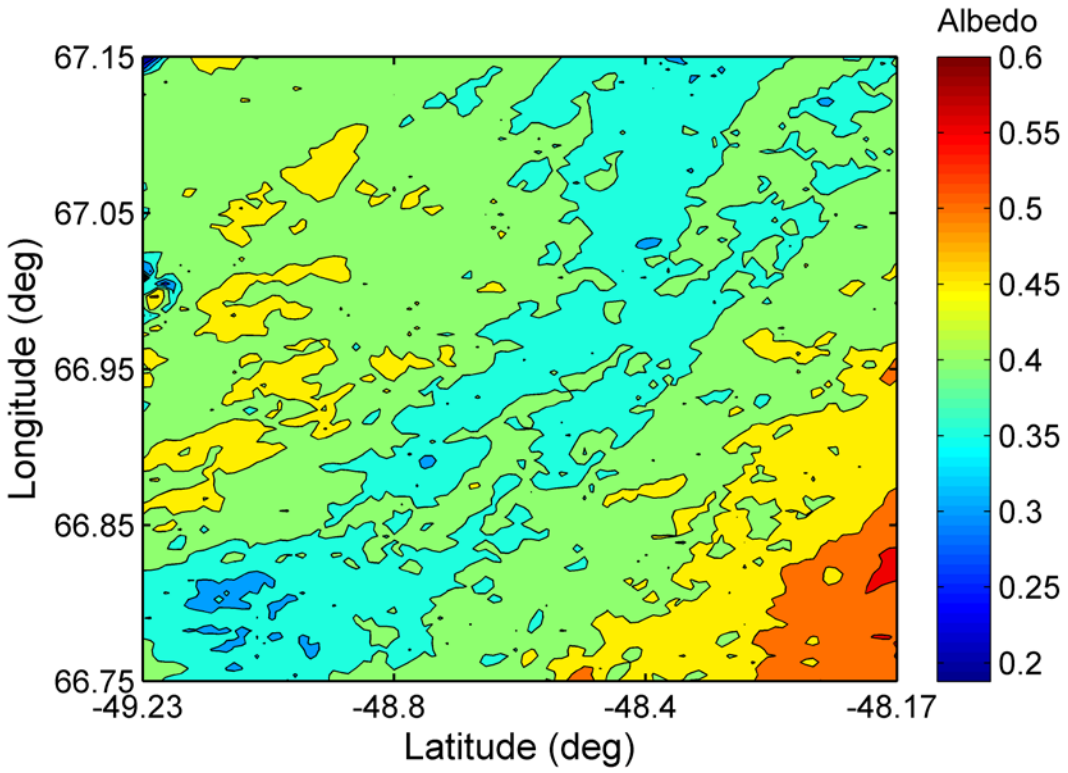

New Figure. MODIS 2012 spatial average for the 100x100 spatial extent. A region of dark ice, known as the 'dark band', extends through our study area (cyan blue color).

4. You state the 'seasonal changes in GrIS ablation zone albedo are not exclusively a function a darkening surface from ice crystal growth' and I do completely agree. The current SMB models do not claim that either for the ablation zone, because the major variability the ablation zone albedo in these models is driven by the deposition/change/disappearance of snow. Consequently, these models also have the bimodal distribution with sudden changes (e.g. sudden disappearance of snow or the suddent albedo reduction due to localized melt within the snowpack). Again, here you will have to prove that the bimodal distribution is effectively not the result of the disappearing (already degraded) snow instead of the evolving ice itself (i.e., completely independent of previous snowfall events) and/or what the contribution of (degraded) snow to this bimodal distribution is?

    - Indeed, after careful analysis, we found that the 2013 bimodal distribution was due to the presence of snow and ice. However, in 2012, a more complex distribution emerges as the snow melt, revealing a region of lower albedo known as the 'dark-band'. We explain how this has been addressed in the revised paper in reviewer 1 Comment #3 above. Furthermore, we will correct our manuscript text to clarify that the presence/absence of snow cover is an important driver for surface albedo.

5. Is the spatial or temporal variability of importance? I do have the impression that the spatial variability in 'ice albedo' is an order of magnitude more important than the temporal variability (E.g., the difference between pixel 1 and 2 is bigger than the within pixel variability, certainly if you assume that the biggest temporal variability is driven by appearance/disappearance of snowfall (e.g. 29/6 or 7/7)). If you then take into consideration that for example Van Angelen et.

al. already accounts for the spatial variability in ice albedo, the uncertainty of the existing SMB's, which is the motivation for your research, reduces significantly. I certainly think this should be discussed in your paper.

- In our revised manuscript, we will explain that the spatial distribution of snow cover and background ice albedo is very important to understand the temporal change in MODIS distributions in 2012 and 2013. For example, in 2012 when snow melt is more pronounced and reaches higher elevations, the 'dark band' is exposed and results in a mode with lower albedo.

- We will rewrite our Introduction section to acknowledge that the SMB model RACMO2 (as implemented by van Angelen et al. (2012)) accounts for spatially distributed ice albedo, and considers the impact of black carbon contaminants on albedo. Finally, we will rewrite our Introduction to make clear that the motivation for our research is not to critique SMB models, but to understand ablation zone albedo because of its role in ice sheet surface ablation.

6. Although I agree with the Short Comment of Pope that it is good that you provide so much information on the processing of the ASD data, I think large part of this processing (e.g. section 3.4 and Fig. 2-3) can be moved to a supplementary material as I think it diverts the reader of your main message. Moreover, some of this processing should be improved (e.g., the use of different wavelengths, etc.) to avoid wrong interpretations (see detailed comments).

   - We will dedicate the information related to the ASD data processing to an Appendix section. This new appendix will include section 3.4 and Figures 2-4. This appendix will describe our improved processing that address the concerns raised by the reviewers about accounting for wavelengths (see response to Dr. Pope's Comment #4) and in the Detailed Comments below.

7. The hypothetical albedo distributions based on ASD albedo (400-700nm) values for distinct surfaces and the fractional surface coverage area from Chander et. al. (2014) is prone to many assumptions that are wrong or difficult to justify. Therefore, it is very difficult to draw any conclusion from it. In my opinion, it is an interesting thinking exercise, but it stays far from the real bimodal distributions that will be much more blurred due to i) broadband values instead of overestimated albedo differences in the 400-700nm, ii) uneven standard deviations for different surface types (see detailed comments). This blurring is also what I tend to see in Fig. 10 and therefore I would remove this analysis as it will give you an overestimation of the real bimodality.

   - The authors believe that incorporating the computed albedo distribution analysis is an important part of the study. To our knowledge, no other studies have attempted to theorize and characterize the albedo distributions of distinct surface types in the ablation area of the GrIS. In the revised manuscript, we will correct the issues raised by the reviewer, namely i) correct calculation of broadband albedo and ii) provide different standard deviations for each surface type.

8. By comparing melt rates relative to the early summer ice melt rates, the underestimation in the existing SMB models and the importance of this study is overestimated. For example, existing SMB models with a fixed ice albedo use values of typically 0.5-0.45, but that locally go much lower (e.g. Van Angelen et. al. 2012), whereas Moustafa et. al. compare melt relative to melt with

albedo values of 0.7. Off course, this will result in strong increases in melt rate when compared relative to unrealistic high ice albedo values with unrealistic low melt rates.

- We will clarify that the melt rate calculations were made to examine the seasonal changes in MODIS albedo. No comparison with SMB models was made. Furthermore, we will remove the last sentences in the conclusions that stated that SMB models need to incorporate seasonal evolution of surface types. We will rewrite the conclusions to make it more nuanced, and it will read:

  Continued atmospheric warming coinciding with a darkening ice surface will increase the ice sheet surface meltwater production and runoff. Here, we show the importance of the distribution of dirty ice surfaces, which are likely the result of accumulation of impurities melted out from internal ice layers rather than contemporary deposition of atmospherically transported dust. Future research should investigate the importance of surface accumulation of impurities and if its surface area can change to significantly influence GrIS albedo and surface ablation.

Response to Detailed comments

1. p4738 L 7 "excluded in surface mass balance models" : Depending on how you define a surface mass balance, I do not completely agree. For example, Van Angelen et. al. (2012) included a spatially variable background albedo in RACMO which accounts for the spatial variability in surface properties once the snow is gone. Also MAR, for example, allows for ponding water, etc..

   - We will add in that these surface properties, such as ponding water, and snow spatial distributions, are characterized in SMB models. See also our response to reviewer 2 Specific Comment #2.

2. p4738 L20: "are not exclusively a function of darkening from the surface from ice crystal growth": that is absolutely true, but the existent models also do not claim that. See major comments 1-3

   - This particular line does not include a reference to SMB models. However, we hear the reviewers concerns about ensuring accurate representation of the state-of-the art SMB models, and believe that the many revisions to our manuscript described at many places in this response address those concerns satisfactorily.

3. p4739 L22-28: Any idea what the effect of increased roughness on the changes in albedo is?

   - We will add a sentence describing the current understanding about roughness changes, albedo and melting. It reads:

     Not many studies have quantified the effects of surface roughness on bare ice albedo in the ablation zone, besides macroscopic surface features (e.g., Warren et al., 1998; Zhuravleva and Kokhanovsky, 2011). Chandler et al. (2014) indicates that seasonal development of topographical features, as well as the transition from snow to bare ice, can have implications for sensible and latent heat fluxes, yet is rarely

characterized in the ablation zone.

- In the discussion section, we will mention a need to address this in follow up research. It will read:

  Future work should examine the importance of increased surface roughness on changes in albedo.

4. p4740 L7: Add “and crevasses and other types of roughness begin to form” ?

   - We will add ‘crevasses and other types of surface roughness’ as an additional mechanism for lowering surface albedo in the ablation area, as requested.

5. p4740 L24-28: You are perhaps too optimistic about satellite albedo estimates and too hard for the RCM albedo description. This should be more nuanced.

   - We will rewrite this sentence to make it more nuanced. The new sentence reads: *Remotely-sensed and modeled albedo has been validated with ground measurements from dispersed Greenland Climate Network Automatic Weather Stations (GC-Net AWS; Knap and Oerlemans, 1996; Steffen and Box, 2001). These comparisons reveal that MOD10 satellite product provides albedo estimates with an overall RMSE of 0.067 (Stroeve et al., 2006). Early implementations of RCM used constant albedo values for bare ice or very simple schemes, which resulted in very large intra-model differences in runoff (42% Vernon et al., 2013). More recent RCM implementation allow for spatially distributed bare ice albedo that evolve with grain size growth and contamination of black carbon on snow (Van Angelen et al., 2012, Alexander et al . 2014).*

6. p4749 L28: "relatively smooth terrain" I understand what you mean, but this might be confusing for the non-experienced reader. I would change it to "lack of surface roughness in the RCMs"

   - We will change the text to ‘lack of surface roughness in the RCMs’ instead of ‘smooth terrain in the RCMs’ as requested.

7. p4749 L29: Perhaps it is worth to mention the Van Angelen et. al. (2012) already has a spatially variable ice albedo scheme.

   - We will revise the text and mention the existence of ‘a spatially variable ice albedo scheme in RCMs (Van Angelen et al., 2012)’.

8. p4741: L9-29: I think this section, which provides a complete summary of your manuscript is perhaps too long as it reads more as an abstract.

   - We have shortened this paragraph as requested.

9. p4743 L8: “in close proximity”: is close proximity enough when you have only a 1.1m footprint? If there is only close proximity, you are sampling different plots for each transect overpass (and I think you are anyway). Therefore, and given the large fine scale spatial variability (as seen in Fig. 5), you are obtaining transects which are very difficult to compare.

   - We will clarify that we are not aiming to do a point-by-point comparison for the different ASD transect dates. Instead, we are comparing them based on their smoothed spatial patterns (i.e., 50 m bins averages in Fig. 5b) and their overall distributions. We recognize that these are not identical points, but are sufficient to capture the general spatial pattern along the transect given the similarity of our bin-averages.

- We will add a sentence that reads:

  While samples were not taken from exactly the same sites preventing a point-by-point comparison, the transect sample distribution and smoothed spatial patterns can be analyzed for change over time.

- We also revised our calculation of the ASD footprint and found it to be ~0.18 m (see our response to reviewer 2 Specific Comment #10).

10. p4743 L14 "spectra > 1.0" based on the assumption that you have an equal amount of outliers in each side of the mean, you will underestimate the final albedo, because you tend to remove only the postive (>1) outliers. Can you comment on that?

    - We will add the sentences below to comment on the issue raised by the reviewer. Note that while this makes the section longer, it will now appear in the Appendix section. It reads:

      Apparent outliers were identified using the Spectral Analysis and Management System software (SAMs) to identify outliers. Outliers were defined as raw spectra that were significantly different to the other spectra across the entire spectral range (visible and near-infrared wavelengths) taken for the same sample. For June 16, 20 spectra were deemed outliers (total spectra collected = 555); June 19, 17 spectra were deemed outliers (total spectra collected = 560); and June 25, 12 spectra were deemed outliers (total spectra collected = 480). The outliers for these transect dates comprise less than 4% of all spectra collected, and thus, likely had an insignificant impact on the final albedo calculations. On June 17, spectra with unrealistic >1.0 values were collected, as will be shown later all data from this day were considered low-quality and removed from the dataset.

11. p4743 L15: To obtain broadband albedo you should never (!) average over the entire spectral range, but you should apply a weighted average based spectral response curve and the amount of incoming radiation per wavelength. Otherwise you will obtain albedo data that are not comparable to the albedo values derived from broadband sensors (See for example Table 3). Given these large discrepancies (0.1), I also think it is very difficult to interpret the melt rates calculated based on these visible albedo values.

    - We will recalculate broadband albedo as a weighted average based on the spectral response curve as requested. We have described this further in our response to reviewer 2 General Comment #4.

12. p4743 L24-25: Can you give an idea (+ add it to the text) of the amount of observed tilt as it can give an indication of the albedo uncertainty

    - We do not have observed tilt information for the AWSs, however we have calculated reasonable uncertainty ranges caused by tilt and will add them to the manuscript. The calculations are based on the equation given by Van den Broeke et al. (2004), Journal of Atmospheric and Oceanic Technology. The text reads as:

      Based on Fig. 3b in Van den Broeke et al. (2004), a theoretical tilt of 1º on 18 January at Kohnen station, Antarctica (75ºS, 0º) is associated with ~15 W m^{-2} offset in net shortwave at noon local time. This is associated with an absolute error of 5% with a tilt of 1º. Here, we assume double the uncertainty (± 10%) since tilt information was not recorded.

13. p4744 L5: (e.g. Lhermitte, S., Abermann, J., Kinnard, C. (2014). Albedo over rough snow and ice surfaces. The Cryosphere, 8(3), 1069–1086. doi:10.5194/tc-8-1069- 2014 or Warren, S., Brandt, R., Hinton, P. (1998). Effect of surface roughness on bidi- rectional reflectance of Antarctic snow. Journal of Geophysical Research, 103(E11), 25.)

    - We will add the citation on surface roughness effects on snow and ice albedo, as requested.

14. p4744 L16: Although the differences between data sets are logical (I expect higher albedos for 300-1100nm than for the entire SW spectrum), it complicates comparison as the absolute differences between the data sets are almost bigger than the spatial and temporal variability. Therefore, it is important to include a rough correction for the different spectral ranges (e.g. based on a reference spectrum) .

    - We are not aware of any simple conversion from MODIS broadband albedo to the 300-1100 nm range based on the reference spectrum. However, we have calculated the relative weight of the reference spectrum in the 325-1075 nm range (corresponding to the ASD wavelength range), compared to the MODIS range (300–3000 nm), to show that the ASD visible and near-infrared wavelengths are dominating albedo, which suggests that spatial and temporal comparisons are sound. We have added the following to the manuscript to clarify this point:

      Direct comparison of α_{ASD}, α_{MET}, *and* α_{MOD} *are not possible, and* α_{MOD} *is expected to have lower values than the other two datasets. However, relative comparisons of spatial and temporal patterns are reasonable, because the MODIS albedo is dominated by the ASD visible and near-infrared (i.e., 325-1075 nm) wavelengths. In a standard Top-of-Atmosphere solar irradiance reference spectrum, the 325-1075 nm range comprises 80.52% of the total irradiance in the 300-3000 nm range.*

15. p4744 L17: What do you mean by similar results and do you effectively expect that? For example, based on the spectral differences I do expect for the 300-1100nm data a higher albedo for the white ice and a lower albedo for the dark ice compared to the broadband albedo values.

    - We will clarify that we expect to see similar temporal and spatial variability, but not similar absolute values. The new sentence reads:
      The three albedo dataset's different wavelength ranges prevent comparison of absolute values. However, the dominance of reflectance in the ASD visible and near-infrared wavelengths (325-1075 nm) in determining broadband albedo means that temporal and spatial variability can be compared among the three datasets.

16. p4744 L18: Are mean ASD data per MODIS pixel a reasonable assumption? I have my doubts. Firstly, because the MODIS observations have footprints that often are much larger and include data from neighboring pixels (i.e. pixel 2 data in pixel 1 data and vice versa). It is true that the MODIS pixels data are resampled to a fixed grid, but this does not remove the larger footprint effects (See for example Dozier, J., Painter, T. H., Rittger, K., Frew, J. E. (2008). Time-space continuity of daily maps of fractional snow cover and albedo from MODIS. Advances in Water Resources, 31(11), 1515–1526. doi:10.1016/j.advwatres.2008.08.011). So this implies that both pixel 1 and 2 are oftennot that separable and certainly not allow a clear separation of the ASD measurements. This should be discussed.

- As mentioned previously, we are not attempting to conduct a 1:1 comparison between MODIS and ASD albedo data. The intent of the ASD data averaged per MODIS pixel was meant to examine how our data falls within the MODIS seasonal pattern. The authors will address the reviewer here by: 1) clarifying in the manuscript that we are not conducting a comparison of absolute values, and 2) improve the discussion regarding issues of MODIS pixel separability and include a reference to the Dozier et al. (2008) paper.

17. p4745 L3-13: What is the temporal resolution to calculate CC? Every second, minute, 15mins, hourly? And how do you define variability (range? standard deviation?)

    - We will clarify in the manuscript that the temporal resolution is every second. The text reads:

      As a proxy for cloud cover, relative cloud cover, hereafter CC, was calculated every second as the ratio of modeled clear-sky and observed incoming solar radiation similar to Box (1997).

    - We will clarify in the manuscript that variability here refers to the range in CC during transect times.

18. p4745 L6: How do you account for surface albedo values in the Iqbal model as the Clear sky incoming radiation is strongly dependent on the surface albedo (e.g. Sedlar, J., Tjernström, M., Mauritsen, T., Shupe, M. D., Brooks, I. M., Persson, P. O. G., et al. (2010). A transitioning Arctic surface energy budget: the impacts of solar zenith angle, surface albedo and cloud radiative forcing. Climate Dynamics, 37(7-8), 1643–1660. doi:10.1007/s00382-010-0937-5)

    - The Solar Radiance model does not account for surface albedo values. It only solves for incoming radiation, not outgoing radiation (which would then need to account for surface albedo values). The model computes total incoming solar flux through a horizontal surface, zenith declination, solar azimuth, direct beam irradiance on a surface normal to the beam, and the diffuse component on a horizontal surface. As far as we can tell, Sedlar et al's paper shows that net solar radiation is dependent on surface albedo, not incoming solar radiation.

19. p4745 L18-19: 662 and 239: is that average incoming radiation or average variability?

    - We will clarify that these values are the average incoming and outgoing radiation during transect dates.

20. p4746 L3-14: You spend a large amount of text on discussing why you are only using 3 of six transects. I think that is not completely relevant for your story and could therefore be moved to supplementary material.

    - We will follow the reviewer's recommendation to separate the quality control of transect data from the Methods section, and move the quality control assessment and associated figures (i.e., Figures 2-4) of the ASD data to the Appendix section.

21. p4746 L9: "reduced the amount of longwave radiation" I would expect clouds to increase the longwave radiation? Or do you mean longer wavelength SW radiation? Anyway, I think it is best to remove all cloudy ASD observations from your data set.

    - We agree with the reviewer and will revise the sentence to state that cloudy conditions

effectively increase the amount of longwave radiation at the ice surface.

22. p4746 L20-26+Fig.4: I would not draw any conclusion from this figure. First of all, there is no linear relation apparent at all (six points with a ASD albedo of 0.5-0.6 and a highly variable MET albedo + one clear outlier) so any interpretation is not very meaningful. Secondly, how come you have 5 points (base) and 4 points (top) for the ASD data if you only have three useful transects?

    - We have revised Figure 4 to account for a couple of errors, see response to Dr. Pope's ASD Data Collection Comment #5 and reviewer 2 Specific Comment #19. The updated figure exhibits better agreement between α_{ASD} and α_{MET}.

23. p4747 L9: Why do you suddenly restrict your wavelengths to only the 400-700nm range? This makes again any comparison very difficult and would overestimate the albedo differences between white and dirty ice compared to the values of the broad- band albedo. This will cause overestimation in all your later results.

    - We will revise the manuscript to use the 325-1075 nm wavelength range. See more details in response to reviewer 2 General Comment #22.

24. p4747 L11: Which bimodal distribution? This is completely unclear in this part of the text if you haven't read the next parts yet.

    - We will revise the analysis to only incorporate high quality broadband α_{ASD} measurements from the 16, 19, and 25 June transects. α_{ASD} spectra made within 40 m of ablation stakes were individually assessed to classify each surface type into two distinct groupings: clean and dirty ice.

    - We agree with the reviewer that 'bimodal' is not an appropriate description of the histograms. To clarify, we will rewrite the text in the following way:
      At Sites D and E, albedos of white and dirty ice, hereafter $\alpha_{ASD\,DW}$, $\alpha_{ASD\,DD}$, $\alpha_{ASD\,EW}$, *and* $\alpha_{ASD\,ED}$, *were estimated from the histograms of* α_{ASD} *observations made within 40 m of stakes for each transect date. Manual inspection of each of the spectrums at Sites D and E confirm that samples with* $\alpha_{ASD} < 0.4$ *are qualitatively similar to typical spectrum for wet or debris rich ice as shown in Pope and Reese (2014), and distinctly different from* α_{ASD} *above 0.4.*

25. p4747 L18: By taking the 400-700nm albedo data you overestimate the differences in albedo between white and dark snow and you tend to separate the bimodal distribution much more than would occur in reality in the broadband spectrum.

    - We have replaced the 400-700 nm albedo with 325-1075 nm albedo, which will minimize the error pointed out by the reviewer.

26. p4747 L22: I think it is not very realistic to fix *s* to a fixed value as I expect the white ice values to have much higher standard deviations than the darker surfaces due to the non-linearity of albedo decrease to increasing impurity/melt. You also can see this in Figure 8. Moreover, why do take a standard deviation of 0.09, when your observations show much larger standard deviations (e.g. Table 3)

    - We have computed additional standard deviations for each surface type to address the reviewer's comment. We will add in additional standard deviations into our calculation to take into account the expected higher standard deviations associated with the white ice albedo values. The standard deviations will be unique for each

distinct surface type's spectral albedo.

- A standard deviation of 0.09 was selected based on the average standard deviation of all α_{ASD} for each surface type. The standard deviations in Table 3 correspond to all α_{ASD} measurements collected for each transect date, excluding the α_{ASD} measurements associated with distinct surface types. We are removing Table 3 from the manuscript (see response to reviewer 2 Specific Comment #19).

27. p4747 L24-28: I think that using fractions from another study over another year determined over a very small footprint may help to provide a nice thinking exercise, but give very little indication of what is actually happening in reality. Moreover, as you tend to overestimate the differences between, for example, dark and white ice (see previous two comments) I believe your modeled bimodal distribution is overestimating the bimodal distribution observed in reality. Therefore, I would recommend to remove this analysis from the manuscript.

    - We decided to keep the modeled distribution. Prior studies, to our knowledge, have not attempted to model the overall albedo distribution of the ablation area in this way. We believe these computed distributions inform the subsequent interpretation of the MODIS distributions, and may be of value for future ablation area albedo research. Finally, we have corrected the issue the reviewer is raising with overestimating the difference between dark and white ice by replacing visible albedo with broadband albedo.

28. p4747 L10: 463m is indeed the resolution for the zenith observations but the final effective resolution will almost always be different depending each overpass (see also earlier comment)

    - Yes, 463 m spatial resolution assumes that the MODIS pixel data was collected at nadir. We have revised the sentence to read:
      The spatial resolution of the original MOD10A1 data is 463 m at zenith observations (exact resolution varies with overpass time),…

29. p4749 L14: Is it day-to-day variability or are you just sampling different sites? Based on my earlier comment, I tend to believe the latter.

    - We agree with the reviewer, and will rewrite the text to clarify this. The text will read:

      While discrete α_{ASD} observations often differ from the nearest observation made at another transect time due to slight day-to-day changes in sample location (fig. 5a), …

30. p4749 L15 "spatial range? You mean spatial variability?

    - We have corrected the sentence to say 'spatial variability' as requested.

31. p4749 L23 "uneven decline" I understand what you mean, but it is a very confusing way to formulate it.

    - We rephrased the sentence to clarify the meaning. The new sentence will state that the α_{base} and α_{top} follow a 'non-linear decline', as requested.

32. p4749 L26 "inconsistent decline" What is inconsistent about it? It is completely consistent to me. A steady decline + noise + some snowfall events

- We agree that the term 'inconsistent decline' is a poor choice to describe the figure. We will rephrase this sentence in the following way to better describe the figure:
  The MOD10A1 albedo time series declines from June 1st to June 21st. A snowfall event on June 28-29 raised MOD10A1 albedo compared to the June 21st values. July MOD10A1 albedos exhibited some temporal variability, but were generally lower at the end than the start of the month. August MOD10A1 albedo increased from early to late in the month with a snowfall event on 18 August, triggering large increases in albedo values above 0.75.

33. p4745 L3-4: "The general darkening observed in α_{base}". Sorry, but I do not see that general darkening, as it seems to be a darkening followed by a increase in albedo again.

    - We agree that "general darkening" does not describe α_{base} well. We will rewrite the sentence as such:

      High-quality daily average broadband $\alpha_{ASD\ Pixel\ 1}$ and $\alpha_{ASD\ Pixel\ 2}$ data don't exhibit the increase in albedo at the end of June, as seen in the α_{base} and α_{top} data, which may be reflected by differences in footprint sizes. Instead, $\alpha_{ASD\ Pixel\ 1}$ and $\alpha_{ASD\ Pixel\ 2}$ data exhibit a steady decline over the month of June, while $\alpha_{MOD\ Pixel\ 1}$ and $\alpha_{MOD\ Pixel\ 2}$ data remain relatively constant over the same time period.

34. p47450 L4-6: "temporal variability shows general agreement". Sorry, again I do not see that general agreement. α_{MET} decreases followed by an increase, whereas α_{ASD}'s only decline. α_{MODIS}'s seem to be fairly constant over the period when α_{ASD}'s decline.

    - We agree with the reviewer (see also reviewer 1 comment #33 response above), and will rephrase the sentence in the following way:
      Absolute magnitudes among the three ground- and satellite-derived albedo products diverge due to sensor, wavelength range and spatial resolution differences. However, all products have higher albedo values in the first than the last observation in the month of June, prior to the 28-29 June snowfall event.

35. p4750 L13-22: Isn't an overestimation (factor 2) of the difference in melt rates (ob- served difference light-dark=2.31 10 -7m/s, vs. calculated difference light-dark=4.63 10 -7m/s) resulting in an overestimation (factor 2) of the effect of albedo difference on increased melt rates?

    - We will recompute melt rates since the ablation rates were not converted to SI units properly (see response to Dr. Pope's Distribution Discussion Comment #8).

36. p4751 L8: see my earlier comments, but I believe you severely overestimate the bi- modal distribution (e.g. by too high difference between white and dark ice, by underer timating the standard deviation (especially for white ice), etc.)

    - We will recalculate the computed distributions with additional standard deviations for each surface type. See response to reviewer 1 Detailed Comment #26.

37. p4751 L12-17 "darker surfaces progressively populate" Is it dark surface that grow or is it just the (degraded) snow that disappears? Similarly, is the dichotomy not the result of disappearing snow and thus possibly already included in the SMB models?

    - See our previous response to Dr. Pope's Distribution Discussion Comment #8. The darker surface that progressively grows is a result of degraded snow that disappears to expose the impurity-rich ice surface beneath. We will revise the manuscript to explain that disappearing snow plays an important role in governing surface albedo.

- It is our understanding that SMB models consider impurities from dust deposition, but not from melted out sediments (e.g., dark band). We will revise our discussion to make it more nuanced about SMB models and include advances to SMB albedo schemes as described in Alexander et al . (2014) and van Angelen et al. (2012).

38. p4751 18-21: I do think the results in Fig.11 are overestimating the melt rate effects (see my previous comments)
    - We agree with the reviewer and will recalculate the melt rates using broadband albedo instead of visible albedo. We will also clarify that these melt rates were not absolute values, but were modeled in relatively simplistic terms to quantify relative changes in ablation rates related to distinct surface types.
39. p4751-4752 L22-2: Aren't you here also stating that the difference is due to the presence/(dis)appearance of snow? Consequently, it could already be in the SMB models.
    - After careful analysis presented in Dr. Pope's Distribution Discussion Comment #8, we find that the reviewer is correct. In the revised manuscript, we will clarify that at the 100x100 and 150x150 spatial extent, it is likely that the transition from snow to ice may have contributed to this bimodal distribution seen in Fig. 12.
40. p4752 L3-7: If I am correct MOD10A is giving direct beam albedo (i.e. black sky albedo), which is strongly dependent on the solar zenith angle. So how much of that variation would be caused by variations in SZA?
    - From what we understand, the MOD10A1 product provides daily black sky albedo in the absence of modeled or observed aerosol optical depth information (e.g., Stroeve et al., 2013). As such, the MOD10A1 albedo data may be classified as a directional-hemispherical reflectance (DHR) case, different from our ASD albedo data (bi-hemispherical reflectance). As identified in several studies, the accuracy of albedo data retrieved from both satellite and observational systems declines as the SZA increases, particularly beyond ~70 - 75°. However, since we are focusing our analysis on summer months (primarily June to September), SZAs are minimized (e.g., see Box et al., 2012). As such, SZA should not influence the MOD10A1 albedo retrievals used in this study. We will update the manuscript with this information to clarify for the reader.
41. p4752 7-9 + Fig.14: I do think the results in Fig.14 are overestimating the melt rate effects (see my previous comments)
    - We agree and will revise the manuscript accordingly. See similar response to reviewer 1 Detailed Comment #38.
42. p4752 L27 "due to fluctuations in diurnal shortwave fluxes": What do you mean by that? Isn't the unsteady decline driven by small snowfall/redistribution effects, etc?
    - The unsteady decrease in albedo during our field campaign in late June 2013 was linked to fluctuations in daily radiation fluxes, and by extension, a brief cooling period (see figures in response to Dr. Pope's Distribution Discussion Comment #8), disallowing the albedo to decline continuously as we may expect it to otherwise (refer to α_{base} and α_{top} lines in Figure 6). Based on visual assessment in the field, and continuous monitoring of the site, no snow fell in our study area between 8-26 June 2013.
    - We will clarify in the manuscript that the fluctuation in diurnal shortwave fluxes refers to variability in daily incoming and outgoing solar radiation.
43. p4753 L9 I don't agree with these assumptions and I think they tend to overestimate your bimodal distribution (see earlier comments)

- We will add a sentence to clarify that the bimodal distribution is an idealized representation that likely overemphasizes the two modes. It will read:
  Compared to reality, the modeled distribution probably overemphasizes each mode and does not account for darkening of each surface type due to ice crystal growth over the melting season.

44. p4753 L14: "abrupt shifts" Could these shifts not just be the shift from (degraded) snow to ice, or from dry snow to wet snow? And isn't that exactly what Alexander et al. formulate?
    - We will revise the text to clarify that these abrupt shifts are due to snow to ice transitions. See response to earlier comments.
45. p4753 L24-27: "and not solely grain size metamorphism" I do agree, but neither Box or Tedesco, nor any other SMB model, do claim that either. Both Box and Tedesco clearly indicate that the longer exposure of ice and the lower summer snowfall was responsible for the lower albedo values in the ablation zone.
    - We have removed the reference to Box and Tedesco as requested. We have also rewritten the manuscript to emphasize the importance of snow to ice transition in overall albedo.
46. p4753-54 L28-2 I do agree, but as you can see in the figure, the initial drop or the partial snow variability is much more important (albedo variability of 0.2) than the the subsequent decrease due to darkening (albedo variability of maximum 0.1)
    - To address the concern of the reviewer, we will revise the sentence in the following way:
      Consistent with Chandler et al. (2014), the initial drop in ablation zone albedo is likely due to the transition from dry to wet, and patchy snow surfaces. Successive lowering of albedo after snow melt is predominantly due to an increase ice crystal size and possibly also by expansion of darker surface area coverage (e.g., cryoconite holes, accumulation of impurities, and stream organization).
47. p4753 L4:'Substantial' are the differences also equally substantial if you compare to a more realistic reference albedo values of 0.4-0.35 that would be used as a background ice albedo for this region?
    - We will recalculate the computed distributions, using more realistic reference albedo values for bare ice, to reevaluate relative melt rates. Figure 11 will be redone, as discussed in earlier responses, to address reviewer comments. The manuscript will be updated accordingly.
48. p4753 L17 "Previous studies have ..." I do not agree (see earlier comments)
    - This statement will be revised and nuanced, see our response to comments above (see reviewer 1 Detailed Comments #45).

Response to Anonymous Referee #2

Response to General Comments: It is stated in the conclusions that abrupt shifts in albedo can occur as a result of changing dust concentrations. Abrupt shifts primarily occur for MODIS data, and seem more likely to be associated with changes in snow cover, while the observed changes at local sites (which are presumably snow-free) are actually more gradual. The conclusion that abrupt changes in albedo can be associated with sudden changes in impurities does not seem to be supported by the data and should be revised.

- We will revise the text to reflect the reviewer's comment as requested.

1. The authors suggest that "white ice" albedo is greater than 0.6, similar to the albedo of snow (Figs. 8 and 9). Thus the bimodal distribution of albedo over ice may be similar to the bimodal

distribution for areas including both snow and ice. These numbers are higher than the cited range for bare ice (p.4740, line 10) of between 0.3 and 0.6. If the authors are certain that "white ice" is indeed ice and not firn or snow, the observation that ice albedo can be higher than 0.6, and that changes in ice albedo can occur over the course of a season, are important findings of this study and should be emphasized. If there is a possibility that there is snow cover present in the study area, the manuscript should be revised throughout to consider this possibility. In the case of MODIS data, I think that snow likely plays a role in the albedo distributions. The authors should more thoroughly discuss differences in the distributions and changes in the distributions for local data vs. MODIS data.

- We are not going to make this a distinction between white ice or firn. We will remove the term white ice, and refer to this instead as 'high albedo' for clean surfaces and 'low albedo' for dirty surfaces. High albedo appears to be pure ice, free of snow. Low albedo is ice with impurities.
- In the discussion, we will discuss why white ice is likely not firn (it's unlikely to form along the low reaches of the ablation area). We will also address that the likely sources of variability in the 2012 MODIS pentad averages (e.g., related to shifts in meltwater ponding). See additional comments in response to reviewer 1 Major Comment #3.

2. The authors should discuss the discrepancy between the observed distribution along the transect over which ASD measurements were taken, and the bimodal distribution inferred from the surface types of Chandler et al. (2014), which appear to have very different peaks. Figure 1 suggests that the transect passes over relatively bright areas, while the MODIS pixels and the area of Chandler et al. (2014) may cover a wider range of values. Also, it was noted that during sampling with the ASD, streams and cryoconite holes were not sampled, which would seem to reduce the frequency of dark surfaces sampled. The discrepancy should be noted in the results and discussed in the discussion section.

- We will add a text to explain that the modeled bimodal distribution is idealized and can only be compared qualitatively to MODIS distributions. Furthermore, we will explain in the discussion that the transect is under sampling dark surfaces, as requested.

3. The procedure used for calculating broadband albedo values (P. 4743, Lines 14-16) appears to involve simply averaging albedo over a series of spectral intervals, which would assign too much weight to albedo values where incoming solar radiation is small. The best way to calculate broadband albedo would be to integrate incoming and out- going shortwave radiation and divide the total outgoing amount by the total incoming amount. Please recalculate broadband albedo values if possible.

- We will recalculate broadband α_{ASD} as requested. The process will be repeated for individual spectra associated with a known surface type. The process of recalculating broadband α_{ASD} will be included in the Methods section of the ASD appendix.

4. In some cases, the authors use "broadband albedo" and in other cases use "visible" albedo values for a smaller wavelength range. It would seem that broadband albedo would be more indicative of changes in absorbed energy and hence the energy avail- able for melt. The authors should explain why different wavelength ranges are used, use broadband albedo in all cases, or perhaps compare differences in results for "visi- ble" vs. "broadband" albedo if there are substantial differences.

- We will compute broadband α_{ASD} in all cases throughout our analysis (e.g., Figures 5, 7-9,

10-11, and 14; Tables 2 and 4). See above for how we will compute broadband α_{ASD} (reviewer 2 General Comment #4). Depending on these results, we will either use broadband α_{ASD} in all cases or compare differences in results for visible and broadband α_{ASD}, if the differences are substantial.

5. I suggest moving the discussion of melt rates (P. 4750, Line 13 – P. 4751 Line 6, and perhaps Lines 7-11) to a separate section (Section 4.3) that follows the discussion of albedo distributions (Section 4.2). This would allow the manuscript to flow better and would allow the authors to introduce the bimodal distribution of albedo before present- ing results regarding its influence on melting.

    - We will move the text containing the discussion of melt rates to after the discussion of albedo distributions, as requested.

Response to Specific Comments

1. Consider revising "ablation zone" to "ablation area" through- out.

    - We will replace 'ablation zone' with 'ablation area' throughout the entire paper, as requested.

2. P. 4738, Line 7: The statement that the role of distinct surface types on surface albedo is "excluded in surface mass balance models" is not true. The MAR and RACMO models, for instance, account for the presence of bare ice. Perhaps a statement such as "not represented in detail. . ." or "represented in a relatively simple manner" is more accurate.

    - We will add in 'represented in a relatively simplistic manner', as requested.

3. P. 4739, Lines 9-12: The feedback also involves a melt- induced increase in the percentage of the surface covered by bare ice, impurities and meltwater, which further enhances melting. Please include these effects.

    - We will revise the manuscript to mention an increase in debris, meltwater ponding, and bare ice facies as additional effects of the feedback.

4. P. 4739, Lines 15-16: Again, while some processes such as the transport of dust are generally not included in RCMs, some processes, such as the presence of surface water and bare ice are accounted for (though perhaps in a relatively simplistic manner). Please clarify.

    - We will clarify that bare ice and surface water are accounted for, albeit in a relatively simplistic manner, in RCMs (e.g., MAR; Alexander et al. 2014), and some models account for black carbon concentration on snow surfaces (e.g., RACMO2; van Angelen et al. 2012). We will also explain that processes such as dust/sediment accumulation, the distribution of cryoconite holes, and spatial variability in debris-covered ice are generally not included in RCMs.

5. P. 4740, Line 25: Alexander et al. (2014) indicate some discrepancies between MODIS albedo products.

    - We will revise the text to include a statement highlighting the exception to reasonable albedo estimates identified in satellite products, namely the discrepancies between MODIS albedo products, as requested. We will add the reference to Alexander et al. (2014).

6. P. 4740, Line 26: “Physically unrealistic” seems too extreme. The latest version of RACMO (van Angelen et al., 2012) uses (realistic) MODIS background albedo. The schemes employed by MAR account for the presence of bare ice and capture the change in albedo as bare ice is exposed. Please revise.
    - We will revise the text to state that it’s represented in relatively simplistic terms. See response above to reviewer 2 Specific Comment #4.
    - We will reword the text to acknowledge that RACMO uses realistic MODIS background albedo data and that MAR accounts for the presence of bare ice and changes in snow cover.
7. P. 4740, Line 30: The word “poor” suggests that there is something wrong with the schemes used. Perhaps, “relatively simplistic” is more accurate.
    - We will include ‘relatively simplistic’ as requested.
8. P. 4742, Lines 21- 22: Since the foreoptic was used, perhaps it would be better to indicate the field of view with the foreoptic?
    - We will clarify that only a RCR was attached to the ASD. See additional response to Dr. Pope’s ASD Data Collection Comment #3.
9. P. 4742, Line 22: Is the diameter of the spot 1.1m or is the area 1.1m2 ? Please clarify.
    - We have revised the calculation of the spot size after finding an error with the calculation. The new estimate is ~0.18 m. We will explain that the spot size refers to the diameter, as requested.
10. P. 4743, Line 14: Perhaps “albedo spectra” should read “spectral albedo values”?
    - We will correct to ‘spectral albedo values’ as requested.
11. P. 4743, Lines 14-16: As noted in the general comments, the statement “Broadband αASD . . .” is ambiguous. Is broadband albedo calculated by averaging albedo values over each spectral interval provided by the spectrometer.
    - We will recalculate broadband albedo, as requested. See response to reviewer 2 General Comment #4.
12. P. 4744, Line 11: This is a bit unclear. Change “MOD10A1 albedo” to “MOD10A1 albedo for pixels”.
    - We will change it to ‘MOD10A1 albedo for pixels’ as requested.
13. P. 4744, Line 17: Please define “similar results”. For example, results would be expected to be similar for the distribution of albedo values and tem- poral changes in albedo.
    - We will reword this section to provide a better description. See response to reviewer 1 Detailed Comment #15.
14. P. 4745, Lines 10-13: These two sentences probably could be removed as the information seems redundant.
    - We will remove the two sentences to avoid redundancy as requested.
15. P. 4745, Lines 18, 19: Are the “average” values in parenthesis the average range of diurnal variability? Please clarify.
    - We will clarify that in the text as requested.
16. P. 4745, Lines 19-21: Since CC is derived from observed incoming SW, it seems self-evident that they would be well correlated. Perhaps this sentence should be removed. If the authors wish to keep it, the phrase “yet on average, remained low” is unclear and should be revised. Also, since CC is based on a combination of modeled clear-sky SW and observed SW, perhaps this should read

"Derived CC reveals" rather than "CC simulations reveal".

- We kept the sentence to show that the model was able to adequately capture cloud conditions during transect dates. The phrase will be revised for clarification as requested.

17. P. 4745, Lines 26-27: Could hysteresis also result from changing surface conditions over the course of a day?
    - We will revise the text to acknowledge that the hysteresis may also partly be due to changing surface conditions.
18. P. 4745, Lines 20-26: Given the high range of variability that is observed along the transect, the comparison shown in Figure 4 seems unnecessary. It appears that the average αASD over the entire transect is being compared with the albedo at the stations, but this is somewhat unclear. I suggest removing this figure, or alternately comparing station measurements with αASD measurements within a small radius of the weather stations.
    - We will clarify that Figure 4 compares the first and last α_{ASD} measurements for each transect date that is closest to the AWSs. Only α_{ASD} measurements from high quality transect dates were used in the updated figure (see response to Dr. Pope's ASD Data Collection Comment #5).
19. P. 4745, Line 25: Table 3 is only mentioned here in passing. Please provide more discussion of the data shown in Table 3 or alternately, remove it.
    - We will remove Table 3 from the manuscript.
20. P. 4746, Line 1: Here it is stated that Top Met Station measurements are excluded, but it appears that the measurements continue to be mentioned in the results and discussion section. Please clarify.
    - We will exclude the Top Met Station in the revised manuscript except for in Figure 4.
21. P. 4747, Line 10: Why are "visible" albedo values used here while albedo values for the entire spectrum are used in other analyses? See general comment 5.
    - We will recompute our data using broadband α_{ASD} values. See response to reviewer 2 General Comment #5.
22. P. 4747, Line 15: Please provide a few more details regarding how cryoconite hole albedo was parameterized.
    - We will revise the manuscript and better explain how cryoconite holes albedo was parameterized, as requested. The text will be as follows:

      Cryoconite hole albedo, hereafter α_{cryo}, was parameterized using published values of Bøggild et al. (2010). Here, broadband albedos for damp cryoconite material and cryoconite basin surface types under clear-sky and overcast conditions were averaged together to estimate α_{cryo}.
23. P. 4747, Line 25: Perhaps the authors can refer to the figure from Chandler et al. (2014) that shows fractional changes in surface types, for clarity.
    - We will add in the reference to the relevant figure (i.e., Fig. 6 from Chandler et al., 2014) as requested.
24. P. 4749, Lines 2-7: The additional terms (such as net LW radiation and sensible and latent heat fluxes) could be mentioned for clarity.
    - We will add in these terms for clarity as requested.

25. P. 4749, Line 17: Do the authors mean that the station values are "distinctly different" from average αASD?
    - We will clarify in the manuscript that we are referring to the α_{base} and α_{top} values being 'distinctly different' on ASD transect dates. The text will read:
      α_{base} and α_{top} are distinctly different from one another on the three transect dates (Fig. 6), reflecting the surfaces they were installed on.
26. P. 4750, Line 1: Are the values for 28 June and 14 August switched here? It may be better to report the trend over this period as the variability is rather high.
    - Yes, the values appear to be switched, and will be corrected in the manuscript. We will report results as a trend over this period, as requested. See related responses to reviewer 1 Detailed Comments #32 and #33.
27. P. 4750, Line 2-4: This claim can only be made for the month of June. Please clarify.
    - We will clarify that this is for the month of June as requested.
28. P. 4750, Line 23: Mention turbulent heat fluxes in addition to longwave radiation.
    - We will mention turbulent heat fluxes as requested.
29. P. 4750, Lines 23-24: "Relative melt rates between. . ." The calculations capture the fact that melt rates are substantially different, but not the magnitude of the difference between melt rates. Please revise for clarity.
    - We will revise the manuscript as requested. The text will read:
      Regardless of this, relative melt rates between light and dark surfaces are considerably different, and thus useful for investigating seasonal melt rate changes as described next.
30. P. 4750, Lines 26-27: To the contrary, there seems to be a wider range of ablation rates for "dark" rather than "white" ice. Please revise.
    - We will correct to reflect the wider range of ablation rates for dark ice as requested.
31. P. 4751, Lines 1-6: Could it be that sensible heat flux from stream water, which is not accounted for in radiative estimates, can lead to increased melting?
    - We will include this as an additional process that may not have been accounted for in the radiative estimates. The text will be as follows:
      Considerable spread in ablation rates for stream observations could be explained by varying stream depth (Legleiter et al., 2014). The depth of these ice streams determines the attenuation and scattering of radiant energy, thereby influencing the observed albedo measurements. Sensible heat flux from the stream water, not accounted for in radiative estimates, may also be a mechanism for increased melting.
32. P. 4751, Line 9: Clarify that these are computed frequencies for the nearby region of Chandler et al. (2014).
    - We will clarify that these are computed albedo frequencies for a nearby area of Chandler et al. (2014)'s study, as requested.
33. P. 4751, Line 18: As noted in the general comments, please mention differences between the appearance of the distributions for αASD vs. those derived from the data of Chandler et al. (2014).
    - We will mention differences between the appearance of the distributions between the in situ α_{ASD} and Chandler albedo data as requested. See our response to reviewer 2 General Comment #3 and reviewer 1 Detailed Comment #38.
34. P. 4752, Lines 18-20: For the MODIS data this could easily be a result of snow melt exposing impurity rich ice below, since the albedo values for "white ice" and snow are similar. In fact this seems to be a more plausible reason for a sudden shift in albedo.

- Yes, this is a more likely result for the MODIS data. We identified a snowfall event at the end of June that likely contributed to the bimodal distribution seen in Fig. 12. This will be restated to reflect changes associated with our strategy and response to Dr. Pope's Distribution Discussion Comment #8.

35. P. 4753, Lines 2-4: Perhaps note that MODIS albedo (shown in Fig. 6) is observed to decrease nonlinearly, with a smaller rate of change towards the end of the season. Also, since an alternative explanation is provided in the subsequent sentence, "mitigates" should be replaced by "may mitigate". van den Broeke et al. (2011), p. 378, attribute a gradual decline in albedo over the course of a season to the gradual removal of snow patches from the surface. Perhaps this is also a possibility at this location, unless the authors observed no snow patches during the field expedition.
    - The authors will note that the MODIS albedo exhibits a nonlinear decrease over the melt season, with smaller changes in variability near the end of the summer season (as seen in Fig. 6).
    - We will include the possibility of snow patch removal on the ice surface as a contributor to changes in ablation area albedo (although snow was not observed in our study area during the field campaign in June 2013) in the Discussion section. We will revise the text as follows:
      Accumulation of exposed below-surface impurities (Wientjes and Oerlemans, 2010) and the gradual erosion of snow patches in local depressions on the ice surface (van den Broeke et al., 2011) may mitigate the rate of change in ablation area albedo.
36. P. 4753, Line 5: Replace "ground albedo" with "surface albedo" to avoid confusion with the albedo of tundra in proglacial areas.
    - We will replace 'ground albedo' with 'surface albedo' as requested.
37. P. 4753, Lines 17-22: Alexander et al. (2014) also used a lower resolution of 25 km, which may limit the ability to distinguish between dust and ice in some areas. However, the results of this study suggest that "white ice" can have an albedo similar to that of snow, which means that the distribution for ice may be similar to that for areas covered by both snow and ice.
    - We will acknowledge that the different results seen in Alexander et al. (2014) may also be related to the lower resolution of the MAR model.
38. P. 4753, Line 25: Tedesco et al. (2011) and Box et al. (2012) discuss the role of grain size metamorphism at higher elevations, where it may play a role in changing snow albedo. However, both studies indicate that the exposure of bare ice (i.e. a change from light to dark albedo) likely plays an important role in changes in albedo in the ablation zone. What is different about the findings here is that a shift from high to low albedo is observed for areas that are apparently snow-free. Please revise.
    - We will revised this statement to reflect that the transition from high to low albedo was observed as a primary mechanism for lowering albedo in the snow-free, lower reaches of the ablation area.
39. P. 4753, Lines 27-28: For the MODIS data there do seem to be abrupt transitions, perhaps associated with the addition and removal of snow. In the case of the observed and computed albedo distributions, the changes seem more gradual, perhaps in association with impurity changes. Please note these differences.
    - The reviewer is correct, and we will revise and note these differences in the manuscript accordingly. See response to Dr. Pope's Distributed Discussion Comment #8.
40. P. 4754, Lines 7-11: As noted above, the observed abrupt shifts in MODIS distributions may be a result of snow addition or removal rather than changes in impurities, so the statement that changes

in deposition of impurities will likely result in abrupt shifts in albedo seems to be a bit of a stretch.

- We will revise the manuscript to clarify that in the 2013 MODIS albedo distributions, it appears that the bimodal distribution seen is actually from the addition and removal of snow. We will include a new analysis of the 2012 MODIS albedo distributions, which likely cannot be explained by transitions from snow to ice or vice versa. Instead, the 2012 MODIS albedo distributions likely reflect abrupt shifts in ablation zone albedo from the exposure of impurities on the ice surface as well as ice crystal growth and possible expansion of dirty ice areas. See response to Dr. Pope's Distributed Discussion Comment #8. Differences in the observed shifts in the MODIS albedo distributions for 2012 and 2013 melt seasons will be added into the Discussion section of the manuscript.

41. P. 4755, Line 1: "of which these processes. . ." is awkward. Please remove or include in a new sentence.

- We will remove 'of which these processes' as requested.

42. Figure 1: The text within the inset is hard to read. Can the text or inset be made slightly larger? Also, there is no scale bar for the inset.

- We will make the text within the inset and the inset itself larger as requested. A scale bar will be added in the inset into Figure 1 as requested.

43. Figure 1, Caption: Indicate that the yellow boxes show MODIS pixel extents.

- We will indicate in the caption that the yellow boxes show the MODIS pixel extents as requested.

44. Figure 4: As noted above, I suggest removing this figure. If the figure is included or revised, the x and y axes should be adjusted to have the same range, and the graph should be made square so that both axes are scaled equally. The difference in the axes results in the appearance of a weak relationship between the variables, although there is some correlation indicated by the statistics.

- We will keep Figure 4 in the manuscript. It will be updated per reviewer suggestions. See the response to Dr. Pope's ASD Data Collection Comment #5 and reviewer 2 Specific Comment #19.

45. Figure 6: The circles used to indicate individual MODIS measurements don't show up on the legend. If possible please revise the legend.

- We have updated Figure 6 below.

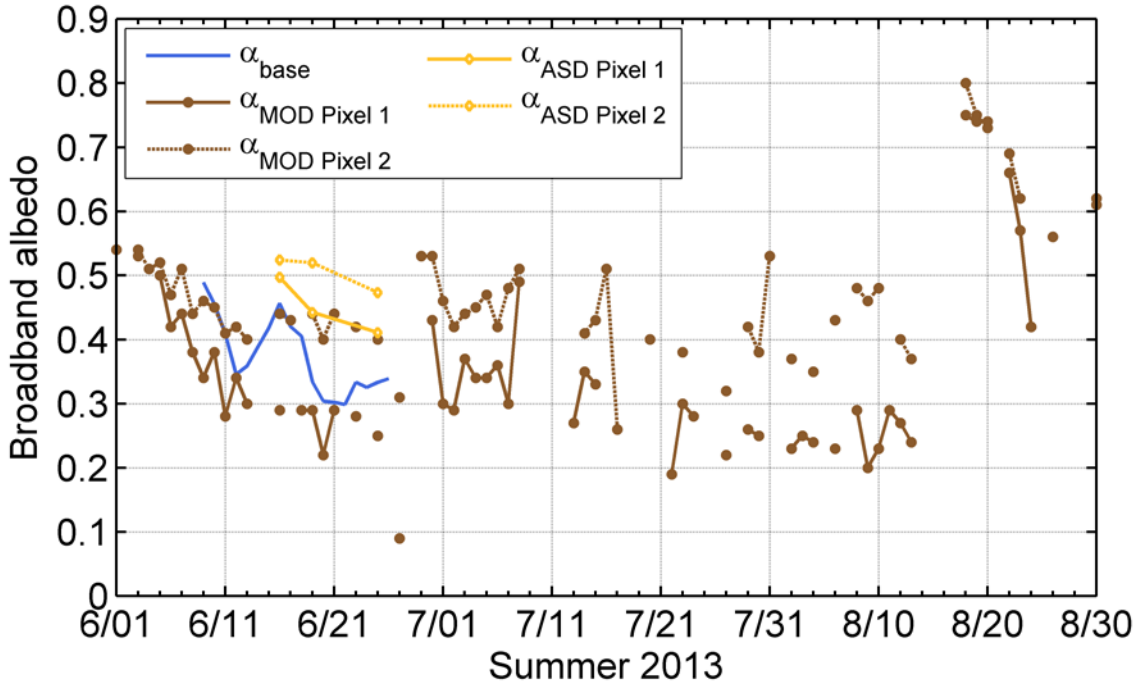

Updated Figure 6. High-quality daily average broadband $\alpha_{ASD\ Pixel\ 1}$ and $\alpha_{ASD\ Pixel\ 2}$, α_{base} (for SZA < 70°), and $\alpha_{MOD\ Pixel\ 1}$ and $\alpha_{MOD\ Pixel\ 2}$ time series for the 2013 melt season. $\alpha_{ASD\ Pixel\ 1}$ and $\alpha_{ASD\ Pixel\ 2}$ pixel-averaged values correspond to high-quality ASD transect dates 16, 19 and 25 June. Note, α_{top} was removed as requested (see reviewer 2 Specific Comment #20).

46. Figure 9, Caption: Mention that the distributions are computed for the site of Chandler et al. (2014)

- We will include that the distributions were computed for a nearby site of Chandler et al. (2014) as requested.

47. Figure 11, Caption: Mention in the caption what the melt rates are relative to.

- We will include in the caption that the melt rates were relative to 'early summer ice (1 Jun)' distribution as requested.

Response to Technical Corrections:

1. P. 4738, Line 13: Change "30 August." to "30 August 2013." for clarity.
   - Changed to include the year as requested.
2. P. 4739, Line 22: Change "Large-scale" to "The large-scale".
   - Included 'the' at the beginning of the sentence as requested.
3. P. 4739, Line 25: Change "lack of" to "a lack of"
   - Added 'a' as requested.
4. P. 4741, Lines 18-19: Suggest changing "surface type's fractional area" to "fractional area

of surface types".

- Switched to 'fractional area of surface types' as requested.

5. P. 4741, Line 22: Change "changing albedo and surface type coverage's impact on" to "impact of changing albedo and surface type coverage on"
   - Changed the sentence to 'impact of changing albedo and surface type coverage on' as requested.
6. P. 4744, Line 24: Change "were" to "was".
   - Changed to singular form as requested.
7. P. 4745, Line 10: "information" can be removed.
   - Removed unnecessary word as requested.
8. P. 4745, Line 26: Fig. 3a is referred to here, but αtop measurements are not provided in Fig. 3a. Please revise.
   - Revised to say that α_{top} measurements are not shown, as requested.
9. P. 4745, Line 4: Should the reference be to Fig. 3a rather than 3b?
   - The reference is to Fig. 3b. Fig. 3a refers only to SZA dependence. The reference to the hysteresis in α_{top} measurements is misplaced and will be removed from the sentence. This statement was intended to highlight that only the Base Met Station CC was presented in Fig. 3b, and relate it back to the hysteresis observed in the albedo observations collected at the Top Met Station. This will be clarified in the manuscript.
10. P. 4748, Line 4: Change "data is" to "data are".
    - Changed to 'data are' as requested.
11. P. 4748, Line 26: Remove "to" from "≥ to".
    - Removed 'to' as requested.
12. P. 4749, Line 15: Change "αASD spatial range" to "The spatial range of αASD".
    - Changed the sentence to 'the spatial range of α_{ASD}' as requested.
13. P. 4749, Line 25: Change "by" to "for".
    - Replaced 'by' with 'for' as requested.
14. P. 4750, Line 6: Change "temporal variability show a general agreement" to "there is a general agreement with regards to temporal variability" or something similar.
    - Switched the sentence to say that 'there is general agreement with regards to temporal variability' as requested.
15. P. 4750, Line 9: Change "within 10 m" to "within a 10 m"
    - Added in 'a' as requested.
16. 16. P. 4752, Line 11: Change "GrIS's" to "GrIS"
    - Changed to singular form as requested.

~~Bimodal~~Multi-modal albedo distributions in the ablation ~~zone~~area of the southwestern Greenland Ice Sheet

S.E. Moustafa[1], A.K. Rennermalm[1], L.C. Smith[2], M.A. Miller[3] ~~and~~, J.R. Mioduszewski[1], L.S. Koenig[4,5,*], M.G. Hom[6,7], and C.A. Shuman[4,8]

[1]{Department of Geography, Rutgers, The State University of New Jersey, 54 Joyce Kilmer Avenue, Piscataway, NJ 08854-8045, USA}

[2]{Department of Geography, University of California, Los Angeles, 1255 Bunche Hall, P. O. Box 951524, Los Angeles, CA 90095-1524, USA}

[3]{Department of Environmental Sciences, Rutgers, The State University of New Jersey, 14 College Farm Rd, New Brunswick, NJ 08901-8551, USA}

[4]{Cryospheric Sciences Laboratory, NASA Goddard Space Flight Center, 8800 Greenbelt Road, Greenbelt, MD, 20771, USA}

[5]{Cooperative Institute for Research in Environmental Sciences, University of Colorado Boulder, 216 UCB, Boulder, CO, 80309, USA}

[6]{Biospheric Sciences Laboratory, NASA Goddard Space Flight Center, 8800 Greenbelt Road, Greenbelt, MD, 20771, USA}

[7]{Science Systems and Applications, Inc., 10210 Greenbelt Rd, Lanham, MD, 20706, USA}

[8]{Joint Center for Earth Systems Technology (JCET), University of Maryland, Baltimore County, 1000 Hilltop Circle, Baltimore, MD, 21250, USA}

Correspondence to: S.E. Moustafa (~~samiah.moustafa@rutgers.edu)~~(samiah.moustafa@rutgers.edu)

*L.S. Koenig is now at National Snow and Ice Data Center, University of Colorado, 1540 30th Ave., Boulder CO 80303, USA

Formatted: Subtitle

Abstract

Formatted: Normal

Surface albedo is a key variable controlling solar radiation absorbed at the Greenland Ice Sheet (GrIS) surface, and thus, meltwater production. Recent decline in surface albedo over the GrIS has been linked to enhanced snow grain metamorphic rates, earlier snowmelt, and amplified ice-albedo feedback from atmospheric warming. However, the importance of distinct surface types on ablation ~~zone~~area albedo and meltwater production is still relatively unknown~~, and excluded in surface mass balance models~~. In this study, we analyze albedo and ablation rates using in situ and remotely-sensed data. Observations include: 1) a new high-quality in situ spectral albedo dataset collected with an Analytical Spectral Devices (ASD) spectroradiometer measuring at 325–1075 nm, along a 1.25 km transect during three days in June 2013; 2) broadband albedo at two automatic weather stations; and 3) daily MODerate Resolution Imaging Spectroradiometer (MODIS) albedo (MOD10A1) between 31 May ~~and~~ 30 August~~.~~ 2012 and 2013. We find that seasonal ablation ~~zone~~area albedos in 2013 have a bimodal distribution, with snow and ice facies characterizing the two ~~alternate states. This suggests that an abrupt switch from high to low albedo can be triggered by a modest melt event, resulting in amplified surface ablation rates.~~peaks. Our results show that ~~such~~ a shift from a distribution dominated by high to low albedos corresponds to an observed melt rate percent difference increase of 51.~~6% during peak melt season~~5% (between 10 – 14 July and 20 – 24 July, 2013). ~~Furthermore,~~ In contrast, melt rate variability caused by albedo changes from pentad-to-pentad before and after this shift was much lower, and varied between ~10-

30% in the melting season. In 2012, a more complex multimodal distribution emerges, reflecting a transition from light to dark-dominated surface, as well as sensitivity to the so called 'dark band' region in southwest Greenland. In addition to a darkening surface from ice crystal growth, our findings demonstrate that seasonal changes in GrIS ablation ~~zone~~area albedo~~ are not exclusively a function of a darkening surface from ice crystal growth, but rather~~ are controlled by changes in the fractional coverage of snow, bare ice, and impurity-rich surface types. ~~As~~ Thus, seasonal variability in ablation area albedo appears to be regulated primarily as a function of bare ice expansion at the expense of snow, surface meltwater ponding, and melting of outcropped ice layers enriched with mineral materials, enabling dust and impurities to accumulate. As climate change continues ~~to warm, regional climate models should consider~~in the Arctic region, understanding the seasonal evolution of ice sheet surface types in Greenland's ablation ~~zone~~area is critical to improve projections of mass loss contributions to sea level rise.

1 Introduction

Surface albedo, defined as the bihemispherical reflectance integrated across the visible and near-infrared wavelengths (Schaepman-Strub et al., 2006), is a key variable controlling Greenland Ice Sheet (GrIS) surface melting~~, is defined as the ratio of reflected to incident solar radiation upon a given surface (Schaepman-Strub et al., 2006).~~. During the melt season, surface albedo modulates absorbed solar radiation at the ice surface, and consequently, the surface energy and mass balance of the ice sheet (Cuffey and Paterson, 2010). Over the last decade, an observed decline in albedo has been linked to less summer snow cover, expansion of bare ice area, and enhanced snow grain metamorphic rates from atmospheric warming~~, and~~ amplified by the melt-albedo feedback (Box et al., 2012; Stroeve et al., 2013; Tedesco et al., 2011). This positive feedback ~~entails snow grain growth owing to melt~~involves increased melting, and exposure of bare ice, impurities and meltwater ponding, reducing surface albedo,

thereby increasing solar radiation absorption, and thus, accelerating melt further (Box et al., 2012; Tedesco et al., 2011).

The GrIS surface has a wide range of surface types with different albedos, including snow, ice, dust and sediment-~~covered ice~~rich impurities, cryoconite holes, melt- ponds, and streams. Yet, the importance of these surface types on ablation ~~zone~~area albedo, and thus, meltwater production over the melt season is still relatively unresolved~~, unquantified, and excluded in surface mass balance (SMB) models~~ (Rennermalm et al., 2013). ~~Understanding~~Current state-of-the-art surface mass balance (SMB) models, such as Modèle Atmosphérique Régionale (MAR) v3.2 and Regional Atmospheric Climate MOdel (RACMO2), consider some variability in surface types by including the presence of meltwater ponding, snow, black carbon concentrations on snow, and bare ice surfaces to characterize seasonal variations in ablation area albedo (Alexander et al., 2014; Van Angelen et al., 2012). Furthermore, RACMO2 is capable of utilizing realistic MODIS background albedo data (Van Angelen et al., 2012), thereby representing the impact of surface types spatially aggregated to the MODIS resolution. However, few studies have utilized these modeling tools to understand how the distribution of surface types ~~on~~are changing ablation ~~zone~~area albedo (e.g., Alexander et al. 2014). This is increasingly important due to enhanced surface melt ~~in 2007-2012~~ associated with anomalously warm atmospheric circulation patterns in 2007-2012 that may become more frequent in the future (Hall et al., 2013; Nghiem et al., 2012; Tedesco et al., 2013~~) as well as~~). Additionally, some studies suggest that a new control of ice sheet albedo is the deposition and accumulation of light-absorbing impurities advected from snow-free areas and forest fires outside of Greenland (Dumont et al., 2014; Keegan et al., 2014).

~~Large~~The large-scale decline in albedo has been greatest in southwest Greenland (-0.04 to -0.16 per decade trend in June and August, respectively; Stroeve et al., 2013). This is related to stronger warming trends (2-4 °C in some regions; Hanna et al., 2014), early melt onset, a lack of wintertime accumulation (van den Broeke et al., 2008), expansion of bare ice

area (Tedesco et al., 2011), high concentration of impurities (cryoconite, dust, and soot), melting of outcropped ice layers enriched with mineral content (Wientjes and Oerlemans, 2010; Wientjes et al., 2011), and enhanced meltwater production and runoff (e.g., Mernild et al., 2012). Seasonal changes in the distribution of different surface types in southwest Greenland's ablation ~~zone~~area have considerable influence on the spatiotemporal variability of surface albedo (Chandler et al., 2014; Knap and Oerlemanns, 1996; Konzelmann and Braithwaite, 1995). During the melt season, surface albedo decreases as cryoconite hole coverage increases (Chandler et al., 2014), melt ponds and supraglacial rivers form efficient drainage networks (Lampkin and VanderBerg, 2013; Kang and Smith, 2013; Smith et al., ~~in review, 2014),~~2015), crevasses and other types of roughness begin to form, and impurities accumulate from exposure of the underlying ice surface (Wientjes and Oerlemans, 2010). Albedo in western Greenland's ablation ~~zone~~area averages around ~0.41 for the duration of the melt season (Wientjes et al., 2011), but can vary between > 0.80 for fresh snow, to 0.30-0.60 for bare ice (Cuffey and Patterson, 2010), and ~0.10 for cryoconite surfaces (Bøggild et al., 2010; Chandler et al., 2014; Knap and Oerlemans, 1996). Furthermore, negative albedo trends since 2000 (Box et al., ~~2012) are linked to a darkening of the ice surface from increased surface coverage of meltwater, cryoconite holes, and impurity rich surface types (Bøggild et al., 2010; Chandler et al., 2014; Wientjes and Oerlemans, 2010).~~ 2012) are linked to an expansion of areas of ablation relative to accumulation facies.

Changes in surface albedo are typically characterized from the MODerate Resolution Imaging Spectroradiometer (MODIS) and the Advanced Very High Resolution Radiometer (AVHRR) satellite sensors (e.g., Chandler et al., 2014; Stroeve et al., 2013; Wang et al., 2012; Wright et al., 2014) or modeled with regional climate models (RCMs) such as Regional Atmospheric Climate Model (RACMO2; Van Meijgaard et al., 2008) and Modèle Atmosphérique Régional (MAR; Fettweis, 2007). Remotely-sensed and modeled albedo has been validated with ground measurements from dispersed Greenland Climate Network Automatic Weather Stations (GC-Net AWS; Knap and Oerlemans, 1996; Steffen and Box, 2001). These comparisons reveal that satellite products provide reasonable albedo estimates

(Box et al., 2012; Stroeve et al., 2005, 2006, 2013), ~~but~~although discrepancies between different MODIS albedo products have been identified (Alexander et al., 2014). Despite this, RCM surface albedos remain ~~physically unrealistic~~represented in relatively simplistic terms, particularly in regions that frequently experience prolonged bare ice ~~regions~~exposure like southwest Greenland (Fettweis et al, 2011; Fitzgerald et al., 2012; Rae et al., 2012; Van Angelen et al., 2012). This is attributed to ~~its relatively smooth terrain~~a lack of surface roughness in the RCMs (Ettema et al., 2010), and ~~poor~~relatively simplistic bare ice and impurity albedo schemes (Alexander et al., 2014), resulting in large inter-model differences in runoff (42% variance; Vernon et al., 2013~~).~~), despite the existence of spatially distributed ice albedo schemes and inclusion of black carbon contaminants on snow surfaces (Van Angelen et al., 2012). Recent ~~ground~~surface albedo observations and snow model simulations of impurity-rich surfaces have been linked to enhanced ice sheet melt (Chandler et al., 2014; Dumont et al., 2014; Keegan et al., ~~suggest~~2014), suggesting that incorporating seasonal changes in the albedo distribution of distinct surface types ~~would~~might improve accuracy of modeled meltwater runoff ~~(Chandler et al., 2014; Dumont et al., 2014; Keegan et al., 2014)~~ and GrIS sea level rise contributions ~~(Rennermalm et al., 2013).~~. These findings point to the importance of a detailed assessment of high spectral, spatial, and temporal resolution albedo data to quantify how different surface types control ablation ~~zone~~area albedo, and therefore, melt.

~~Here, we~~In this study, we report the results of an assessment of ablation area albedo along the southwestern GrIS for the 2012 and 2013 melt seasons. We use 1) a new high-quality in situ spectral albedo dataset collected with an Analytical Spectral Devices (ASD) spectroradiometer measuring at 325–1075 nm, along a 1.25 km transect during three days in June 2013; 2) in situ broadband albedo at two automatic weather stations; and 3) daily MODerate Resolution Imaging Spectroradiometer (MODIS) albedo (MOD10A1) product (Hall et al., 2012) between 31 May – 30 August 2012 and 2013 to investigate how ice sheet surface types influence surface albedo and ~~melting by analyzing a new in situ surface albedo dataset, MODIS albedo, and~~ablation rates; and 4) summer seasonal changes in surface type

coverage reported in literature. ~~High~~First, we describe the collection of high-quality in situ spectral albedo ground, automatic weather station broadband albedo, and ablation stake measurements ~~were~~ collected ~~three times~~ during ~~the~~ early 2013 ~~melting~~melt season along a fixed transect in the GrIS ablation ~~zone. Only a few studies have collected similar measurements in central and northeast Greenland (e.g., Bøggild et al., 2010; Wright et al., 2014). Our albedo transects were compared with continuous surface albedo measurements collected via automatic weather stations situated at each end of the transect, and~~ area. From the MODIS daily albedo ~~(MOD10A1)~~ data~~. Albedos for distinct surface types were identified in the in situ dataset, and were combined with surface type's~~, we estimate seasonal changes in the albedo distributions by using fractional area of surface types from a nearby site (1030 m a.s.l.; reported by Chandler et al., ~~2014) to estimate seasonal changes in the albedo distribution.~~ 2014). These distributions were compared with seasonal changes in computed albedo distributions derived from ~~MOD10A1. Finally, the~~ in situ albedo and ablation stake data. Thirdly, the impact of changing albedo and surface type ~~coverage's impact~~ coverage on surface melt ~~in southwest Greenland's ablation zone~~ was quantified and compared with transect ablation stake measurements~~ installed along the transect. Viewed collectively,~~. Finally, we compare these ~~albedo measurements provide a detailed first assessment of~~results with 2012 MOD10A1 data to better understand the overall frequency distribution, spatiotemporal variability, and ablation rates associated with dominant surface types in southwest Greenland's ablation ~~zone. To the authors' knowledge, the present~~area. This study is the first high spatial, temporal, and spectral resolution albedo dataset collected in the southwestern GrIS ablation ~~zone~~area.

2 Study site description

The study site is located on the southwestern GrIS approximately 30 km northeast of Kangerlussuaq, Greenland (Fig. 1). Albedo measurements were collected along a 1.25 km transect situated between ~510 to 590 m a.s.l., well within the ablation ~~zone~~area for this

region (mean equilibrium line altitude of 1553 m a.s.l.; van de Wal et al., 2012). Two meteorological stations, referred to as Base and Top Met Stations, were installed near the transect end points by Site E and A, respectively (Fig. 1) to derive independent measurements of in situ broadband albedo (300-1100 nm), hereafter α_{base} and α_{top}. In addition, ablation stakes were installed at five sites along the albedo transect and by the Base Met Station to measure ice surface ablation rates. Ice sheet surface types examined included white ice, shallow supraglacial streams, and dirty ice, where dirty ice was qualitatively distinguished from white ice based on visible surface sediments. Visual assessment in the study area revealed that snow had melted before mid-June and no snowfall events occurred between 8-26 June 2013. A few small melt ponds (< 1 km^2) were observed in the study area, but likely not in sufficient quantity to explain discrepancies between in situ and MODIS albedo-derived estimates.

3 Methods

3.1 Field spectroscopy measurements

High spatial (~10 m posting), temporal (1-2 days), and spectral (1 nm) resolution spectral albedo measurements, hereafter α_{ASD}, were measured at 325-1075 nm using an ASD Fieldspec HandHeld 2 Spectroradiometer (PANalytical, formerly ASD Inc.), fitted with a Remote Cosine Receptor (RCR) foreoptic. The ASD was mounted on a tripod at 0.4 m distance, and with no foreoptic attached~~,~~ (i.e., bare fiber), had a 25º field-of-view, corresponding to a spot size of ~~1.1~~0.18 m diameter on the surface.

Spectral albedos were measured along the transect starting at Site E and ending at Site A on 16, 17, 19, 21, 24, and 25 June, 2013 between 1000 and 1800 local time (1200 – 2000 GMT). ~~As will be shown in section 3.4, after rigorous quality control, only transect observations made on the 16, 19, and 25 June were used in analyses.~~ After rigorous quality control (see Appendix A), only transect observations made on the 16, 19, and 25 June were

used in analyses.~~At the start of each transect, the ASD was calibrated to current hemispherical atmospheric conditions by orienting the RCR skyward, along a nadir viewing angle. Subsequent measurements were taken with the ASD rotated 180° to view the ice surface. Under changing sky conditions, the instrument was recalibrated. Each transect consisted of ~100 sample locations, roughly 10 m apart. Despite changing ice conditions rapidly deteriorating temporary location markers, global positioning system (GPS) locations reveal that sample sites in consecutive transects were gathered in close proximity (Fig. 1). Sample sites along the transect were selected based on distance. If a spectrum site intersected with a stream, melt pond, or cryoconite hole, the nearest ice surface was sampled instead. To capture spectral albedo of different ice surface types, separate measurements of streams, dirty ice, and white ice were collected.~~ ~~At each sample location, five consecutive spectra were recorded and averaged. Apparent outliers and physically unrealistic albedo spectra (> 1.0) were removed from the dataset.~~ Broadband α_{ASD} were calculated by averaging albedo over its entire spectral range at each site along the transect. These measurements were compared with MOD10A1 and meteorological station data, as described in section 3.3.

3.2 Continuous broadband albedo measurements at meteorological stations

~~The Top Met Station was installed upon a homogenous white ice surface, and the Base Met Station was installed above a heterogeneous surface of mixed white and dirty ice. Both stations measured solar radiation fluxes every 0.5 h at 300-1100 nm, using S-LIB-M003 silicon pyranometers and a U30 data logger (Table 1; ± 5% or 10 W m^{-2} precision; Onset Computer Corp., 2010) from 8 – 26 June.~~Two AWSs, the Top and Base Met Stations, were installed at each end of the transect to independently measure broadband (300-1100 nm) albedo from 8-26 June 2013, hereafter α_{base} and α_{top}. See Appendix A for details on surface installation conditions and tilt uncertainty estimates. This analysis suggests that α_{top} were compromised by surface roughness effects, and thus, α_{base} alone is used for most analyses.

~~Sensors were attached to a pole drilled into the ice at 1.5 m above the surface, and were kept relatively constant at this height, but occasionally tilted off level. The Top Met station was re-drilled and installed at 0.5 m height after a period of heavy melting.~~

Daily average broadband albedo was computed using shortwave flux measured at SZAs < 70° (Stroeve et al., 2005) to minimize the cosine response error inherent to the pyranometers (uncertainty increases by ± 5% for SZAs > 70°; Onset Computer Corp., 2010). Expected accuracy of α_{base} and α_{top} is ± 10% based on the intrinsic accuracy and cosine response error of the pyranometers. Additional sources of error not quantified here include~~:~~ ~~meteorological station tilt (e.g., van den Broeke et al., 2004),~~ tower shadowing~~,~~ and surface roughness effects on measured surface albedo~~.~~ (e.g., Lhermitte et al., 2014).

3.3 MODIS albedo data

Daily MODIS broadband albedo (300-3000 nm) was acquired from the MOD10A1 product (Version 005) from NASA's Terra satellite (Hall et al., 2006; Klein and Stroeve, 2002). High-quality flagged MOD10A1 albedo data (periods of high SZA and cloudiness were excluded; Schaaf et al., 2011) from 31 May to 30 August 2012 and 2013 (when SZAs are minimized; e.g., Box et al., 2012) were used in two analyses. First, MOD10A1 albedo ~~corresponding to the~~for pixels overlapping with our transect site (Fig. 1), hereafter $\alpha_{MOD\ Pixel\ 1}$ and $\alpha_{MOD\ Pixel\ 2}$, were compared with observations as described ~~in section 3.3.~~below. Second, distributions of MOD10A1 albedo were examined at ~~four~~three spatial extents as described in section 3.~~6~~5.

Broadband $\alpha_{MOD\ Pixel\ 1}$ and $\alpha_{MOD\ Pixel\ 2}$ were compared with α_{ASD}~~, α_{base}~~, and α_{top}~~.~~ ~~Although the three albedo products~~$_{base}$. Direct comparison of α_{ASD}, α_{base}, and α_{MOD} absolute values are ~~calculated over~~ not possible due to different wavelength ranges, and ~~not~~α_{MOD} is expected to ~~match 1:1, they should~~have lower values than the other two datasets. However, relative comparisons of spatial and temporal patterns are reasonable, because the α_{MOD} is

Formatted: Not Superscript/ Subscript

dominated by the ASD visible and near-infrared (i.e., 325-1075 nm) wavelengths. In a standard Top-of-Atmosphere solar irradiance reference spectrum, the 325-1075 nm range comprises 80.52% of the total irradiance in the 300-3000 nm range. The dominance of reflectance in the ASD visible and near-infrared wavelengths in determining broadband albedo means that α_{MOD} can be used qualitatively to provide ~~similar results~~spatiotemporal context. High-quality broadband (325-1075 nm) α_{ASD} data within pixels 1 and 2, hereafter $\alpha_{ASD\ Pixel\ 1}$ and $\alpha_{ASD\ Pixel\ 2}$, were averaged together to indirectly validate $\alpha_{MOD\ Pixel\ 1}$ and $\alpha_{MOD\ Pixel\ 2}$ data, and to facilitate comparison between in situ and remotely-sensed observations. While absolute values will differ between the datasets, and issues of MODIS pixel separability may exist due to off-nadir footprint effects (Dozier et al., 2008), the difference shouldn't change spatial and temporal patterns.

~~3.41.1 Quality control of α_{ASD} data~~

~~To ensure a high-quality α_{ASD} dataset, an impact assessment of variable cloud conditions (i.e., irregular lighting due to transient clouds) and high SZAs during late afternoon albedo transect collections were made. Key et al. (2001) reported a 4-6% increase in albedo, on average, under cloudy conditions. Albedo readings have also been reported as unreliable at SZAs beyond 70°, due to an increase in diffuse radiation reaching the ice surface (Schaaf et al., 2011; Stroeve et al., 2005; Stroeve et al., 2013; Wang et al., 2012).~~

~~As a proxy for cloud cover, relative cloud cover, hereafter CC, was calculated as the ratio of modeled clear-sky and observed incoming solar radiation similar to Box (1997). 'Clear-sky' incoming shortwave fluxes at the surface were calculated with a solar radiance model (Iqbal, 1988). Model inputs of water vapor content, surface pressure, aerosol optical depth at 380 and 500 nm, and ozone optical thickness were estimated from the Kangerlussuaq AEROsol Robotic NETwork (AERONET) station (Holben et al., 2001). SZA was also modeled with the solar radiance model using latitude, longitude, time of day, and day of year~~

information at the Base Met Station. α_{ASD} collected under high CC variability and SZAs approaching extreme angles were subsequently removed. Filtering α_{ASD} data under these criteria ensured the production of a high quality dataset necessary for subsequent analysis.

Cloud cover and radiative conditions varied among transects (Fig. 2). The majority of α_{ASD} measurements were made at small SZAs (~1030-1200 local time), except on 21 and 24 June, when observations were made in late afternoon (1530-1630 and 1640-1750 local time, respectively). Incoming solar radiation fluxes exhibited considerable diurnal variability (average 662 ± 83 W m^{-2}). Outgoing solar radiation displayed similar variability at lower magnitudes (average 239 ± 18 W m^{-2}) during transect dates. CC simulations reveal daily variability in cloud conditions roughly consistent with incoming solar radiation observations, yet on average, remained low (~0.13). Half-hourly α_{base} and α_{top} observations changed linearly with SZA, yet remained fairly stable during transect times (Fig. 3a). Above 80° SZA, half hourly α_{base} and α_{top} variability increased, confirming that 70° SZA was a suitable threshold for daily average albedo calculations. Installation tilt likely contributed locally to "unstable" α_{base} observations at higher SZAs. Similarly, a hysteresis observed in α_{top} observations (Fig. 3a) is attributed to a low installation height (0.5 m). These effects can compromise the accurate representation of illumination and viewing geometries, resulting in reduced albedo estimates at high SZAs (Kuhn, 1974; Wang et al., 2012; Dumont et al., 2012). As such, Top Met Station measurements, and α_{base} at SZAs greater than 70º, were excluded.

High CC variability, instead of consistently high CC, was found to be responsible for saturating α_{ASD} readings on 17, 21, and 24 June (Fig. 3b, only α_{base} shown due to a high hysteresis present in α_{top}). Continuous recalibration of the ASD instrument on 17 and 24 June was inadequate to overcome variable lighting conditions resulting in saturated α_{ASD} readings ($\alpha > 1$). During 21 June, α_{ASD} data did not saturate despite variable sky conditions (0.01-0.52 CC range). Variable cloud conditions on 17, 21, and 24 of June effectively reduced the amount of downwelling longwave radiation relative to shortwave radiation available at the surface, of which, the net effect results in a larger portion of solar radiation available to be

~~reflected by the ice surface (Grenfell and Perovich, 2004; Román et al., 2010; Wang et al., 2012). This can translate to an increase in spectral albedo estimates by ~0.06 over active melting ice surfaces (Grenfell and Perovich, 2004).~~

~~Despite the shortcomings and uncertainties identified in transect radiative and surface conditions, a high-quality albedo dataset was produced. Optimal SZA, CC, and radiative conditions were observed for 16, 19 and 25 June. α_{ASD} data collected on 17, 21, and 24 June were identified as low quality based on their dependence on SZA, CC variability, and issues with albedo saturation, and subsequently removed from further analysis (Fig. 3). High quality α_{ASD} and α_{base} and α_{top} data agree reasonably well (Fig. 4). As much as 40% of α_{ASD} variance is explained by α_{base} and α_{top}, and the linear regression model slope between the two datasets is close to one ($\alpha_{ASD} = 0.77\alpha_{MET} + 0.14$, where α_{MET} and α_{ASD} are X and Y, respectively and α_{MET} is α_{base} and α_{top} combined). The discrepancy is likely due to differences in exact sample locations and instrumentation. Tables 2 and 3 provide summary statistics related to high quality α_{ASD} and transect conditions.~~

Formatted: Indent: First line: 0"

~~3.5~~3.4 Ablation and albedo at dominant surface types

Surface melting between 8 – 26 June was estimated using ablation stakes installed at the Base Met Station, hereafter M_{base}, and at five sites across the albedo transect, hereafter $M_{stakeXY}$, where X denotes Sites A-E, and Y denotes surface type - white ice (W), dirty ice (D), or shallow 5-10 cm deep streams (S) (Fig. 1). Bamboo poles were used as stakes (Hubbard and Glasser, 2005), and ablation rates were recorded every 1-3 days by measuring the distance between the bamboo pole top and ice sheet surface at cm-scale resolution.

α_{ASD} spectra were made within 30 m of ablation stakes to identify representative surface type albedos. With the exception of Site D, all sites were relatively homogenous. At Site D, the two surface types could be classified into distinct groupings: clean and dirty ice. Albedos

of ~~white~~clean ice at Sites A~~, B, and~~ C, and E, hereafter α_{ASD_AW}, α_{ASD_BW}, ~~and~~ α_{ASD_CW}, and α_{ASD_EW}, were estimated by averaging ~~visible (400-700 nm)~~broadband α_{ASD} observations made within ~~10~~30 m of stakes for each transect date. At ~~Sites~~Site D~~ and E~~, albedos of ~~white~~clean and dirty ice, hereafter α_{ASD_DW}~~, α_{ASD_DD}, α_{ASD_EW},~~ and α_{ASD_ED}DD, were estimated from the ~~bimodal distribution~~histograms of α_{ASD} observations made within ~~10~~30 m of stakes for each transect date. At the M_{base} stake, no albedo observations were made. Instead, α_{ASD_DD} is assumed to be representative of albedo at the Base Met Station, hereafter α_{MET_base}. Stream albedo, hereafter α_{stream}, was determined from occasional α_{ASD} measurements at various shallow surface streams between 13-25 June. Cryoconite hole albedo, hereafter α_{cryo}, was parameterized using published values ~~of Bøggild et al. (2010).~~ (from Bøggild et al., 2010) of broadband albedo averaged together for damp cryoconite material and cryoconite basin surface types under clear-sky and overcast conditions.

~~3.6~~3.5 Melt season albedo distributions

Two types of melt season albedo distributions were constructed: 1) computed distributions based on broadband α_{ASD} for distinct surfaces and fractional surface coverage area from Chandler et al. (2014); and 2) observed MODIS-derived distributions.

The computed distributions were constructed by assuming that the albedo distribution for each distinct surface is represented by a normal distribution N($\bar{x}$,s), with $\bar{x} = \overline{\alpha_{ASD}}$ representing surface type and standard deviation, s, ~~fixed to 0.09.~~different for each surface type. Four distributions were constructed: ~~white~~clean ice N(0.~~68~~56, 0.~~09~~07), dirty ice N(0.~~23~~19, 0.~~09~~05), shallow streams N(0.~~26~~23, 0.09), and cryoconite holes N(0.10, 0.~~09~~05). Relative surface coverage of these four dominant surface types was derived at five distinct time periods (1 June, 19 June, 18 July, 28 July, and 5 August) over the 2012 melt season from Chandler et al. (2014; see Fig. 6a-g) to represent transient ice surface conditions, classified here as “early summer ice”, “dirty ice exposure”, “melt”, “darkening ice”, and “late summer

ice", respectively. (Table 3). A composite distribution for each distinct time step was calculated as the weighted mean of surface type distributions, where the weights were determined by their relative surface coverage area. Since Chandler et al. (2014) data is are from 2012, results were not directly comparable with 2013 MOD10A1 data, but should capture melt season evolution.

To validate compare with the computed distributions, high-quality 2012 and 2013 MOD10A1 data were used to construct observed albedo distributions at four three spatial scales (20x20, extents (50x50, 100x100, and 150x150 pixel extents; Fig. 1). The spatial resolution of the original MOD10A1 data is 463 m, at nadir (exact resolution varies with overpass time), corresponding to study areas of 9.3, 23.2, 46.3, and 69.5 km^2 for the four three spatial extents, respectively. Using a kernel smoothing density estimator, the average probability density distribution was computed at 0.01 albedo bin widths (range from 0.05 to 1). The seasonal average albedo distribution was calculated at the four three spatial scales extents, and five-day average albedo distributions and spatial averages were calculated for the 100x100 pixel scale. for 2012 and 2013 MOD10A1 data.

3.6 Identification of snowfall events

To identify possible snowfall events in our study area and MODIS spatial extents, hourly precipitation and air temperature measurements collected by a meteorological station, hereafter 660 Met Station, installed near the ice sheet edge at the proglacial and ice sheet margin interface (Fig. 1), was examined. Near surface air temperature measurements from the shorter Base Met Stations time series (available from 8 – 26 June 2013) were also examined to estimate temperature differences between the proglacial and ice surfaces. To validate that solid precipitation fell, NASA's WorldViewer was utilized to browse daily MODIS reflectance imagery (bands 7-2-1 and 3-6-7) to identify textural and brightness changes related to precipitation events.

Formatted: Indent: First line: 0.4"

3.7 Computation of relative melt rates

~~Relative~~To examine seasonal changes in MODIS albedo, and estimate the importance of distinct surface types, relative surface melt rates were computed using the net shortwave solar radiation equation ~~(assuming net longwave radiation terms are negligible), using~~, observed values of incoming solar radiation from the Base Met Station on 16, 19, and 25 June, and ~~visible~~broadband albedo values for computed and observed distribution methods. Net solar radiation (E_R) varies as a function of incoming solar radiation ($E_S^{\downarrow}$) and albedo (α_s), where units of energy are represented as W m^{-2}:

$$E_R = E_S^{\downarrow}(1 - \alpha_s) \quad (1)$$

~~(Cuffey and Patterson, 2010). Melt rate, defined as the heat needed to melt snow/ice when near-surface temperatures are ≥ to 0 °C, was computed in units of m s^{-1}:~~

Melt rate, defined as the heat needed to melt snow/ice when near-surface temperatures are ≥ 0 °C, was computed in units of m s^{-1} (Cuffey and Patterson, 2010):

$$M = (E_R * \Delta t)\left(L_f * \rho_w\right)^{-1} \quad (2)$$

where Δt is the time interval (s); L_f is latent heat of fusion (3.34 x 10^5 J kg^{-1}); and ρ_w is density of water (1000 kg m^{-3}). Since the meteorological station datasets lack surface energy balance terms (i.e., net longwave radiation, sensible and latent heat fluxes) required to compute the entire energy budget, calculating absolute melt rates was not possible. Instead, the percent difference in estimated melt rates was computed for each distribution relative to the early melt season ablation rates (mean of ~~3.50~~4.40*10^{-7} m s^{-1} for "early summer ice" computed distribution; mean of 2.~~31~~70*10^{-7} m s^{-1} for 31 May – 4 June observed MODIS distribution).

4 Results

4.1 Spatiotemporal patterns in ablation ~~zone~~area albedo

Spatial variability of broadband α_{ASD} along the transect follows a consistent pattern on all three dates, averaging low values (0.~~55~~50 ± 0.~~06~~04) the first ~300 m, followed by increased albedo, reaching a plateau of 0.~~74~~64 ± 0.~~09~~07 at ~600 m, and remaining nearly constant with the exception of a dip to 0.~~48~~44 ± 0.02 at ~900 m (Fig. ~~5a~~2a). While ~~individual~~discrete α_{ASD} ~~sites exhibit high day-to-day variability (Fig. 5a~~observations often differ from the nearest observation made at another transect time due to slight day-to-day changes in sample location (Fig. 2a), data averaged in 50 m bins covary spatially along the transect gradient (Fig. ~~5b). α_{ASD}~~2b). The spatial ~~range~~ variability of broadband α_{ASD} is considerable and varies between a minimum of 0.~~15 (25~~14 (19 June) and a maximum of 0.~~86~~75 (16 June; Table ~~2). α_{base} and α_{top} are distinctly different on the three transect dates (Fig. 6). For instance, on 16 June, daily average albedo ranged from 0.40 to 0.64 (difference of 0.24), while on 25 June ranged from 0.32 to 0.54 (difference of 0.22) at α_{base} and α_{top}, respectively (Table 2).~~1). The high spatial variability in α_{ASD} over short distances is indicative of the heterogeneous surface that characterizes the field site and surrounding ablation ~~zone~~area, not necessarily captured in α_{base} ~~and α_{top}~~-observations.

Formatted: Not Superscript/ Subscript

Temporal variability in daily average α_{base} follows a non-linear decline from 8-26 June 2013 starting at 0.49 and ending at 0.34 (Fig. 3). ~~and α_{top} follows an uneven decline from 8-26 June, with α_{base} consistently ~0.2 lower than α_{top} (Fig. 6). This general decline is observed through the entire melting season by $\alpha_{MOD\ Pixel\ 1}$ and $\alpha_{MOD\ Pixel\ 2}$. The MOD10A1 albedo time series illustrates an inconsistent reduction in albedo of the ice surface, averaging 0.29 on 28 June and 0.43 on 14 August. Fresh snow fell on ~18 August, abruptly increasing MOD10A1 albedo to above 0.75. High quality, pixel-averaged daily broadband $\alpha_{ASD\ Pixel\ 1}$ and $\alpha_{ASD\ Pixel\ 2}$ confirm the general darkening observed in α_{base} and α_{top}; $\alpha_{MOD\ Pixel\ 1}$ and $\alpha_{MOD\ Pixel\ 2}$. While absolute magnitudes among the three ground- and satellite-derived albedo products diverge~~

~~due to sensor and spatial resolution differences, temporal variability show general agreement.~~ An increase in α_{base} of 0.11 between June 12 and 16 might be related to tilt errors, which influenced what part of the increasingly heterogeneous surface the instruments were monitoring. Indeed, the net lowering of α_{base} by 0.15 between 8-26 June is confirmed and observed from June to mid-August for $\alpha_{MOD\ Pixel\ 1}$ and $\alpha_{MOD\ Pixel\ 2}$. $\alpha_{MOD\ Pixel\ 1}$ and $\alpha_{MOD\ Pixel\ 2}$ drop from values slightly above 0.5 in June to 0.24 and 0.37, respectively, around mid-August. In between these dates, sudden increases in albedo could be caused by occasional snowfall events, where the difference in tundra and ice sheet near surface air temperatures is ~3 °C (Fig. 4). A brief snowfall event on 28-29 June (Fig. 4) raised MOD10A1 albedos from 0.31 to 0.53 between 27 June and 30 June, respectively. July MOD10A1 albedos exhibited some temporal variability, but were generally lower at the end than the start of the month. It is unclear if they were triggered by snowfall events. While precipitation events occurred several times on the tundra in July, it is unknown if these events extended to the ice sheet and if temperatures were sufficiently cold to trigger snow rather than rain (Fig. 4). August MOD10A1 albedo increased from early to late in the month with a snowfall event on ~18 August, triggering large increases in albedo to values above 0.75. High-quality daily average broadband $\alpha_{ASD\ Pixel\ 1}$ and $\alpha_{ASD\ Pixel\ 2}$ data don't exhibit the slight increase in α_{base} at the end of June (0.04 from 22-26 June), which may be reflected by differences in footprint sizes, less temporal α_{ASD} sampling frequency, and α_{base} tilt errors. Instead, $\alpha_{ASD\ Pixel\ 1}$ and $\alpha_{ASD\ Pixel\ 2}$ data exhibit a steady decline over the month of June, while $\alpha_{MOD\ Pixel\ 1}$ and $\alpha_{MOD\ Pixel\ 2}$ data remain relatively constant over the same time period. Absolute magnitudes among the three ground- and satellite-derived albedo products diverge due to sensor, wavelength range and spatial resolution differences. However, all products have higher albedo values in the first than the last observation in the month of June, prior to the 28-29 June snowfall event.

Albedos of dirty and ~~white~~clean ice surfaces are distinctly different for each ablation stake site (Table ~~4). This is illustrated by the clear separation between high and low albedo distributions of visible α_{ASD}~~ 2). Broadband α_{ASD} spectra made within ~~10~~30 m ~~radius~~ of

ablation ~~stake sites D and E, where both dirty and white ice surface are observed (~~stakes were individually assessed to classify each surface type into two distinct groupings: clean and ~~Fig. 7). A threshold of 0.5 was used to separate darker and lighter surfaces at Sites D and E (white surfaces included α_{ASD_DW} and α_{ASD_EW}; dark surfaces included α_{ASD_DD}, α_{ASD_ED}, α_{stream}, and α_{cryo}).~~

~~Ablation rates are typically higher for dark surfaces (~~dirty ice ~~and streams) than light surfaces (white ice; Fig. 8). White ice surfaces have higher visible α_{ASD} values (mean of 0.69), corresponding to lower average ablation rates ($5.80*10^{-7}$ m s^{-1}). In contrast, dirty ice and stream surfaces have lower mean visible α_{ASD} values (0.26), corresponding to higher average ablation rates ($7.00*10^{-7}$ m s^{-1}). The observed mean difference between white and dark surface ablation rates is 0.02 m d^{-1}. Melt rate calculations (Eqn. 1 and 2) resulted in higher average ablation rates ($3.50*10^{-7}$ m s^{-1} for white surfaces and $7.00*10^{-7}$ m s^{-1} for dark surfaces, corresponding to a mean difference of $4.63*10^{-7}$ m s^{-1}). Differences between observed and calculated melt rates could be due ablation stake measurement errors and simplification of calculations (e.g., no consideration of longwave radiation). Regardless of this, relative melt rates between light and dark surfaces are captured by the calculations, and thus useful for investigating seasonal melt rate changes as described next.~~

~~The spread in observed white ice visible albedo values results in greater variability in observed ablation rate estimates (~~Fig. ~~8). In contrast, minimal visible albedo variability is observed for dirty ice and stream surfaces. As such, grouping these two ice surface types into a 'darker surface' type classification is justified. Differences in ablation rates for stream surfaces are due to a lack of albedo data. While ablation rates were measured at several ablation stake stream sites, only occasional α_{ASD} measurements were collected over these surfaces. Considerable spread in ablation rates for stream observations could be explained by varying stream depth (Legleiter et al., 2014). The depth of these ice streams determines the attenuation and scattering of radiant energy, thereby influencing the observed albedo measurements.~~ 5). Only Site D had both dirty and clean ice surfaces. Manual inspection of

Formatted: Comment Reference

individual spectra at Site D confirm that samples with $\alpha_{ASD} < 0.4$ are qualitatively similar to typical spectra for wet or debris rich ice as shown in Pope and Reese (2014), and distinctly different from α_{ASD} above 0.4 (Fig. 5).

Formatted: Indent: First line: 0"

4.2 Melt season albedo distributions

Formatted: Heading 3

Formatted: Font: Times New Roman

~~4.2~~4.2.1 2013 computed vs. observed distributions

Computed albedo frequencies using typical albedo values for four distinct surface types (Table 3) and changing area fractions of these surfaces identified at a nearby site by Chandler et al. (2014) reveal a bimodal distribution as the melt season progresses (Fig. ~~9~~6). The relative strength of the first and secondary modes change as the fractional area of darker surfaces expands from "dirty ice exposure" to "melt" distributions and onwards. At the start of the melt season, the abundance of lighter surfaces coincides with a higher probability of high ~~visible~~broadband α_{ASD} values. Here, snow and clean ice surfaces dominate and gradually degrade, exposing the impurity-rich surface underneath. As darker surfaces progressively populate the ablation ~~zone~~area with the onset of the melt season, computed albedo distributions predict a concomitant higher probability of lower albedo. Thus, there is an apparent dichotomy between darker and lighter surfaces 'competing' to control the overall albedo distribution of the ablation ~~zone~~area. A transition towards a ~~left-skewed~~ distribution ~~is likely~~biased towards lower albedo values is due to darker surfaces shifting the overall distribution~~ to lower albedo values~~, and is confirmed by high-quality ~~visible~~broadband α_{ASD} distributions (Fig. ~~10~~7). Relative melt rates increase sharply (by ~~41.8 ± 2~~25.7%) from "dirty ice exposure" to "melt", coinciding with a strengthening of the second, lower mode in the computed albedo distribution (Fig. ~~11).~~ 8). Once the secondary mode is established, a smaller increase in melt rates occurred as the mode strengthens between "melt" to "darkening ice" and finally to "late summer ice" (6.7% and 9.1%, respectively).

Observed MOD10A1 albedo distributions at ~~four~~three spatial extents (Fig. ~~12~~9) reveal that the ~~computed~~ bimodal ~~distribution above~~distributions (cf. Fig. ~~9) is~~6) are manifested in reality~~.~~ at the 100x100 MODIS pixel (px) extent (i.e. 46.3 km^2). While the spatial extent of the MOD10A1 sample influences the seasonal average albedo distribution, two distinct surface types - dark and light surfaces - dominate the seasonal signal (Fig. ~~12~~9). At the smallest spatial ~~scale (20x20~~extent (50x50 px – i.e., ~~9.3~~23.2 km^2), lower albedos from darker surfaces of the lower ablation ~~zone~~area control the density distribution, while at the largest spatial ~~scale~~extent (150x150 px – i.e., 69.5 km^2), the probability distribution is primarily influenced by higher albedos from lighter surfaces (e.g., snow) of the upper ablation area. The central tendencies of each mode are ~0.46 and ~0.72, which is much larger than in the computed distributions (~0.18 and ~0.56; cf. ~~Fig. zone.~~6).

The bimodal distribution identified in the observed 100x100 px MODIS albedo distribution in 2013 (Fig. 9) is the result of snow and ice surfaces characterizing the two peaks, as each mode centers around typical values of snow and clean ice, respectively. As such, the observed MODIS bimodal distribution is associated with a transition from ice to snow, rather than a change from clean to dirty ice, which caused the two modes in the computed distribution (Fig. 6). Indeed, analysis of 2013 meteorological observations reveal that short term snowfall events that fell on top of the underlying ice can result in variations in ablation area albedo (Fig. 3 and 10). In 2013, the bimodal distribution at the 100x100 px spatial extent is likely the result of snow deposition or redistribution of blowing snow on top of the ice surface (Fig. 9 and 10).

MOD10A1 albedo at the 100x100 px (i.e., 46.3 km^2) spatial ~~scale~~extent, transitions from a ~~high,~~ unimodal distribution with high albedo values at the start of the melt season (31 May – 4 June), to a bimodal-like distribution with intermediate albedo values at mid-melt season (20 – 24 June), and shifts abruptly to a new, ~~low~~ unimodal distribution with low albedo values at peak melt season (30 July – 3 August; Fig. ~~13).~~ 10). By assuming an unchanged radiation budget, the relative impact of albedo distribution changes on melt rates

Formatted: Comment Reference

Formatted: Comment Reference

was quantified. The abrupt shift from a lighter- (high albedo) to darker-dominated (low albedo) surface corresponds to an observed melt rate percent difference increase of 51.~~6~~5% between 10 – 14 July and 20 – 24 July pentad average albedo distributions (Fig. ~~14). —~~14). Before and after this shift, melt rates changed much less from pentad-to-pentad, ranging between ~10-30%, with the exception of the dramatic drop of 103.3% when the melt season ends in late August.

The bimodality seen in the 30 June – 4 July pentad (Fig. 10) coincides to a brief period of higher MODIS albedo values (~0.6 – 0.7), indicative of snow. Identification of a snowfall event on 28-29 June 2013 (Fig. 4), confirms the source of the bimodal distribution observed in the 30 June – 4 July pentad (Fig. 10), corresponding to a brief "jump" in the probability density distribution to higher albedos.

4.2.2 Differences between 2012 vs. 2013 observed albedo distributions

While the 2013 MODIS albedo bimodal distribution shown in Fig. 9 and 10 are a result of snow and ice albedo, analysis of MODIS 2012 data reveal a more complex, multi-modal albedo distribution (Fig 15). These distributions cannot be explained by the presence or absence of snow and ice alone. The 2012 MODIS is characterized by generally lower albedo, with six out of nine pentad albedo distributions ranging mostly between 0.2 and 0.5, compared to three out of nine pentad albedo distributions in 2013 (cf. Fig. 10 and 11). These low albedos are confirmed by the average seasonal MODIS 2012 albedo distributions, where a higher probability of albedos are centered on ~0.35, compared to two peaks at ~0.45 and ~0.7, in 2013 at the 100x100 px spatial extent (cf. Fig 12 and 16). The higher probability of these very low albedos observed in 2012 are likely due to dust, sediment, and impurity-rich ice in the so-called 'dark-band' region (Wientjes and Oerlemans, 2010). The identification of this dark zone feature is presented in section 4.2.3.

4.2.3 2012 vs. 2013 spatial maps

The presence of the dark band region is confirmed by the diagonal band of very low albedo (< ~0.35) in the 2012 MODIS seasonal average at the 100x100 px extent (Fig. 12). However, the presence of the dark band region is not visible in 2013, where albedo gradually increases from west to east (Fig. 13). The lack of the dark zone feature in 2013 is likely due to snow covering the dark band for most of the season. Overall, 2012 exhibits substantially lower ablation area albedos (Fig. 11), while 2013 reveals higher ablation area albedos in the MODIS spatial averages (Fig. 10). The large inter- and intra-annual variability in MODIS ablation area albedo may be indicative of the large spatial variability in surface types that characterize the lower elevations of the ablation area. Alternatively, a larger distribution in cryoconite hole coverage may have also contributed to low albedos (~0.25) observed in the 2012 MODIS seasonal averages (Fig. 15).

4.3 Relative melt rates

Observed ablation rates, derived from stake readings, are typically higher for dark surfaces (dirty ice and streams) than light surfaces (clean ice; Fig. 16). Clean ice surfaces have higher broadband α_{ASD} values (mean of 0.57), corresponding to lower average ablation rates ($5.38*10^{-7}$ m s^{-1}). In contrast, dirty ice and stream surfaces have lower mean broadband α_{ASD} values (0.24), corresponding to higher average ablation rates ($6.75*10^{-7}$ m s^{-1}). The observed mean difference between light and dark surface ablation rates is $1.37*10^{-7}$ m s^{-1}. Melt rate calculations (Eqn. 1 and 2) resulted in a lower average ablation rate for clean ice surfaces ($4.24*10^{-7}$ m s^{-1}) and a higher average ablation rate for dark ice surfaces ($7.56*10^{-7}$ m s^{-1}), corresponding to a mean difference of $3.33*10^{-7}$ m s^{-1}. Differences between observed and calculated melt rates could be due ablation stake measurement errors and simplification of calculations (e.g., no consideration of longwave radiation or turbulent heat fluxes).

Regardless, in both cases relative melt rates between light and dark surfaces are considerably different, and thus useful for investigating seasonal melt rate changes as described next.

The spread in observed clean ice broadband albedo values results in greater variability in observed ablation rate estimates (Fig. 16). In contrast, minimal broadband albedo variability is observed for dirty ice and stream surfaces. As such, grouping these two ice surface types into a 'darker surface' type classification is justified. Few dirty ice albedo measurements were sampled as compared to clean ice surfaces. Differences in ablation rates for stream surfaces are due to a lack of albedo data. While ablation rates were measured at several ablation stake stream sites, only occasional α_{ASD} measurements were collected over these surfaces. Considerable spread in ablation rates for stream observations could be explained by varying stream depth (Legleiter et al., 2014). The depth of these ice streams determines the attenuation and scattering of radiant energy, thereby influencing the observed albedo measurements. Sensible heat flux from the stream water, not accounted for in radiative estimates, may also be a mechanism for increased melting.

Formatted: Tab stops: 1.42", Left

5 Discussion

5.1 ~~GrIS's~~ The importance of surface types on observed and computed ablation ~~zone~~area albedo

GrIS ablation area albedos are strongly influenced by the presence or absence of impurity-rich debris on its surface. ~~White~~Clean ice and dust-covered, dirty ice have distinctly different albedos, resulting in a left-skewed albedo distribution at ~~the~~mid- and end of June~~. This suggests that an abrupt switch from high to low albedo can be triggered by a modest melt event, resulting in amplified melt rates.~~ (Fig. 7). This pattern is supported by computed and remotely-sensed albedo distributions, revealing that a ~~bimodal~~multimodal distribution develops seasonally~~, with two alternate states.~~. A modest melt or snowfall event can trigger a sudden switch from a high to low albedo mode~~, resulting in augmented~~ or vice versa,

drastically changing ablation rates. These findings suggest that a shift in dominant surface type from ~~white~~snow to bare ice, and clean ice to impurity-rich ~~ice~~ surfaces is an important driver in abruptly increasing seasonal ice sheet melt rates.

The first quality-controlled in situ ablation ~~zone~~area albedo dataset collected along a 1.25 km transect during three days in June 2013 is presented. Albedo data collected during in situ transect dates resemble an early summer ice surface classified in Chandler et al. (2014) and Knap and Oerlemans (1996; Fig. 6). Here, remaining snow cover and superimposed ice gradually melts, revealing underlying impurities and ~~last ablation season's~~ cryoconite holes. Visual assessment and continuous monitoring in the field revealed that the ice surface along the transect was snow-free from 8-26 June 2013. This period corresponds to ~~an unsteady~~a non-linear decrease in albedo (Fig. ~~6) primarily due to fluctuations in diurnal shortwave fluxes, which is responsible for~~3). Accumulation of exposed below-surface impurities (Wientjes and Oerlemans, 2010), the gradual erosion of snow patches in local depressions on the ice surface (van den Broeke et al., 2011), as well as the activation and development of ~~an efficient surface meltwater routing~~the hydrologic system~~,~~ and ~~increase in~~ cryoconite hole coverage (Chandler et al., 2014~~). Accumulation of exposed below surface impurities (Wientjes and Oerlemans, 2010) mitigates~~) may mitigate the rate of change in ablation ~~zone~~area albedo. Turbulent sensible heat fluxes from adjacent pro-glacial areas ~~may function as~~provide an ~~alternative~~additional explanation for the non-linear decline in ground albedo measurements, serving to limit the melt-albedo feedback's influence (van den Broeke et al., 2011).

~~An increase in debris rich and stream surfaces over the melting season (Fig. 9) is likely responsible for the left-skewed distribution identified in the observed α_{ASD} distribution (Fig. 10).~~ Under the assumptions that distinct surface types follow a normal distribution, a bimodal probability distribution preferentially develops as ablation ~~zone~~area albedo decreases rapidly over the melt season due to development of an efficient meltwater drainage system, increase in cryoconite hole coverage, and accumulation of debris-rich

sediments (Fig. 6). An increase in debris-rich and stream surfaces over the melting season (Fig. ~~9).~~6) is likely responsible for the enhanced frequency of low albedo values identified in the observed α_{ASD} distribution from 16-25 June (Fig. 7). However, the observed changes at transect sites appear to be more gradual than for the MODIS data (Fig. 10 and 15). This may be due to a lack of snow cover influencing the local albedo distribution and a lower temporal sampling frequency. The lack of a pronounced secondary mode with lower albedo values in the observed left-skewed distributions (Fig. 7) compared to the modeled bimodal distribution (Fig. 6) may be related to different melt season conditions (2012 vs. 2013), and corresponding range of surface types captured along the transect, which undersamples dark surfaces (e.g., dirty ice and stream surfaces; Fig. 5). While, Chandler et al. (2014) surface types cover a wider range of surface types, and thus, albedos.

Compared to reality, the computed distribution (Fig. 6) probably overemphasizes each mode and does not account for darkening due to ice crystal growth over the melting season. The observed albedo distributions reveal abrupt and variable shifts in the seasonal albedo distribution (Fig. ~~13~~10 and 11). At certain spatial ~~scales~~extents, these albedo distributions transition from a high- to low-dominated mode (Fig. ~~12~~9), enabling enhanced melt rates (Fig. ~~11~~8 and 14). Alexander et al. (2014) also observed bimodal albedo distributions for Greenland's ablation ~~zone~~area by analyzing MAR and MODIS products between 2000-2013. ~~In contrast to this study,~~ Alexander et. al. (2014) attributes the dominant modes to the presence of snow and ice (and firn). This is in agreement with the analysis of the 2013 conditions, but disagrees with 2012 conditions. This discrepancy could be due to the larger study area ~~in Alexander et al. (2014), which may include~~that includes areas unaffected by dust from deposition and outcropped ice layers~~.~~, and a thirteen-year averaging period suppressing outlier years like 2012 used in Alexander et al. (2014).

The bimodal albedo distribution and shift from a higher to a lower albedo mode centering at values below 0.4 (Fig. ~~9~~6, 10, and ~~13~~11) indicate that a switch in dominant surface type (i.e., from light to dark) during the melt season, and not solely grain size

Formatted: Indent: First line: 0.49"

metamorphism, ~~as suggested in Box et al. (2012) and Tedesco et al. (2011),~~ are largely responsible for lowering albedo in snow-free ablation ~~zone albedo~~areas. Furthermore, results from the MODIS data (Fig. 10 and 11) suggest that a transition from a light- to dark-dominated surface is abrupt rather than gradual~~.~~, likely associated with the addition and removal of snow. The transition is more gradual in the left-skewed observed (Fig. 7) and computed albedo distributions (Fig. 6), likely reflecting changes in impurity content and different time stamps. Consistent with Chandler et al. (2014), the initial drop in MODIS ablation ~~zone~~area albedo is likely due to the transition from dry to wet, and patchy snow surfaces~~, while successive~~. Successive lowering of albedo after snow melt is predominantly due to an increase ~~in~~ice crystal size and possibly also by expansion of darker surface area coverage (e.g., cryoconite holes, accumulation of impurities, and stream organization~~), where the darker, lower albedo surface mode dominates.~~) and melting of dust-enriched ice layers. These distributions correspond to percent differences (e.g., 51.5% between 10 – 14 July and 20 – 24 July pentads) in melt rate estimates that are substantial over the melt season (Fig. ~~11~~8 and 14), and highlight the importance of considering the albedo of ablation ~~zone~~area surface types. The higher melt rates associated with darker surfaces (Fig. 16) may lead to lighter surfaces becoming topographically prominent. In theory, this should enhance sensible heat transfer to the lighter surfaces, increasing their ablation. Future studies should consider quantifying the effects of surface roughness on ablation area albedo (e.g., Warren et al., 1998; Zhuravleva and Kokhanovsky, 2011), and the possibility of enhanced ablation of light surfaces following upon adjacent, dark surface ablation.

~~Plausible~~Recent studies have proposed scenarios of future atmospheric warming, where excess deposition of light-absorbing impurities (Dumont et al., 2014) and black carbon from increased forest fire frequency or incomplete fuel combustion (Keegan et al., 2014), will ~~likely result in earlier and abrupt shifts in ablation zone albedo's distribution~~promote accumulation of impurities, contributing to amplified surface melting~~, and thus, enhanced mass loss. These~~. If these findings turn out to be true, these effects will likely be exacerbated in southwest Greenland's ablation ~~zone~~area, where continued negative albedo trends (Stroeve

et al., 2013), and increasingly warmer average summer temperatures (Keegan et al., 2014), in conjunction with bare ice, light-absorbing impurities, and cryoconite holes, are expected to dominate.

5.2 Insights from 2012 and 2013 melt seasons' albedo distributions

The spatial distribution of snow cover and background bare ice albedo is important for understanding temporal changes in 2012 and 2013 MODIS albedo distributions (Fig. 12 and 13). Compared to 2013, snow melt in 2012 was more pronounced and reached higher elevations (Tedesco et al., 2014), allowing the dark band feature to be exposed, resulting in a lower seasonal albedo mode (Fig. 15).

The large albedo distribution changes from one MODIS pentad to another in 2012 (Fig. 11) is likely due to variability in meltwater ponding on the ice surface, and perhaps deposition of wind-blown dust from tundra regions, and not necessarily increases in melted-out debris from internal ice layers at such short timescales. However, exposure of dust and sediment-rich ice surfaces probably caused the high probability of considerably low 2012 MODIS albedo values relative to 2013. This is expected since it was identified as an extreme melt year with early onset snow melt (e.g., Nghiem et al., 2012; Tedesco et al., 2013; Fig. 11 and 15), while 2013 was a normal melt-year in the 1979-2013 context (Tedesco et al., 2014). Given the coarse resolution of the MODIS pixel, it is likely that it averages out finer scale details of distinct surface types (e.g., dirty ice and cryoconite hole surfaces) along the ice sheet edge. It is hypothesized that higher spatial resolution satellite imagery may be able to capture such regions closer to the ice sheet margin. We postulate that the area of these regions may grow in size over the melting season as demonstrated on local scales by Chandler et al. (2014) in situ observations.

The bimodal distribution observed in the 2013 MODIS data (Fig. 6) appears to be governed by the relative extent of clean ice and snow surfaces. This aligns with findings from

current SMB models, as the majority of variability in the overall Greenland ablation area albedo is driven by the deposition, change, and removal of snow (Alexander et al., 2014; Van Angelen et al., 2012). However, 2012 MODIS albedo distributions cannot be explained by transitions from snow to ice and vice versa. Instead, the 2012 MODIS albedo distributions likely reflect abrupt shifts in ablation area albedo from the exposure of impurities on the ice surface in the so-called "dark-band" region as well as ice crystal growth and expansion of dirty ice areas, even with the presence of a few snowfall events. As such, dust and impurities on Greenland's ice sheet surface can influence surface albedo in the ablation area. The current state of SMB models are capable of simulating albedo as a function of meltwater ponding (Alexander et al., 2014) and impurities from atmospheric dust deposition on snow (Van Angelen et al., 2012). The models might be improved by incorporating the melting out of dust and sediments in outcropped ice layers, found in the dark band region.

6 Conclusions

A first high-quality in situ spectral albedo dataset collected along a fixed transect is presented for southwest Greenland's ablation ~~zone~~area. Previous studies have attributed an increase in melt season duration, less snowfall accumulation, enhanced snow grain metamorphism rates and ice-albedo feedback as primary mechanisms for lowering ablation ~~zone albedo; however, these~~ area albedo. Here, we demonstrate an additional control on albedo in the ablation area, namely the distribution of distinct surface types such as snow, clean ice, impurity-rich ice, melt ponds and streams, and also examine their modulation on surface ablation. The spatial extent of each of these surface types result in a multi-modal albedo distributions in the ablation area. Analysis of MODIS data suggest that a ~~bimodal~~multi-modal distribution and consequentially, ~~an abrupt~~a shift from light to dark-dominated surfaces, and sensitivity to melting of outcropped ice layers, characterize seasonal changes in Greenland's ablation ~~zone~~area, and therefore, melt rates. ~~This research provides a new understanding of ablation zone albedo distributions of distinct surface types, and their modulation of surface ablation.~~

Continued atmospheric warming coinciding with a darkening ice surface will ~~alter the distribution of dominant surface types in Greenland's ablation zone. A shift in Greenland's ablation zone albedo distribution, and addition of impurities to its surface, will amplify surface melt and thus, mass loss, of which these processes are not currently realized in SMB models. Future modeling efforts should consider incorporating the effects and evolution of dominant surface types on ablation zone albedo for improved simulation of surface melting and runoff from the southwestern GrIS ablation zone.~~increase the ice sheet surface meltwater production and runoff. Here, we show the importance of the distribution of dirty ice surfaces, which are likely the result of accumulation of impurities melted out from internal ice layers rather than contemporary deposition of atmospherically transported dust. Future research should investigate the importance of surface accumulation of impurities and if its surface area can change to significantly influence GrIS albedo and surface ablation. Finer spatial resolution satellite imagery is needed to adequately characterize the high spatial variability in surface types and their corresponding albedo in the ablation area of the GrIS. Analysis of spatio-temporal variability in albedo using higher spatial resolution imagery may be needed to adequately characterize surface types, particularly for dust and sediment-rich surfaces, to improve our understanding of ablation area albedos' contribution to GrIS mass loss.

Acknowledgements

S.E. Moustafa, A.K. Rennermalm, L.C. Smith and J.R. Mioduszewski were funded by NASA grant NNX11AQ38G~~.~~ and NNX14AH93G. S.E. Moustafa was also funded by NASA Earth and Space Science Fellowship Program NNX12AN98H. Additional funding was provided by Rutgers University Faculty Research Grant. The authors would like to thank ~~Dr. L~~Drs. A. Pope and M.S. ~~Koenig~~Pelto as well as two anonymous reviewers for valuable feedback and commentary.

Formatted: Font color: Auto

Formatted: Font color: Auto

References

Alexander, P. M., Tedesco, M., Fettweis, X., van de Wal, R. S. W., Smeets, C. J. P. P. and van den Broeke, M. R.: Assessing spatio-temporal variability and trends (2000–2013) of modelled and measured Greenland ice sheet albedo, The Cryosphere Discuss., 8(4), 3733–3783, doi:10.5194/tcd-8-3733-2014, 2014.

Van Angelen, J. H., Lenaerts, J. T. M., Lhermitte, S., Fettweis, X., Kuipers Munneke, P., van den Broeke, M. R., van Meijgaard, E. and Smeets, C. J. P. P.: Sensitivity of Greenland Ice Sheet surface mass balance to surface albedo parameterization: a study with a regional climate model, The Cryosphere, 6, 1175–1186, doi:10.5194/tc-6-1175-2012, 2012.

Bøggild, C. E., Brandt, R. E., Brown, K. J. and Warren, S. G.: The ablation zone in northeast Greenland: ice types, albedos and impurities, J. Glaciol., 56(195), 101–113, doi:10.3189/002214310791190776, 2010.

Box, J. E., Fettweis, X., Stroeve, J. C., Tedesco, M., Hall, D. K., and Steffen, K.: Greenland ice sheet albedo feedback: thermodynamics and atmospheric drivers, The Cryosphere, 6, 821-839, doi:10.5194/tc-6-821-2012, 2012.

Van den Broeke, M., van As, D., Reijmer, C. and van de Wal, R.: Assessing and Improving the Quality of Unattended Radiation Observations in Antarctica, J. Atmos. Ocean. Technol., 21(9), 1417–1431, doi:10.1175/1520-0426(2004)021<1417:AAITQO>2.0.CO;2, 2004.

Van den Broeke, M., Smeets, P., Ettema, J., van der Veen, C., van de Wal, R., and Oerlemans, J.: Partitioning of melt energy and meltwater fluxes in the ablation zone of the west Greenland ice sheet, The Cryosphere, 2, 179-189, doi:10.5194/tc-2-179-2008, 2008.

Van den Broeke, M., van de Wal, R. and Smeets, P.: The seasonal cycle and interannual variability of surface energy balance and melt in the ablation zone of the west Greenland ice sheet, The Cryosphere, 5, 377-390, doi:10.5194/tc-5-377-2011, 2011.

Chandler, D. M., Alcock, J. D., Wadham, J. L., Mackie, S. L. and Telling, J.: Seasonal changes of ice surface characteristics and productivity in the ablation zone of the Greenland Ice Sheet, The Cryosphere Discuss., 8, 1337–1382, doi:10.5194/tcd-8-1337-2014, 2014.

Cuffey, K. and Paterson,W. S. B.: The Physics of Glaciers, 4th Edn., Elsevier Inc., Burlington and Oxford, 2010.

Dumont, M., Brun, E., Picard, G., Michou, M., Libois, Q., Petit, J., Geyer, M., Morin, S. and Josse, B.: Contribution of light-absorbing impurities in snow to Greenland's darkening since 2009, Nat. Geosci., 7(7), 509–512, doi:10.1038/ngeo2180, 2014.

Dumont, M., Gardelle, J., Sirguey, P., Guillot, a., Six, D., Rabatel, a. and Arnaud, Y.: Linking glacier annual mass balance and glacier albedo retrieved from MODIS data, The Cryosphere, 6, 1527–1539, doi:10.5194/tc-6-1527-2012, 2012.

Ettema, J., van den Broeke, M. R., van Meijgaard, E., van de Berg, W. J., Box, J. E. and Steffen, K.: Climate of the Greenland ice sheet using a high-resolution climate model – Part 1: Evaluation, The Cryosphere, 4, 511–527, doi:10.5194/tc-4-511-2010, 2010.

Fettweis, X.: Reconstruction of the 1979–2006 Greenland ice sheet surface mass balance using the regional climate model MAR, The Cryosphere, 1, 21–40, doi:10.5194/tcd-1-123-2007, 2007.

Fettweis, X., Tedesco, M., van den Broeke, M., and Ettema, J.: Melting trends over the Greenland ice sheet (1958–2009) from spaceborne microwave data and regional climate models, The Cryosphere, 5, 359-375, doi:10.5194/tc-5-359-2011, 2011.

Fitzgerald, P. W., Bamber, J. L., Ridley, J. K. and Rougier, J. C.: Exploration of parametric uncertainty in a surface mass balance model applied to the Greenland ice sheet, J. Geophys. Res., 117(F1), F01021, doi:10.1029/2011JF002067, 2012.

Grenfell, T. C. and Perovich, D. K.: Seasonal and spatial evolution of albedo in a snow-ice-land-ocean environment, J. Geophys. Res., 109(C1), C01001, doi:10.1029/2003JC001866, 2004.

Hall, D.K., G.A. Riggs and V.V. Salomonson.: "MODIS Snow and Sea Ice Products," 2006: Earth Science Satellite Remote Sensing - Volume I: Science and Instruments, J.J. Qu, W. Gao, M. Kafatos, R.E. Murphy and V.V. Salomonson (eds.), Springer, New York, pp. 154-181, 2006.

Hall, D. K., Comiso, J. C., DiGirolamo, N. E., Shuman, C. A., Box, J. E. and Koenig, L. S.: Variability in the surface temperature and melt extent of the Greenland ice sheet from MODIS, Geophys. Res. Lett., 40(10), 2114–2120, doi:10.1002/grl.50240, 2013.

Hanna, E., Fettweis, X., Mernild, S. H., Cappelen, J., Ribergaard, M. H., Shuman, C. a., Steffen, K., Wood, L. and Mote, T. L.: Atmospheric and oceanic climate forcing of the exceptional Greenland ice sheet surface melt in summer 2012, Int. J. Climatol., 34(4), 1022–1037, doi:10.1002/joc.3743, 2014.

Holben, N., Tanr, D., Smirnov, A., Eck, T. F., Slutsker, I., Newcomb, W. W., Schafer, J. S., Chatenet, B., Lavenu, F., Kaufman, J., Castle, J. Vande, Setzer, A., Markham, B., Clark, D., Halthore, R., Karneli, A., Neill, N. T. O., Pietras, C., Pinker, T., Voss, K. and Zibordi, G.: An emerging ground-based aerosol climatology : Aerosol optical depth from AERONET, J. Geophys. Res., 106(Dll), 12,067–12,097, 2001.

Iqbal, M.: Spectral and total sun radiance under cloudless skies. Physical Climatology for Solar and Wind Energy, R. Guzzi and C. G. Justus, Eds., World Scientific, 196–242, 1988.

Keegan, K. M., Albert, M. R., McConnell, J. R. and Baker, I.: Climate change and forest fires synergistically drive widespread melt events of the Greenland Ice Sheet., Proc. Natl. Acad. Sci. U. S. A., (14), 1–4, doi:10.1073/pnas.1405397111, 2014.

Klein, A. G., & Stroeve, J.: Development and validation of a snow albedo algorithm for the MODIS instrument. Annals of Glaciol., 34(1), 45-52, 2002.

Knap, W. H. and Oerlemans, J.: The surface albedo of the Greenland ice sheet: satellite derived and in situ measurements in the Sendre Stromfjord area during the 1991 melt season, J. Glaciol., 42(141), 364–374, 1996.

Konzelmann, T. and Braithwaite, R. J.: Variations of ablation, albedo and energy balance at the margin of the Greenland ice sheet, Kronprins Christian Land, eastern north Greenland, J. Glaciol., 41(137), 174–182, 1995.

Kuhn, M.: Anisotropic reflection from sastrugi fields. Antarctic Journal of the United States, 9, 123–125, 1974.

Lampkin, D. J. and VanderBerg, J.: Supraglacial melt channel networks in the Jakobshavn Isbrae region during the 2007 melt season, Hydrol. Process., doi:10.1002/hyp.10085, 2013.

Legleiter, C. J., Tedesco, M., Smith, L. C., Behar, a. E. and Overstreet, B. T.: Mapping the bathymetry of supraglacial lakes and streams on the Greenland ice sheet using field measurements and high-resolution satellite images, The Cryosphere, 8, 215–228, doi:10.5194/tc-8-215-2014, 2014.

Van Meijgaard, E., van Ulft, L. H., Van de Berg, W. J., Bosveld, F. C., Van den Hurk, B., Lenderink, G., and Siebesma, A. P.: The KNMI regional atmospheric climate ~~model~~RACMO~~version~~model RACMO version 2.1, Tech. Rep. 302, Royal Netherlands Meteorological Institute, De Bilt, 2008.

Mernild, S. H. and Liston, G. E.: Greenland Freshwater Runoff. Part II: Distribution and Trends, 1960–2010, J. Clim., 25(17), 6015–6035, doi:10.1175/JCLI-D-11-00592.1, 2012.

Nghiem, S. V., Hall, D. K., Mote, T. L., Tedesco, M., Albert, M. R., Keegan, K., Shuman, C. A., DiGirolamo, N. E. and Neumann, G.: The extreme melt across the Greenland ice sheet in 2012, Geophys. Res. Lett., 39(20), 1–6, doi:10.1029/2012GL053611, 2012.

Onset Computer Corp.: Silicon Pyranometer Smart Sensor (Part # S-LIB-M003), 1–6, 2010.

Rae, J. G. L., Aðalgeirsdóttir, G., Edwards, T. L., Fettweis, X., Gregory, J. M., Hewitt, H. T., Lowe, J. A., Lucas-Picher, P., Mottram, R. H., Payne, A. J., Ridley, J. K., Shannon, S. R., van de Berg, W. J., van de Wal, R. S. W., and van den Broeke, M. R.: Greenland ice sheet surface mass balance: evaluating simulations and making projections with regional climate models, The Cryosphere, 6, 1275-1294, doi:10.5194/tc-6-1275-2012, 2012.

Rennermalm, A. K., Smith, L. C., Chu, V. W., Box, J. E., Forster, R. R., Van den Broeke, M. R., Van As, D. and Moustafa, S. E.: Evidence of meltwater retention within the Greenland ice sheet, The Cryosphere, 7, 1433–1445, doi:10.5194/tc-7-1433-2013, 2013.

Román, M. O., Schaaf, C. B., Lewis, P., Gao, F., Anderson, G. P., Privette, J. L., Strahler, A. H., Woodcock, C. E. and Barnsley, M.: Assessing the coupling between surface albedo derived from MODIS and the fraction of diffuse skylight over spatially-characterized landscapes, Remote Sens. Environ., 114(4), 738–760, doi:10.1016/j.rse.2009.11.014, 2010.

Schaaf, C. B., Liu, J., Gao, F., & Strahler, A. H.: Aqua and Terra MODIS albedo and reflectance anisotropy products. In Land Remote Sensing and Global Environmental Change (pp. 549-561). Springer New York, 2011.

Schaepman-Strub, G., Schaepman, M. E., Painter, T. H., Dangel, S. and Martonchik, J. V.: Reflectance quantities in optical remote sensing—definitions and case studies, Remote Sens. Environ., 103(1), 27–42, doi:10.1016/j.rse.2006.03.002, 2006.

L. C. Smith, ~~L. C.,~~V. W. Chu, ~~V. W.,~~K. Yang, ~~K.,~~C. J. Gleason, ~~C. J.,~~L. H. Pitcher, ~~L. H.,~~A. K. Rennermalm, ~~A. K.,~~C. J. Legleiter, ~~C. J., Behar,~~ A. E~~.~~, Behard, B. T. Overstreet, ~~B. T.,~~S. E. Moustafa, ~~S. E.,~~M. Tedesco, ~~M.,~~R. R. Forster, ~~R. R.,~~A. L. LeWinter, ~~A. L.,~~D. C. Finnegan, ~~D. C.,~~Y. Sheng, ~~Y.~~ and J. Balog~~, J.: Supraglacial~~. Efficient meltwater drainage through supraglacial streams and rivers on the southwest Greenland ~~Ice Sheet, Proc. Natl. Acad. Sci., in review, 2014~~ice sheet. Proceedings of the National Academy of Sciences, doi:10.1073/pnas.1413024112, 2015.

Steffen, K. and Box, J.: Surface climatology of the Greenland ice sheet: Greenland Climate Network 1995-1999, J. Geophys. Res., 106(D24), 33951–33964, 2001.

Stroeve, J., Box, J. E., Gao, F., Liang, S., Nolin, A. and Schaaf, C.: Accuracy assessment of the MODIS 16-day albedo product for snow: comparisons with Greenland in situ measurements, Remote Sens. Environ., 94(1), 46–60, doi:10.1016/j.rse.2004.09.001, 2005.

Stroeve, J., Box, J. E., Wang, Z., Schaaf, C. and Barrett, A.: Re-evaluation of MODIS MCD43 Greenland albedo accuracy and trends, Remote Sens. Environ., 138, 199–214, doi:10.1016/j.rse.2013.07.023, 2013.

Stroeve, J. C., Box, J. E. and Haran, T.: Evaluation of the MODIS (MOD10A1) daily snow albedo product over the Greenland ice sheet, Remote Sens. Environ., 105(2), 155–171, doi:10.1016/j.rse.2006.06.009, 2006.

Tedesco, M., Fettweis, X., van den Broeke, M. R., van de Wal, R. S. W., Smeets, C. J. P. P., van de Berg, W. J., Serreze, M. C. and Box, J. E.: The role of albedo and accumulation in the 2010 melting record in Greenland, Environ. Res. Lett., 6(1), 014005, doi:10.1088/1748-9326/6/1/014005, 2011.

Tedesco, M., Fettweis, X., Mote, T., Wahr, J., Alexander, P., Box, J. E. and Wouters, B.: Evidence and analysis of 2012 Greenland records from spaceborne observations, a regional climate model and reanalysis data, The Cryosphere, 7, 615–630, doi:10.5194/tc-7-615-2013, 2013.

M. Tedesco, J. E. Box, J. Cappelen, X. Fettweis, T. Jensen, T. L. Mote, A. K. Rennermalm, L. C. Smith, R. S. W. van de Wal, J. Wahr. The Arctic: Greenland Ice Sheet in "State of the Climate 2013." Bulletin of the American Meteorological Society, 95(7), S136-S137, doi:10.1175/2014BAMSStateoftheClimate.1, 2014.

Van de Wal, R. S. W., Boot, W., Smeets, C. J. P. P., Snellen, H., van den Broeke, M. R. and Oerlemans, J.: Twenty-one years of mass balance observations along the K-transect, West Greenland, Earth Syst. Sci. Data, 4(1), 31–35, doi:10.5194/essd-4-31-2012, 2012.

Wang, Z., Schaaf, C. B., Chopping, M. J., Strahler, A. H., Wang, J., Román, M. O., Rocha, A. V., Woodcock, C. E. and Shuai, Y.: Evaluation of Moderate-resolution Imaging Spectroradiometer (MODIS) snow albedo product (MCD43A) over tundra, Remote Sens. Environ., 117, 264–280, doi:10.1016/j.rse.2011.10.002, 2012.

Wientjes, I. G. M. and Oerlemans, J.: An explanation for the dark region in the western melt zone of the Greenland ice sheet, The Cryosphere, 4, 261–268, doi:10.5194/tc-4-261-2010, 2010.

Wientjes, I. G. M., Van de Wal, R. S. W., Reichart, G. J., Sluijs, A. and Oerlemans, J.: Dust from the dark region in the western ablation zone of the Greenland ice sheet, The Cryosphere, 5, 589–601, doi:10.5194/tc-5-589-2011, 2011.

Wright, P., Bergin, M., Dibb, J., Lefer, B., Domine, F., Carman, T., Carmagnola, C., Dumont, M., Courville, Z., Schaaf, C. and Wang, Z.: Comparing MODIS daily snow albedo to spectral albedo field measurements in Central Greenland, Remote Sens. Environ., 140, 118–129, doi:10.1016/j.rse.2013.08.044, 2014.

Yang, K. and Smith, L. C.: Supraglacial Streams on the Greenland Ice Sheet Delineated From Combined Spectral–Shape Information in High-Resolution Satellite Imagery, IEEE Geosci. Remote Sens. Lett., 10(4), 801–805, doi:10.1109/LGRS.2012.2224316, 2013.

~~Table 1.~~

Table 1. ~~Meteorological station sites and associated variables.~~

~~Site~~	~~Latitude~~	~~Longitude~~	~~Elevation (m)~~	~~Start Date~~	~~End Date~~
~~Base Met Station~~	~~67.151629~~	~~50.027993~~	~~511.3~~	~~8 Jun~~	~~26 Jun~~
~~Top Met Station~~	~~67.146857~~	~~50.001186~~	~~586.0~~	~~14 Jun~~	~~26 Jun~~

Formatted: Body Text, Line spacing: Multip
1.07 li, Tab stops: 6.5", Left

~~Table 2.~~ Descriptive statistics for high-quality albedo transects. SZA and CC listed for Base Met Station only. Brd is used to abbreviate broadband.

Transect Date	Start Time	End Time	Min ~~Vis~~Brd α_{ASD}	Max ~~Vis~~Brd α_{ASD}	Mean ~~Vis~~Brd α_{ASD}	Daily Average α_{base}	Daily Average α_{top}	Min SZA (^{o})	Max SZA (^{o})	Mean SZA (^{o})	Min CC	Max CC	Mean CC
16-Jun	10:32:33	11:53:57	0.~~277~~260	0.~~859~~754	0.~~606~~550	0.404	0.636	45.615	50.454	47.828	0.135	0.176	0.157
19-Jun	10:39:30	11:35:59	0.~~218~~141	0.~~767~~730	0.~~546~~532	0.316	0.541	46.449	49.925	48.093	0.045	0.084	0.065
25-Jun	10:20:29	11:11:00	0.~~151~~210	0.~~855~~670	0.~~608~~490	0.333	0.525	47.963	51.525	49.677	0.119	0.138	0.125

Table ~~3. Summary statistics for high-quality~~ 2. Average broadband ~~and visible α_{ASD} retrievals by transect date reported as mean ± 1σ.~~

~~Transect Date~~	~~Broadband (325 – 1075 nm) α_{ASD} mean and standard deviation~~	~~Visible (400 – 700 nm) α_{ASD} mean and standard deviation~~
~~16-Jun~~	~~0.51 ± 0.096~~	~~0.61 ± 0.126~~
~~19-Jun~~	~~0.48 ± 0.115~~	~~0.61 ± 0.161~~
~~25-Jun~~	~~0.45 ± 0.101~~	~~0.55 ± 0.141~~
~~All Dates~~	~~0.48 ± 0.104~~	~~0.59 ± 0.143~~

Formatted: Font color: Black

Formatted: Font color: Black

~~Table 4. Average visible~~ α_{ASD} within a ~~10~~30 m radius of ablation stake sites and classified by surface type.

Ablation stake sites	α_{ASD} site average	~~White~~Clean surfaces	Dark surfaces
Site A	0.~~750~~641	-	-
Site B	0.~~690~~540	-	-
Site C	0.~~740~~591	-	-
Site D	0.~~490~~432	0.~~652~~530	0.~~274~~243
Site E	0.555	~~0.635~~	~~0.232~~

Table 3. Seasonal evolution (%) of four surface types at five distinct time steps approximated from Chandler et al. (2014).

Time steps	Classified names	Clean ice	Dirty ice	Streams	Cryoconite holes
1 June	Early summer ice	100	0	0	0
19 June	Dirty ice exposure	90	3	1	6
18 July	Melt	60	20	1	19
28 July	Darkening ice	50	30	3	17
5 August	Late summer ice	40	40	6	14

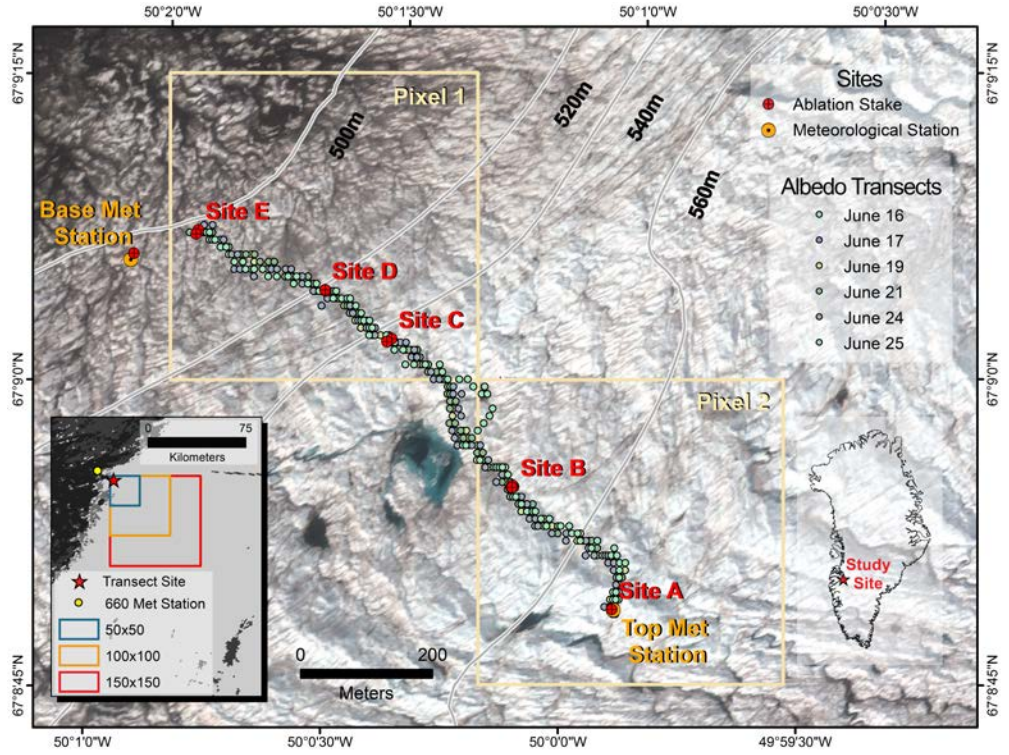

Figure 1. 23 June 2013 WorldView-2 true color image (bands 5, 3, and 2 RGB) of the study site with elevation contours (m), MODIS pixel extents~~,~~ (yellow boxes), and location of the six albedo transects, ablation stake, and meteorological station sites. Location of four MODIS spatial extent regions overlaid on a 31 May 2013 MOD10A1 image (black box inset).

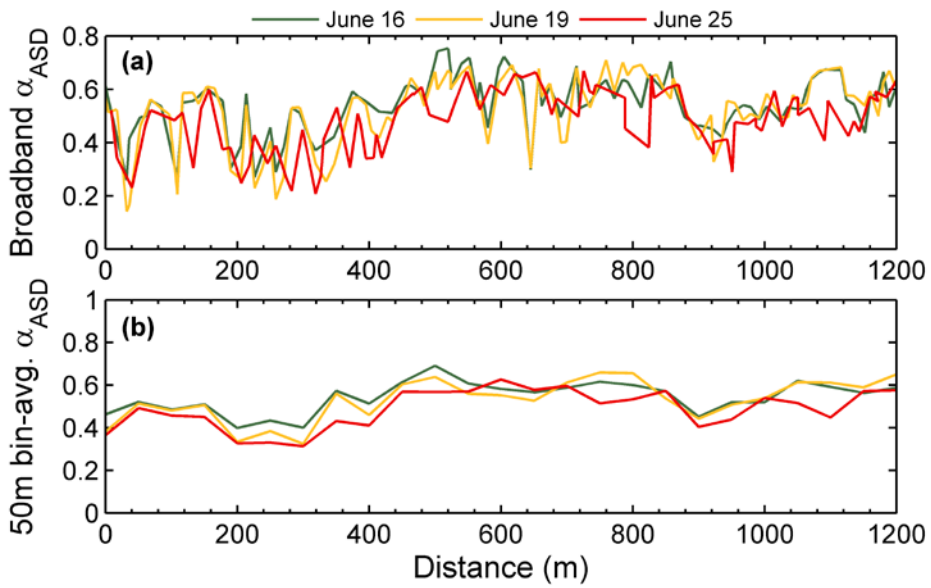

Figure 2. ~~Radiative conditions during transect dates at the Base Met Station, including incoming solar radiation (ISR, black line), outgoing solar radiation (OSR, green line; left y-axis), modeled relative cloud cover (CC, blue stippled line; right y-axis), and solar zenith angles (SZA, yellow line right axis). Red shaded regions show α_{ASD} data collection times.~~

~~Figure 3. Half-hourly broadband α_{base} (a) measurements as a function of SZA. Symbols and colors correspond to transect dates. Transect times correspond to the black line. A SZA threshold at 70° is represented by the red stipple line. (b) Relative *CC* determined at α_{base} as a function of time during transect dates. Symbols and colors correspond to transect dates. Transect times correspond to bold lines.~~

Figure 4. Broadband α_{base} (blue dots) and α_{top} (pink dots) versus α_{ASD} and α_{MET} (i.e., both α_{base} and α_{top}) measurements fitted to a linear regression equation ($R^2 = 0.40$). The value of α_{ASD} error is unknown, but a conservative estimate of ± 0.1 is shown.

~~Figure 5.~~ High-quality ~~visible~~broadband α_{ASD} observations on 16, 19 and 25 June (a), and ~~visible~~broadband α_{ASD} averaged in 50 m bins (b) along the length of the transect starting near Site E (0 m) and ending near Site A (1200 m).

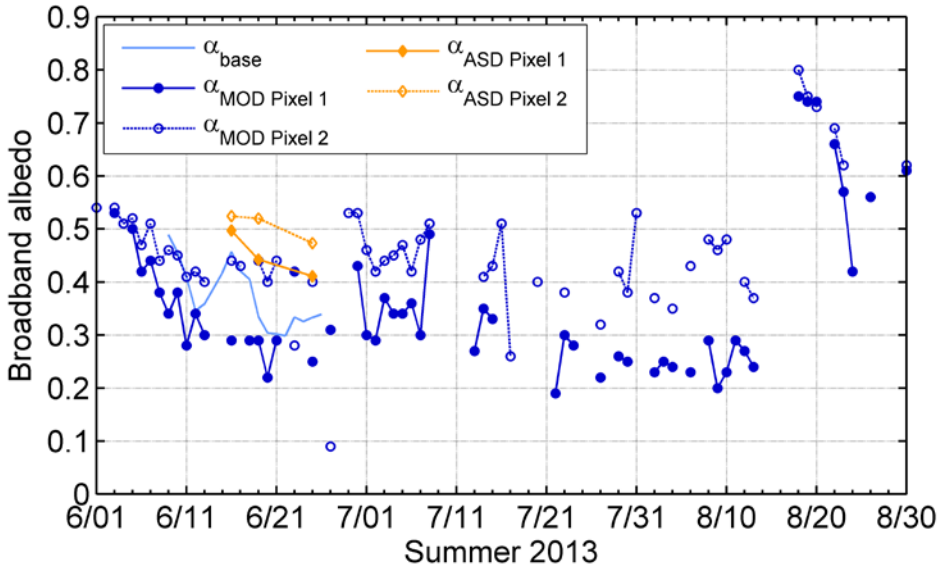

Figure ~~6~~3. High-quality daily average broadband $\alpha_{ASD\ Pixel\ 1}$ and $\alpha_{ASD\ Pixel\ 2}$, α_{base} ~~and α_{top}~~ (for SZA < 70°), and $\alpha_{MOD\ Pixel\ 1}$ and $\alpha_{MOD\ Pixel\ 2}$ time series for the 2013 melt season. $\alpha_{ASD\ Pixel\ 1}$ and $\alpha_{ASD\ Pixel\ 2}$ pixel-averaged values correspond to high-quality ASD transect dates 16, 19 and 25 June.

Formatted: Not Superscript/ Subscript

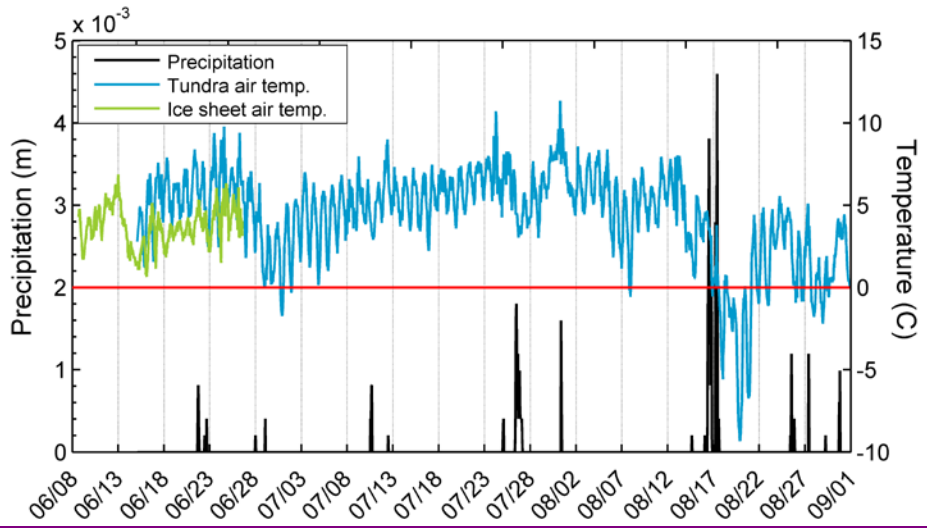

Figure ~~7~~4. Summer 2013 precipitation (left y-axis; black line) and near surface air temperature (right y-axis; blue line) time series collected from a meteorological station installed at the edge of the pro-glacial tundra environment. Base Met Station near surface air temperature time series is available from 8 – 26 June 2013 (green line). The zero degree line is in red.

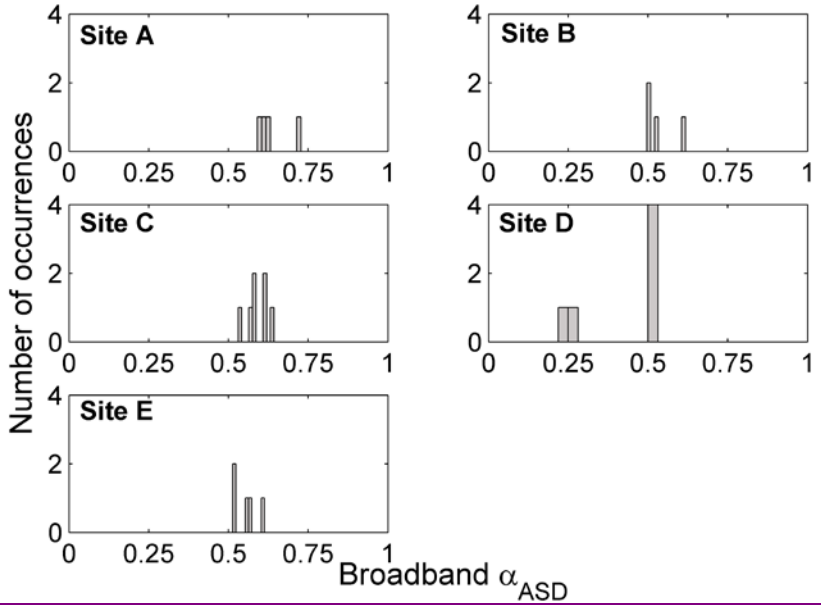

Figure 5. Distribution of ~~visible~~broadband α_{ASD} within ~~10~~30 m radius of ablation stake sites.

~~Figure 8. Observed ablation rates and visible α_{ASD} for different ice surface types.~~

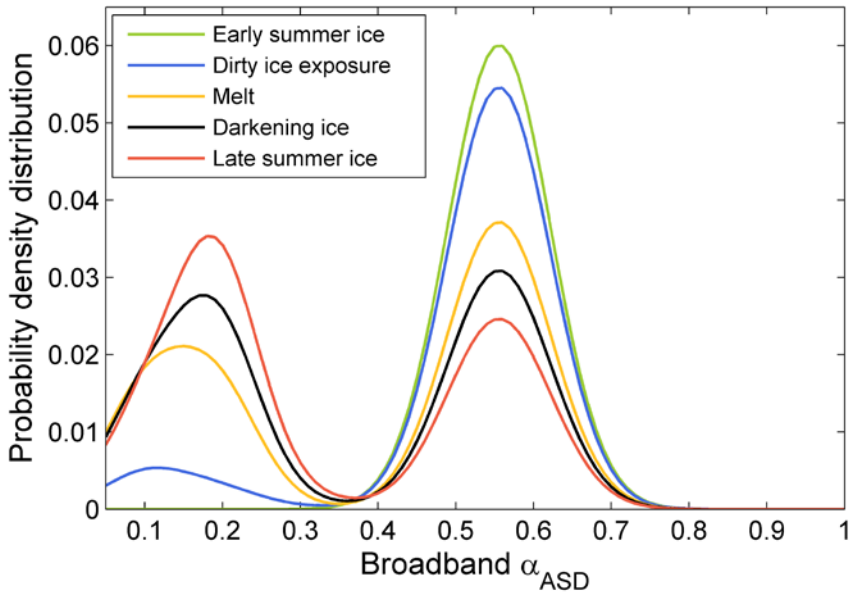

Figure ~~9~~6. Computed albedo distribution for a nearby site of Chandler et al. (2014) simulated across the melt season based on observed ~~visible~~broadband α_{ASD} values for dominant surface types, weighted by their relative surface area coverage. Each surface type is assumed to follow a normal distribution. Computed albedo distributions represent the sum of each surface type's probability distribution function.

Formatted: Left

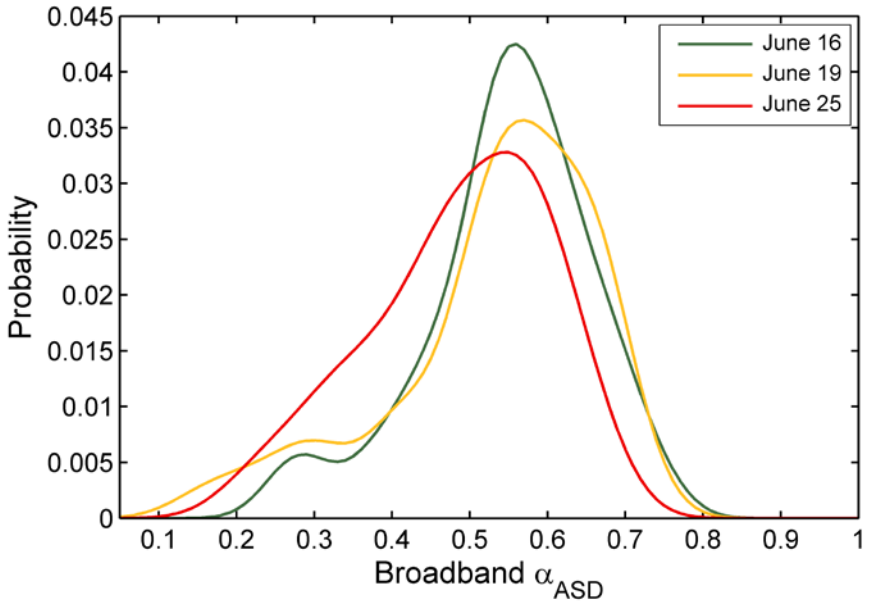

Figure 7. Observed distributions of high-quality broadband α_{ASD} transects on June 16, 19, and 25.

~~Figure 10. Observed distributions of high quality visible α_{ASD} transects on June 16, 19, and 25.~~

~~Figure 11.~~

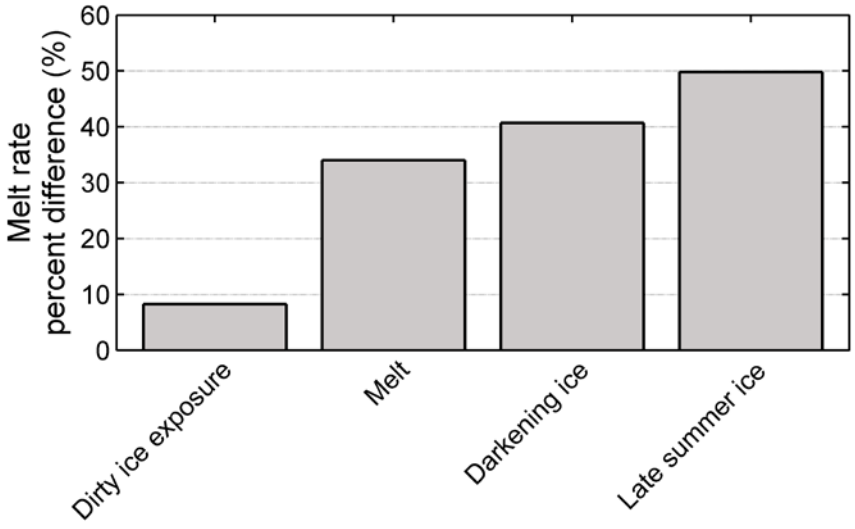

Figure 8. Percent difference in melt rate estimates for different albedo probability density functions and averaged incoming solar radiation conditions at Base Met Station from 16, 19, and 25 June, relative to 'early summer ice (1 June)' distribution.

Formatted: Left

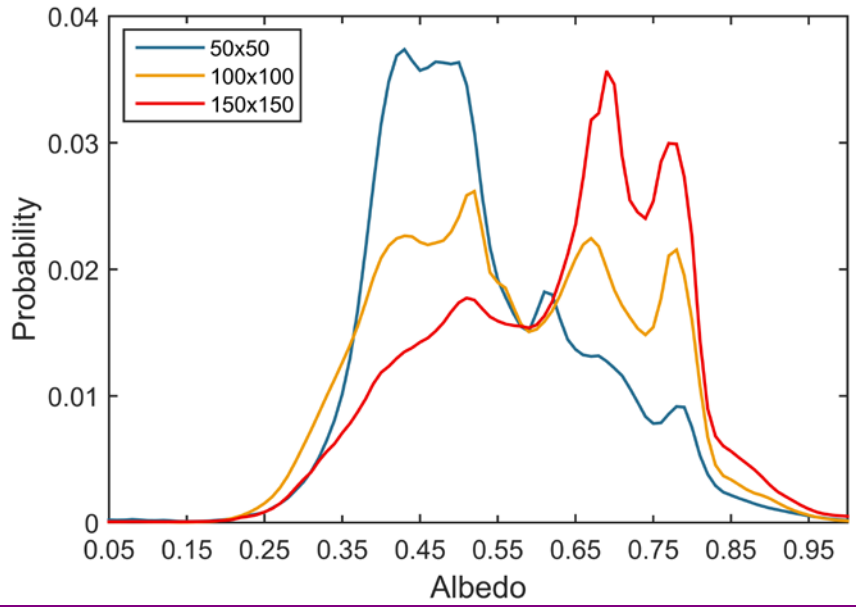

Figure ~~1~~2~~9~~. MOD10A1 2013 seasonal average albedo probability density distributions at ~~four~~three spatial ~~scales. A~~ extents, 50x50 MODIS pixels (px), 100x100 px, and 150x150 px, respectively. The bimodal ~~albedo~~ distribution ~~is evident~~seen at the 100x100 px (46.3 km^2) spatial extent is likely the result of almost equal area of snow and ice facies characterizing the two peaks. In contrast, the right and left skew distributions of 50x50 px and 150x150 px illustrate the dominance of ice and snow surfaces, respectively.

Formatted: Font color: Custom Color(RGB(34,34,34)), Pattern: Clear (White)

~~Figure 13.~~

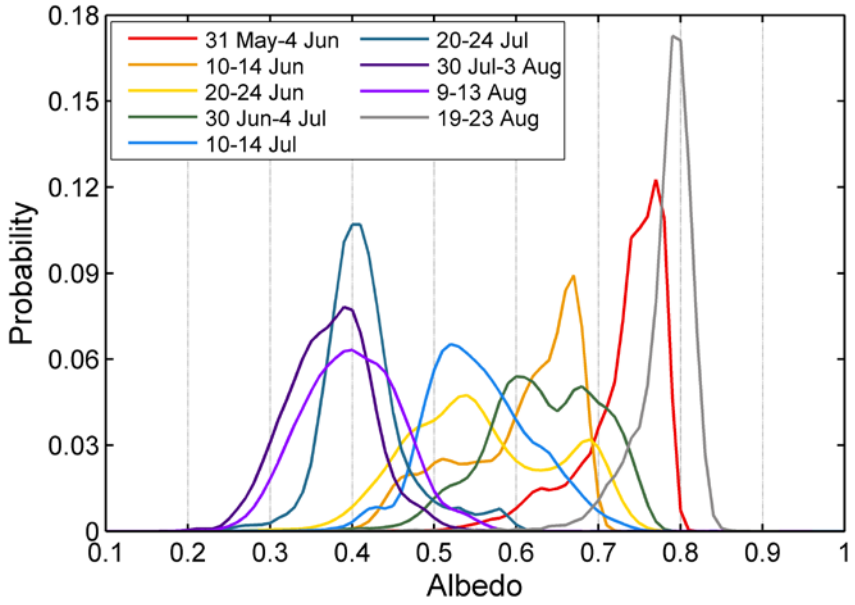

Figure 10. 100x100 ~~pixel scale~~px pentad averages over the 2013 melt season. Every other pentad average line is plotted.

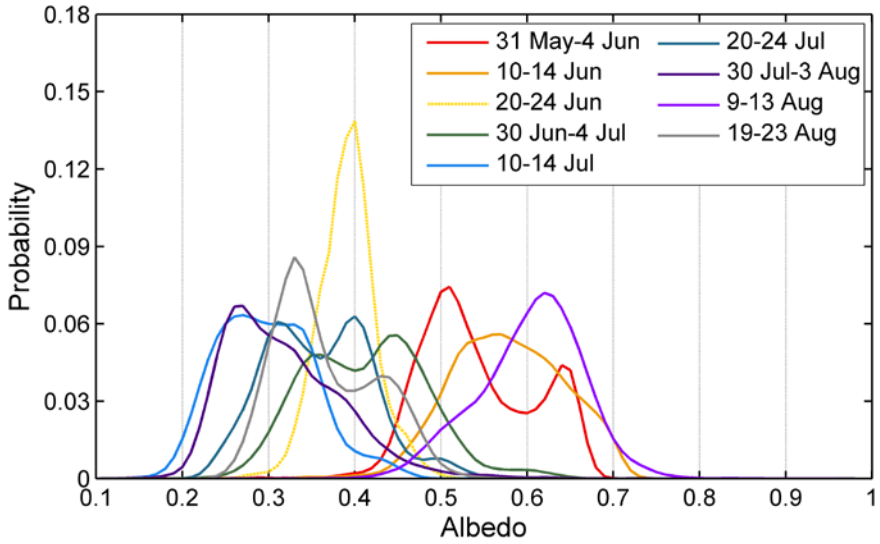

Figure 11. MODIS 100x100 px spatial extent pentad average albedo distributions for the 2012 melt season. Note, the 20-24 June pentad (yellow stippled line) is most likely erroneous due to an outlier in the MODIS data on 21-22 June 2012.

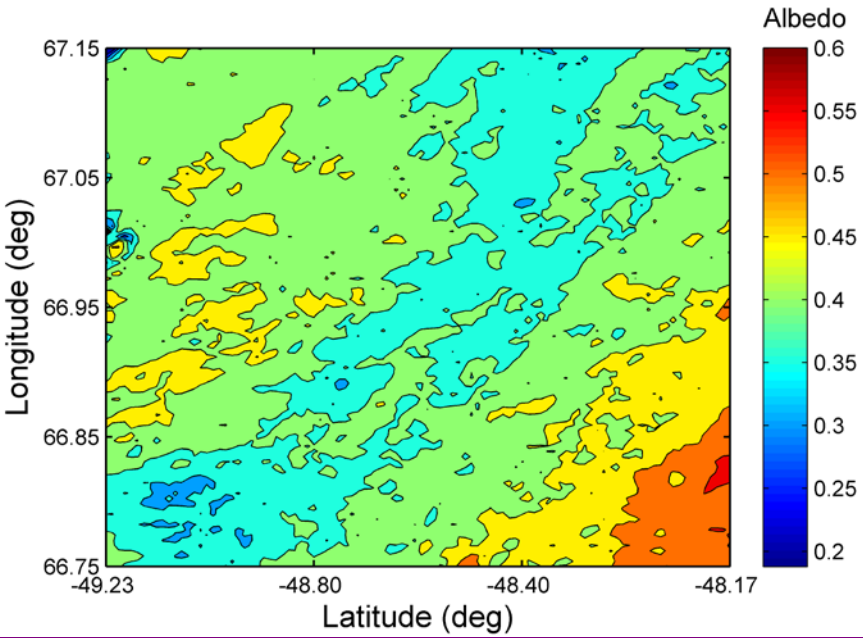

Figure 12. MODIS 2012 seasonal average for the 100x100 spatial extent. A region of dark ice, known as the "dark band", extends through our study area (< ~0.35, shown in cyan blue and blue colors).

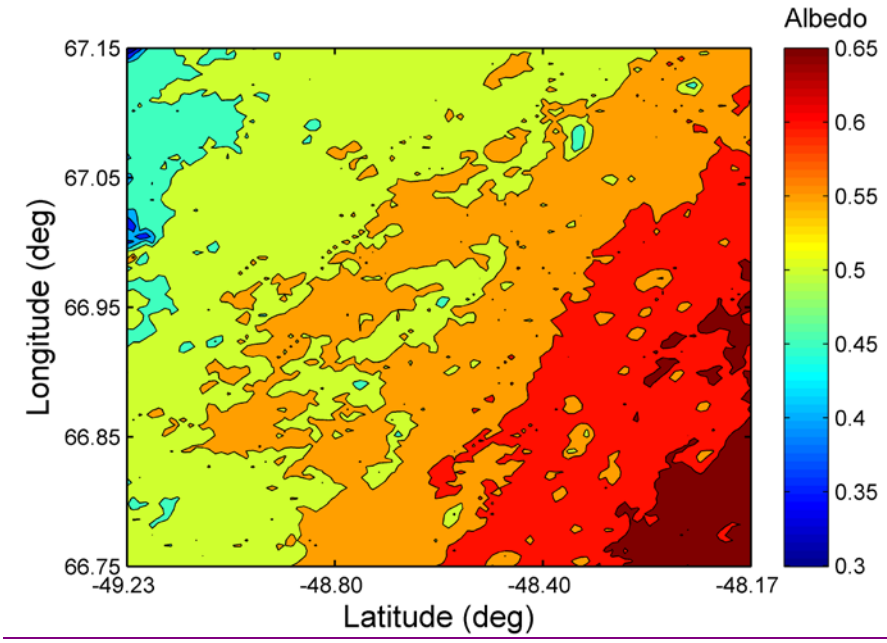

Figure 13. MODIS 2013 seasonal average for the 100x100 px spatial extent. Overall higher MODIS albedo values are observed in 2013, without a "dark band" region surface expression.

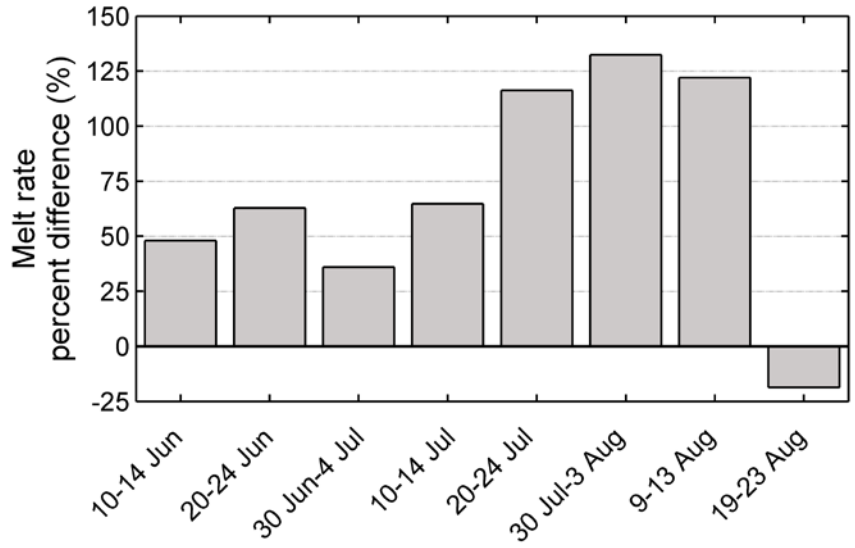

Figure 14. Percent difference in melt rate estimates for 100x100 px pentad ~~averages~~albedo distributions for the 2013 melt season, relative to 31 May – 4 June pentad ~~average~~albedo distribution. Melt rates are calculated with identical radiation budget conditions to isolate the effect of albedo distribution changes.

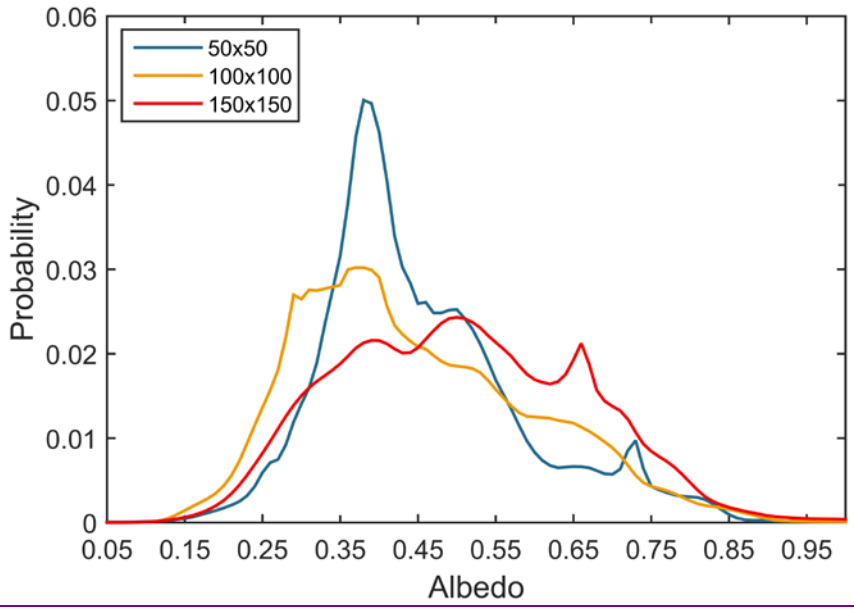

Figure 15. MODIS 2012 seasonal average albedo probability density distributions at three spatial extents. The MODIS 2012 seasonal average albedo probabilities for the 100x100 px and 150x150 px reveal a high probability of low albedo values (0.2 – 0.3). This is likely influenced by the expansion of the "dark band" region in these spatial extents.

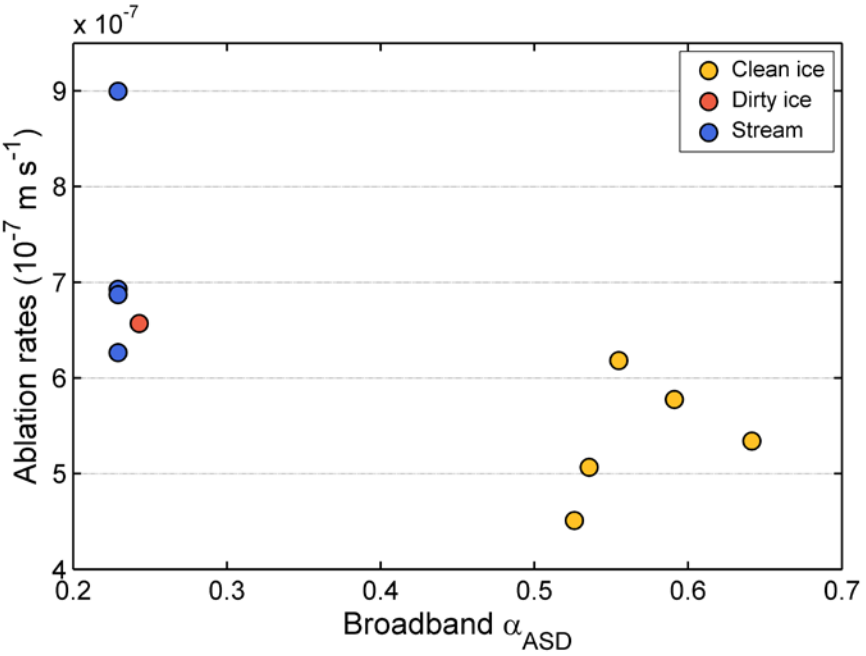

Figure 16. Observed ablation rates and broadband α_{ASD} for different ice surface types.

7 Appendix A

7.1 Field spectroscopy measurements

At the start of each transect, the ASD was calibrated to current hemispherical atmospheric conditions by orienting the RCR skyward, along a nadir-viewing angle. Subsequent measurements were taken with the ASD rotated 180° to view the ice surface. Under changing sky conditions, the instrument was recalibrated. Each transect consisted of ~100 sample locations, roughly 10 m apart. Despite changing ice conditions rapidly deteriorating temporary location markers, global positioning system (GPS) locations reveal that sample sites in consecutive transects were gathered in close proximity (Fig. 1). While samples were not taken from exactly the same sites preventing a point-by-point comparison, the transect sample distribution and smoothed spatial patterns can be analyzed for change over time. Sample sites along the transect were selected based on distance. If a spectrum site intersected with a stream, melt pond, or cryoconite hole, the nearest ice surface was sampled instead. To capture spectral albedo of different ice surface types, separate measurements of streams, dirty ice, and white ice were collected. At each sample location, five consecutive spectra consisting of 10 dark currents per scan and 10 white reference measurements were recorded and averaged.

Apparent outliers were identified using the Spectral Analysis and Management System software (SAMs) to identify outliers. Outliers were defined as physically unrealistic spectral albedo values (> 1.0) and raw spectra that were significantly different to the other spectra across the entire spectral range (visible and near-infrared wavelengths) taken for the same sample. For 16 June, 20 spectra were deemed outliers (total spectra collected = 555); 19 June, 17 spectra were deemed outliers (total spectra collected = 560); and 25 June, 12 spectra were deemed outliers (total spectra collected = 480). The outliers for these transect dates comprise less than 4% of all spectra collected, and thus, likely had an insignificant impact on the final albedo calculations. On 17 June, spectra with unrealistic > 1.0 values were collected, as will be shown in section 7.2 that all data from this day were considered low-quality and removed from the dataset.

1

7.2 Quality-control of α_{ASD} data

To ensure a high-quality α_{ASD} dataset, an impact assessment of variable cloud conditions (i.e., irregular lighting due to transient clouds) and high SZAs during late afternoon albedo transect collections was made. Key et al. (2001) reported a 4-6% increase in albedo, on average, under cloudy conditions. Albedo readings have also been reported as unreliable at SZAs beyond 70°, due to an increase in diffuse radiation reaching the ice surface (Schaaf et al., 2011; Stroeve et al., 2005; Stroeve et al., 2013; Wang et al., 2012).

As a proxy for cloud cover, relative cloud cover, hereafter CC, was calculated every second as the ratio of modeled clear-sky and observed incoming solar radiation similar to Box (1997). 'Clear-sky' incoming shortwave fluxes at the surface were calculated with a solar radiance model (Iqbal, 1988). Model inputs of water vapor content, surface pressure, aerosol optical depth at 380 and 500 nm, and area optical thickness were estimated from the Kangerlussuaq AEROsol Robotic NETwork (AERONET) station (Holben et al., 2001). SZA was also modeled with the solar radiance model using latitude, longitude, time of day, and day of year at the Base Met Station. α_{ASD} collected under high CC variability and SZAs approaching extreme angles were subsequently removed. Filtering α_{ASD} data under these criteria ensured the production of a high-quality dataset necessary for subsequent analysis.

Cloud cover and radiative conditions varied among transects (Fig. A1). The majority of α_{ASD} measurements were made at small SZAs (~1030-1200 local time), except on 21 and 24 June, when observations were made in late afternoon (1530-1630 and 1640-1750 local time, respectively). Incoming solar radiation fluxes exhibited considerable range of diurnal variability (average 662 ± 83 W m^{-2}). Outgoing solar radiation displayed similar range of variability at lower magnitudes (average 239 ± 18 W m^{-2}) during transect dates. Derived CC reveals daily range of variability in cloud conditions roughly consistent with incoming solar radiation observations, yet on average, remained low (~0.13) indicating that the majority of the transect times were collected during nearly cloud-free conditions. During transect times, half-hourly α_{base} changed linearly with SZA, yet remained fairly stable (Fig. A2a). Above 80° SZA, half hourly α_{base} variability increased, confirming that 70° SZA was a suitable threshold

for daily average albedo calculations. Installation tilt, heterogeneous and changing surface conditions likely contributed locally to "unstable" α_{base} observations at higher SZAs. A hysteresis observed in α_{top} observations (data not shown) is attributed primarily to a low installation height (0.5 m), but may also be partly due to changing surface conditions. These effects can compromise the accurate representation of illumination and viewing geometries, resulting in reduced albedo estimates at high SZAs (Kuhn, 1974; Wang et al., 2012; Dumont et al., 2012). As such, Top Met Station measurements, and α_{base} at SZAs greater than 70º, were excluded for most analyses. Despite its limitations, α_{top} were used for α_{ASD} comparison described below.

High range of CC variability, instead of consistently high CC, was found to be responsible for saturating α_{ASD} readings on 17, 21, and 24 June (Fig. A2b). Continuous recalibration of the ASD instrument on 17 and 24 June was inadequate to overcome variable lighting conditions resulting in saturated α_{ASD} readings (> 1). During 21 June, α_{ASD} data did not saturate despite variable sky conditions (0.01-0.52 CC range). Variable cloud conditions on 17, 21, and 24 of June effectively increased the amount of downwelling longwave radiation relative to shortwave radiation available at the surface, of which, the net effect results in a larger portion of solar radiation available to be reflected by the ice surface (Grenfell and Perovich, 2004; Román et al., 2010; Wang et al., 2012). This can translate to an increase in spectral albedo estimates by ~0.06 over active melting ice surfaces (Grenfell and Perovich, 2004).

By removing the majority of shortcomings and uncertainties identified in transect radiative and surface conditions, a high-quality albedo dataset was produced. Optimal SZA, CC, and radiative conditions were observed for 16, 19 and 25 June. α_{ASD} data collected on 17, 21, and 24 June were identified as low-quality based on their dependence on SZA, CC variability, and issues with albedo saturation, and subsequently removed from further analysis (Fig. A2). The first and last high-quality α_{ASD} measurements closest to the AWSs were compared and reveal that they agree reasonably well with α_{base} and α_{top} data (Fig. A3). As much as 62% of α_{ASD} variance is explained by α_{base} and α_{top}, and the linear regression model slope between the two datasets is close to one ($\alpha_{ASD} = 0.26\alpha_{MET} + 0.41$, where α_{MET} is α_{base}

and α_{top} combined). The discrepancy is likely due to differences in exact sample locations and instrumentation. Table 1 provides summary statistics related to high-quality α_{ASD} and transect conditions.

7.3 Installation of meteorological stations

The Top Met Station was installed upon a homogenous clean ice surface, and the Base Met Station was installed above a heterogeneous surface of mixed clean and dirty ice. Both stations measured solar radiation fluxes every 0.5 h at 300-1100 nm, using S-LIB-M003 silicon pyranometers and a U30 data logger (Table 1A; ± 5% or 10 W m^{-2} precision; Onset Computer Corp., 2010) from 8-26 June. Sensors were attached to a pole drilled into the ice at 1.5 m above the surface, and were kept relatively constant at this height, but occasionally tilted off-level. After a period of heavy melting, the Top Met Station was re-drilled and installed at 0.5 m height and remained at this height as melting seized. A very large hysteresis in α_{top} as a function of SZA suggests that the low installation height resulted in α_{top} errors due to a disproportionally large influence of surface roughness on its measurements. Despite not having observed tilt information for the AWSs, we use a theoretical tilt (for Fig. A2b) in Van den Broeke et al. (2004) to provide a reasonable uncertainty range. Assuming a tilt of 1º on 18 January at Kohnen station, Antarctica (75ºS, 0º) is associated with ~15 W m^{-2} offset in net shortwave at noon local time. This is associated with an absolute error of 5% with a tilt of 1º. Here, we assume double the uncertainty (± 10%).

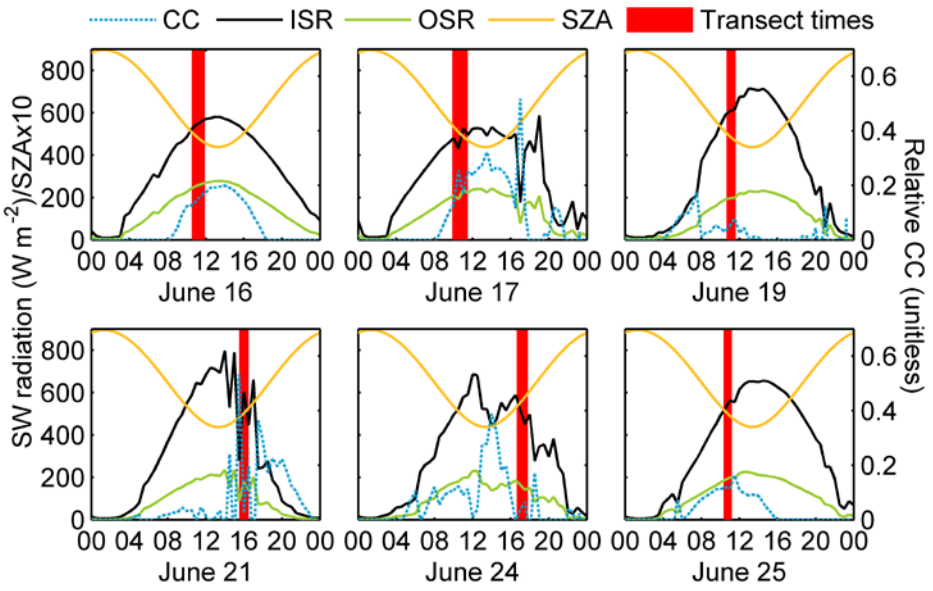

Figure A1. Radiative conditions during transect dates at the Base Met Station, including incoming solar radiation (ISR, black line), outgoing solar radiation (OSR, green line; left y-axis), modeled relative cloud cover (CC, blue stippled line; right y-axis), and solar zenith angles (SZA, yellow line right axis). Red shaded regions show α_{ASD} data collection times.

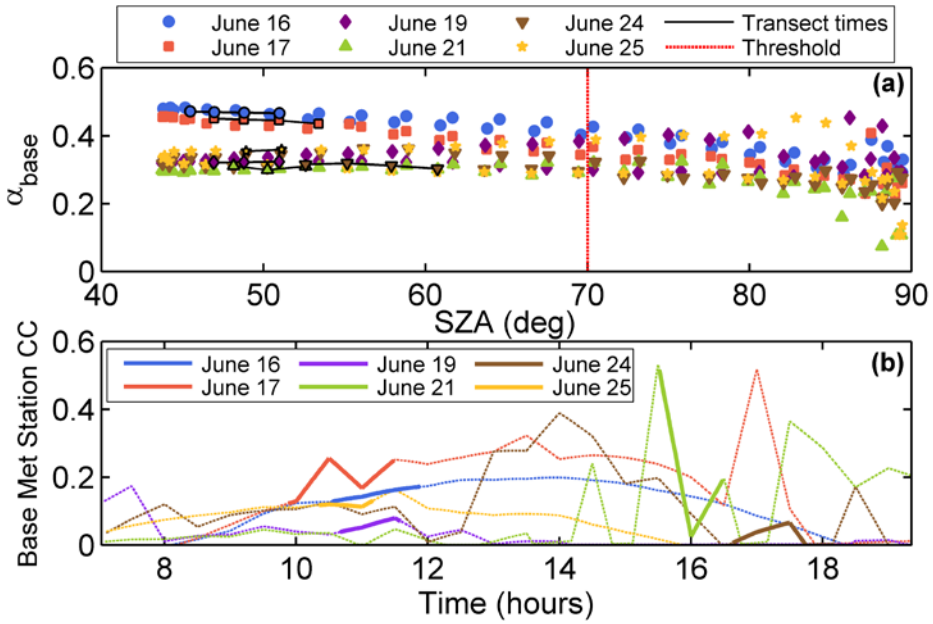

Figure A2. Half hourly broadband α_{base} (a) measurements as a function of SZA. Symbols and colors correspond to transect dates. Transect times correspond to the black line. A SZA threshold at 70° is represented by the red stipple line. (b) Relative CC determined at α_{base} as a function of time during transect dates. Symbols and colors correspond to transect dates. Transect times correspond to bold lines.

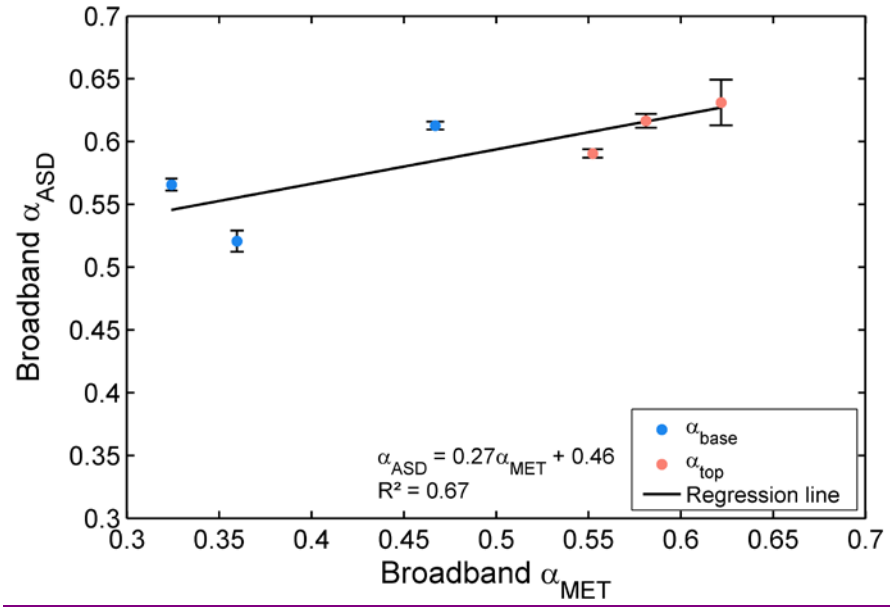

Figure A3. Broadband α_{base} (blue dots) and α_{top} (pink dots) vs. α_{ASD} and α_{MET} (i.e., both α_{base} and α_{top}) measurements fitted to a linear regression equation ($R^2 = 0.67$). The value of α_{ASD} error is based on the standard deviation of individual α_{ASD} measurements.

Formatted: Body Text, Line spacing: Multip 1.07 li, Tab stops: 6.5", Left

Table 1A. Meteorological station sites and associated variables.

Site	Latitude	Longitude	Elevation (m)	Start Date	End Date
Base Met Station	67.151629	50.027993	511.3	8-Jun	26-Jun
Top Met Station	67.146857	50.001186	586.0	14-Jun	26-Jun